
# ROLES FOR THE DNA DAMAGE CHECKPOINT PROTEIN HUS1 IN TISSUE HOMEOSTASIS AND TUMOR SUPPRESSION

by Stephanie Ann Yazinski

---

# ROLES FOR THE DNA DAMAGE CHECKPOINT PROTEIN HUS1 IN TISSUE HOMEOSTASIS AND TUMOR SUPPRESSION

A Dissertation

Presented to the Faculty of the Graduate School

of Cornell University

In Partial Fulfillment of the Requirements for the Degree of

Doctor of Philosophy

by

Stephanie Ann Yazinski

August 2010

# ROLES FOR THE DNA DAMAGE CHECKPOINT PROTEIN HUS1 IN TISSUE HOMEOSTASIS AND TUMOR SUPPRESSION

Stephanie Ann Yazinski, Ph.D.

Cornell University 2010

Cancer is aberrant cellular proliferation that arises due to mutations in growth regulatory genes. DNA damage checkpoint proteins are thought to suppress tumorigenesis by preventing mutation accumulation and by inducing senescence in response to oncogenic stimuli. However, checkpoint proteins may be required for cancer cells to survive the increased stress associated with transformation. There are two main mammalian DNA damage checkpoint pathways, the Atm and Atr pathways. While mutations in the Atm pathway results in increased tumorigenesis, roles for the Atr pathway in tumor development are less well understood, in part because deletion of any component of this pathway, including Hus1, results in embryonic lethality. Hus1, a component of the Rad9-Rad1-Hus1 heterotrimeric, PCNA-like sliding clamp, is recruited to sites of DNA damage for optimal phosphorylation of the Atr target Chk1.

To investigate the physiological function of the Hus1-dependent Atr pathway, our lab developed two systems that bypass the severe phenotypes associated with germline Hus1 inactivation. A conditional allele can be used for tissue specific deletion of Hus1 in adult mice. I have utilized this approach to identify an essential role for Hus1 in the survival and proliferation of mammary epithelium. Notably, Hus1 inactivation in the mammary gland did not result in tumorigenesis, even when combined with p53 inactivation. p53 deficiency exacerbated the effects of Hus1 loss, resulting in increased cell death without compensatory proliferation, revealing a novel role for p53 in mammary gland tissue regeneration. As a second approach, our lab

developed an allelic series in which mice express incrementally reduced Hus1 levels. I used this system to investigate how partial Hus1 impairment affects transformation in cell culture and impacts skin papilloma formation. Reduced Hus1 expression impaired cell transformation by activated oncogenes as measured in cell culture assays. Mice with Hus1 impairment developed significantly fewer and smaller papillomas in a two-step skin carcinogenesis protocol. These results may be due to an inability of Hus1-deficient cells to survive the stresses of neoplastic proliferation due to insufficient genome maintenance. These results suggest that reduced Hus1 levels impair tumor development and that the Atr-dependent pathway may be exploited for cancer therapy.

## BIOGRAPHICAL SKETCH

Stephanie A. Yazinski was born on January 17, 1983 in Scranton, Pennsylvannia. In 2001, she graduated from Scranton Preparatory School, in Scranton, Pennsylvannia and entered the University of Scranton to study Biochemistry. While at the University of Scranton, she worked under the guidance of Dr. George Gomez to understand the timecourse of structural and functional maturation of human olfactory epithelial cells *in vitro*. In 2004, she spent a summer at Youngstown State University and worked under Dr. Thomas Kim to understand the change in proteomic profile of *Penicillium marneffei* before and after infection of macrophage cells. In 2005, she graduated *magnum cum laude* with a Bachelors of Science in Biochemistry and Biomathematics from the University of Scranton. In 2005, Stephanie then moved to Ithaca, New York, and started her Ph.D. studies in the field of Biochemistry, Molecular and Cell Biology under the mentorship of Dr. Robert Weiss. She is studying the roles for the DNA damage checkpoint protein Hus1 in tissue homeostasis and tumor suppression.

This thesis is dedicated in loving memory to my godfather, “the country’s best uncle,”

Thomas J. Kaczmarek, Jr.

ACKNOWLEDGMENTS

I would like to acknowledge the many people who have helped and supported me throughout graduate school. First, I would like to thank my advisor Dr. Robert Weiss for his guidance, patience, and encouragement throughout my thesis work. He has helped me develop the technical and intellectual skills needed to become a successful independent scientist.

I would also like to acknowledge my committee members, Dr. Eric Alani and Dr. John Schimenti. Their valuable advice and research expertise has aided me in my graduate work as well in my professional development.

I would like to express my graditude to the Weiss lab members present and past. I want to show my appreciation to current lab members Kelly Hume, Minxing Li, Gabriel Balmus, Amy Lyndaker, and Jennifer Page and former lab member Xia Xu for their suggestions, helpful discussions, support, and friendship. I especially would like to thank the former undergraduates Lee Gerwitz and Peter Westscott for their help with my projects.

Finally, I would like to acknowledge the unrelenting support and love of my family and friends. Thank you to my fiancé, Steven Rodriguez, for his support, motivation, understanding, and love. I would like to thank my parents for their support in pursuing what I love, and my brother and sister for their constant encouragement. I would especially like to thank my late uncle who inspires me to study what I love and to always keep learning.

TABLE OF CONTENTS


Biographical Sketch iii
Dedication iv
Acknowledgements v
Table of Contents vi
List of Figures viii
List of Tables xi

Chapter 1 Literature Review 1
- 1.1 The Atm and Atr pathways are the two main checkpoint pathways that respond to DNA damage in mammalian cells 2
- 1.2 Hus1 is an essential component of the Atr pathway 6
- 1.3 Defects in the Atr pathway result in genomic instability 9
- 1.4 The Atr pathway plays critical roles in development and tissue homeostasis 11
- 1.5 Defects in the Atr pathway may contribute to tumorigenesis 13
- 1.6 Defects in the Atr pathway may result in decreased tumor development due to non-oncogene addiction 15
- 1.7 Summary and remaining questions 18
- 1.8 Use of Hus1 to understand the role of the Atr pathway in tissue homeostasis and tumor development 19

Chapter 2 Dual inactivation of Hus1 and p53 in the mouse mammary gland results in accumulation of damaged cells and impaired tissue regeneration 24
- 2.1 Abstract 24
- 2.2 Introduction 25
- 2.3 Materials and methods 28
- 2.4 Results 30
- 2.5 Discussion 53
- 2.6 Acknowledgements 57

Chapter 3 A partial defect in the checkpoint protein Hus1 impairs cellular transformation and tumor development 58
- 3.1 Abstract 58
- 3.2 Introduction 59
- 3.3 Materials and methods 62
- 3.4 Results 66
- 3.5 Discussion 101

Chapter 4 Effects of antioxidants on tumorigenesis and genomic instability 109
- 4.1 Introduction 109
- 4.2 Materials and methods 112
- 4.3 Results 115

4.4 Discussion 130

Chapter 5 Summary, Models, and Future Directions 139
5.1 An essential role for Hus1 in mammary gland development and tissue homeostasis 139
5.2 Reduced Hus1 levels result in impaired tumorigenesis 142
5.3 Model for the effect of reduced Hus1 levels on tumorigenesis 144
5.4 Model for roles of the Atr pathway in tumorigenesis 148
5.5 Future Directions 150

Reference 162

LIST OF FIGURES


| | | |
|---|---|---|
| Figure 1.1 | The two main DNA damage checkpoint pathways | 3 |
| Figure 1.2 | Hus1 alleles used for conditional inactivation of Hus1 and partial reduction of Hus1 expression | 21 |
| Figure 2.1 | Depletion of Hus1-deficient cells from mammary glands of conditional Hus1 knockout mice | 32 |
| Figure 2.2 | Mammary glands from conditional Hus1 knockout mice following multiple rounds of pregnancy show depletion of Hus1-deficient cells and grossly normal morphology | 35 |
| Figure 2.3 | Grossly normal mammary gland morphology in conditional Hus1 knockout mice | 37 |
| Figure 2.4 | Significantly increased apoptosis and genome damage in mammary glands from conditional Hus1 knockout mice | 40 |
| Figure 2.5 | Increased retention of Hus1-null cells in mammary glands from p53-dficient conditional Hus1 knockout mice | 42 |
| Figure 2.6 | Increased retention of Hus1-null cells in mammary glands from p53-deficient conditional Hus1 knockout mice at P18 | 44 |
| Figure 2.7 | Aberrant morphology and increased frequency of damaged and dying cells in L4 mammary glands from p53-null conditional Hus1 knockout mice | 46 |
| Figure 2.8 | Significantly reduced epithelial content in mammary glands from p53-null conditional Hus1 knockout mice | 49 |
| Figure 2.9 | Increased genome damage and apoptosis in mammary glands from p53-deficient conditional Hus1 knockout mice | 50 |
| Figure 3.1 | Cells with reduced Hus1 expression are resistant to Large-T antigen induced immortalization | 67 |
| Figure 3.2 | Three immortalized cell lines were derived separately for each genotype | 70 |

| | | |
|---|---|---|
| Figure 3.3 | Cells with reduced Hus1 expression have a decreased probability of forming foci in a contact inhibition transformation assay | 72 |
| Figure 3.4 | Cells with reduced Hus1 expression have a decreased capacity to form colonies in an anchorage independent growth transformation assay | 78 |
| Figure 3.5 | Reduced Hus1 expression caused increased puromycin resistance treatment compared to a cell line with wild-type Hus1 expression | 83 |
| Figure 3.6 | Transplantation of Hus1+ cells infected with Ras and Myc results in larger tumors than transplantation of $Hus1^{Neo/Neo}$ and $Hus1^{Neo/\Delta1}$ infected with Ras and Myc | 86 |
| Figure 3.7 | $Hus1^{Neo/Neo}$ and $Hus1^{Neo/\Delta1}$ mice develop fewer and smaller largest papillomas than $Hus1^{+}$ controls | 89 |
| Figure 3.8 | Papillomas from $Hus1^{Neo/\Delta1}$ mice and $Hus1^{Neo/\Delta1}$ cells have similar proliferation rates | 92 |
| Figure 3.9 | $Hus1^{Neo/\Delta1}$ cells do not show increased sensitivity to DMBA or TPA in culture | 95 |
| Figure 3.10 | Skin of $Hus1^{Neo/\Delta1}$ mice and $Hus1^{Neo/\Delta1}$ cells do not show increased sensitivity to DMBA or TPA | 97 |
| Figure 4.1 | Premature senescence and chromosomal aberrations of $Hus1^{Neo/\Delta1}$ cells can be rescued by antioxidant treatment, but sensitivity of $Hus^{Neo/\Delta1}$ cells to a high dose of aphidicolin cannot be rescued with antioxidant treatment | 117 |
| Figure 4.2 | The heightened level of micronucleus in $Hus^{Neo/\Delta1}$ mice is not rescued by antioxidant treatment | 124 |
| Figure 4.3 | NAC treatment cannot rescue the increased apoptosis seen in $Hus1^{\Delta1/\Delta1}$ embryos | 126 |
| Figure 4.4 | No significant difference in papilloma number or size in wild-type mice treated with NAC and no significant change in proliferation rate within papillomas | 131 |

| | | |
|---|---|---|
| Figure 5.1 | Model for interaction between Hus1 and p53 in maintenance of tissue homeostasis in the mouse mammary gland | 141 |
| Figure 5.2 | Model for reduced Hus1 expression resulting in reduced skin papilloma formation | 143 |
| Figure 5.3 | Model for the effect of reduced Hus1 on transformation | 146 |
| Figure 5.4 | Overall model for the effect of reduced function of Atr pathway on transformation and tumor development | 151 |
| Figure 5.5 | $Hus1^{+}$ MMTV-$Neu^{+}$ and $Hus1^{Neo/\Delta 1}$ MMTV-$Neu^{+}$ mice develop mammary tumors, while $Hus1^{Neo/\Delta 1}$ mice are leaner and develop uterine pathology, regardless of MMTV-Neu transgene status | 154 |
| Figure 5.6 | Intranasal instillation can be used to effectively deliver virus to mouse lungs which can be used to conditionally activate $Kras^{G12D}$ to induce tumor growth | 159 |

LIST OF TABLES


| | | |
|---|---|---|
| Table 2.1 | Genotyping results for weanlings from $Hus1^{Flox/Flox}$ X $Hus1^{+/\Delta 1}$ $Cre^{+}$ breedings | 31 |
| Table 4.1 | Summary of chromosomal aberrations of metaphase spreads of $Hus1^{+/+}$ and $Hus1^{Neo/\Delta 1}$ MEFs treated with NAA or NAC prepared at the given passage number | 118 |
| Table 4.2 | Summary of micronucleus formation over time in $Hus^{+/+}$ and $Hus1^{Neo/\Delta 1}$ mice treated with NAC | 123 |
| Table 4.3 | Summary of histological evaluation of papillomas arising from a two-step skin carcinogenesis treatment in wild-type FVB mice treated with water or NAC | 135 |
| Table 5.1 | Summary of tumor development in MMTV-$Neu^{+}$ $Hus1^{+}$ and MMTV-$Neu^{+}$ $Hus1^{Neo/\Delta 1}$ mice | 156 |

# CHAPTER 1

# LITERATURE REVIEW

The mammalian genome is constantly under assault by both internal stresses such as replication errors and metabolic byproducts, and external stresses such as environmental mutagens and chemical carcinogens, which can result in DNA damage. Despite this, genomic integrity is largely preserved due to highly conserved DNA damage checkpoint mechanisms that have evolved in response to these endogenous and exogenous threats. In a normal somatic cell, DNA damage checkpoint proteins prevent mutation accumulation by halting cell cycle progression, initiating DNA repair, or signaling programmed cell death (Cimprich and Cortez, 2008). These checkpoint pathways play critical roles in embryogenesis, development, and tissue regeneration, ensuring that undamaged cells form a functional, healthy organism.

Because of the role of DNA damage checkpoint proteins in maintaining genomic stability, it is not surprising that checkpoint dysfunction has been shown to result in increased genomic instability and cancer development. However, it has been shown more recently that transformed cells possess a high level of dependence on DNA damage checkpoint proteins in order to survive the increased cellular stress associated with rapid proliferation and transformation. Termed non-oncogene addiction, this reliance of cancer cells on DNA damage checkpoint machinery may be exploited to target cancer cells for death (Luo et al., 2009). These seemingly contradictory effects of checkpoint dysfunction which has both been shown to correlate with tumorigenesis in some instances and to result in inhibition of tumor development in others, may depend on several factors, including affected tissue type, extent of checkpoint reduction, and which specific checkpoints are affected. Understanding which alterations in checkpoint function result in increased tumor

development and which result in tumor inhibition are important for developing cancer therapies. Here, we focus on the roles of DNA damage checkpoint proteins in prevention of genomic instability, in maintenance of tissue homeostasis, and in tumor suppression.

## 1.1 The Atm and Atr pathways are the two main checkpoints that respond to DNA damage in mammalian cells.

### *1.1.1 The Atm pathway*

There are two main, evolutionarily conserved DNA damage checkpoint pathways in mammals, the ATM and ATR pathways, that are activated in response to specific forms of genetic stress (Figure 1.1). The ATM pathway primarily responds to double-stranded breaks (DSBs), such as those that arise from ionizing radiation or fork collapse (Kastan and Lim, 2000; Matsuoka et al., 2000). DSBs are initially recognized by the MRN complex, consisting of MRE11, RAD50, and NBS1, which accumulates at sites of damage and recruits additional components, such as MDC1 and ATM. ATM, a large PI3K related kinase, is subsequently activated through auto-phosphorylation. The phosphorylation of the histone variant, H2AX at these sites of damage allows for retention of this checkpoint response. The large Atm kinase then phosphorylates downstream effector proteins, such as CHK2 and p53 that signals for cell cycle arrest and/or apoptosis. A positive feedback loop forms, recruiting and activating additional checkpoint components which amplifies the checkpoint response, ensuring rapid cell cycle arrest (Kastan and Lim, 2000; Matsuoka et al., 2000). Components of the ATM pathway are non-essential, but are important for genome maintenance. Inactivating mutations in components of the ATM pathway can be tolerated during development and tissue homeostasis, but result in genomic instability and cancer predisposition in mouse models. Additionally, mutations in components of

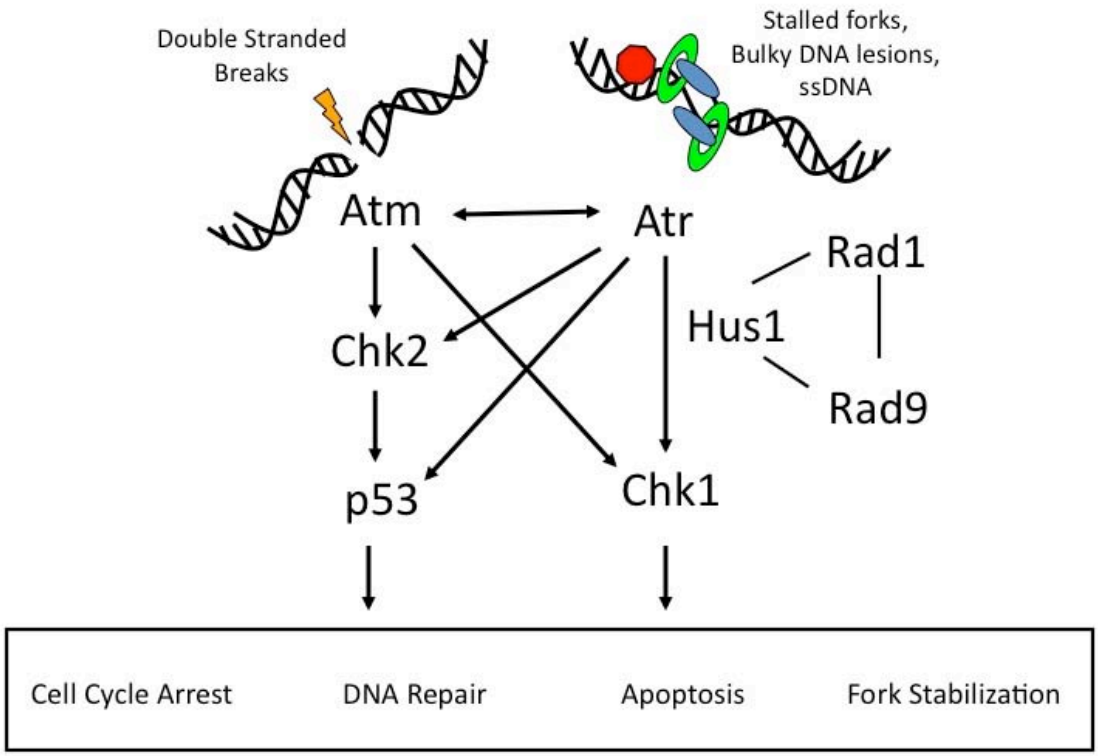


***Figure 1.1.*** **There are two main evolutionarily conserved DNA damage checkpoint pathways, Atm pathway and Atr pathway.** The Atm pathway response primarily to dsDNA lesions, and includes downstream effectors Chk2 and p53. The Atr pathway response to lesions resulting in ssDNA accumulation, and requires the Rad9-Rad1-Hus1 (9-1-1) complex for efficient phosphorylation of downstream effector Chk1. There is significant crosstalk between these pathways, and together they signal for cell cycle arrest, DNA repair, apoptosis, and fork stabilization in response to DNA damage. Inactivation of any component of the Atr pathway results in embryonic lethality.

the ATM pathway are associated with human diseases that show increased rates of cancer development (Bartek et al., 2007). For example, mutations of *Atm* results in the human disease Ataxia Talangiectasia, which also has a predisposition to lymphoma. *Atm* mutant mouse models also show an increased incidence of lymphoma (Shiloh, 2003), and mutations of several ATM pathway components are associated with an increased risk of developing breast cancer (Ahmed and Rahman, 2006). The role of this pathway in maintaining genomic integrity and in the prevention of tumor suppression has been extensively studied due to several mouse models which harbor inactivating mutations in component of this pathway (Shiloh, 2003).

### *1.1.2 The Atr pathway: mechanism*

Roles for the ATR pathway in tumor suppression have been less well characterized than those of the ATM pathway. This is in part due to the embryonic lethality which results from inactivation of any component of the ATR pathway. The ATR pathway is initiated by events resulting in the generation of single-stranded DNA (ssDNA) (Costanzo and Gautier, 2003; Zou and Elledge, 2003), such as stalled replication forks (Cha and Kleckner, 2002; Helt et al., 2005a; Jazayeri et al., 2006) or bulky DNA lesions. These lesions can be generated during S-phase of each cell cycle, triggering Atr activation (Shechter et al., 2004). ATR activation begins when RPA binds to and stabilizes ssDNA (Costanzo and Gautier, 2003; Zou and Elledge, 2003). RPA coated single stranded DNA recruits the ATR-ATRIP complex to the site of damage (Zou and Elledge, 2003). Independently, the RAD17-RFC clamp loader loads the RAD9-HUS1-RAD1 heterotrimeric clamp complex (9-1-1 complex) onto RPA coated single stranded DNA (Bermudez et al., 2003; Ellison and Stillman, 2003; Majka et al., 2006; Zou et al., 2003). The phospho-tail of RAD9 acts to recruit TOPBP1 (Roos-Mattjus et al., 2003), which activates ATR via its ATR activation

domain (AAD), allowing ATR-mediated phosphorylation of CHK1 and other targets (Delacroix et al., 2007; Kumagai et al., 2006). The extent of damage, or the amount of ssDNA generated, can modulate the level of CHK1 phosphorylation (MacDougall et al., 2007). Activated CHK1 can then phosphorylate CDC25A, a critical regulator of cell cycle progression, to prevent cell cycle progression to allow for DNA repair (Sanchez et al., 1997). The ATR pathway is essential; inactivation of any components of this pathway is not compatible with life.

### *1.1.3 Crosstalk between the Atm and Atr pathways*

Though the ATM and ATR pathways primarily are thought to respond to different types of lesions (Helt et al., 2005a) and to activate different downstream effectors, there is evidence of crosstalk between the pathways. Activation of either pathway ultimately results in the phosphorylation of p53, CHK1, or CHK2 (Helt et al., 2005a). ATR has been shown to regulate phosphorylation of p53 in damaged cells (Tibbetts et al., 1999). DNA double stranded breaks, substrates for ATM activation, have been shown to result in CHK1 phosphorylation, a component of the ATR pathway (Jazayeri et al., 2006; Shiotani and Zou, 2009). Similarly, CHK1 activation in response to stalled replication forks is strictly dependent on ATR, whereas the phosphorylation of CHK1 in response to other damage, such as IR-induced lesions, is ATM dependent (Cuadrado et al., 2006; Gatei et al., 2003). A large-scale proteomics analysis revealed that ATM and ATR share several substrates involved in DNA damage response (Matsuoka et al., 2007). Not only can the downstream targets overlap, but there is also evidence for compensation between the two pathways. For example, the loss of CHK1 in thymocytes resulted in heightened activation of CHK2 as well as activation the tumor suppressor p53, while inactivation of CHK2 results in increased activation of CHK1 (Zaugg et al., 2007).

## 1.2 HUS1 is an essential component of the Atr pathway

### *1.2.1 HUS1 structure and function*

One essential component of the ATR pathway is the 9-1-1 complex. The 9-1-1 complex, consisting of RAD9, RAD1, and HUS1, was originally identified in screens for non-essential proteins which induced cell cycle arrest in response to DNA damage (Weinert and Hartwell, 1988). These proteins are evolutionarily conserved from yeast to humans, and were later shown to form a DNA damage-responsive, doughnut-shaped complex (Volkmer and Karnitz, 1999). The 9-1-1 complex and RAD17-RFC are structural orthologs of proliferating cell nuclear antigen (PCNA) and replication factor C (RFC), respectively. RFC is a clamp loader for PCNA, a sliding clamp protein that tethers DNA polymerase to its template, (Griffith et al., 2002; Shiomi et al., 2002). Thus, a heterotrimeric PCNA-like ring structure was predicted (Venclovas and Thelen, 2000) and later confirmed (Dore et al., 2009; Sohn and Cho, 2009; Xu et al., 2009) for the functional 9-1-1 complex. PCNA and the 9-1-1 complex share some similarities, but also perform distinct functions. Both PCNA and 9-1-1 are loaded onto ssDNA. However, PCNA is loaded onto ssDNA at primer-template junctions during replication and can slide over dsDNA, whereas 9-1-1 is loaded onto ssDNA at sites of DNA damage and fork stalling, and is strongly inhibited from sliding over dsDNA (Navadgi-Patil and Burgers, 2009). PCNA moves along as a processivity factor and serves a tether for polymerases δ and ε, while 9-1-1 remains docked at sites of damage and acts as a scaffold for additional checkpoint proteins. Additionally, both PCNA and 9-1-1 may undergo similar post-translational modifications. Both can be ubiquitinated (Fu et al., 2008; Majka and Burgers, 2004) which may function to recruit other factors to the clamps, such as translesion synthesis polymerases (Kannouche et al., 2004; Watanabe et al., 2004), while only PCNA has been shown to be

SUMOylated (Stelter and Ulrich, 2003). Furthermore, both PCNA and 9-1-1 have been shown to stimulate the base excision repair pathway (Wang et al., 2006).

HUS1, one subunit of the essential 9-1-1 component, is a critical member of the ATR pathway (Weiss et al., 2002). Full-length *Hus1* cDNA is approximately 4.2-kb and encodes a 32-kDa mouse HUS1 protein. The *Hus1* gene consists of nine exons and is expressed in a variety of adult tissues and at several stages of embryonic development (Weiss et al., 1999). HUS1, together with RAD9 and RAD1, functions to promote genotoxin induced CHK1 phosphorylation (Weiss et al., 2002). Germline inactivation of *Hus1* results in mid-gestational embryonic lethality due to widespread apoptosis and defective development of essential extra-embryonic tissues (Weiss et al., 2002). HUS1 is particularly important during S phase (Weiss et al., 2003), and HUS1 loss leads to chromosomal instability during DNA replication, triggering increased apoptosis and impaired proliferation through p53-independent mechanisms (Zhu and Weiss, 2007). Therefore, it is not surprising that DNA damage-inducible genes are upregulated in HUS1-deficient embryos, and primary cells from *Hus1*-null embryos contain increased spontaneous chromosomal abnormalities. These findings suggest that loss of HUS1 leads to an accumulation of genome damage that is not compatible with life (Weiss et al., 2000). Consequently, the roles for the 9-1-1 complex in tumor suppression are not yet known.

### *1.2.2 The 9-1-1 complex may play a direct role in translesion synthesis, base excision repair, mismatch repair, and telomere maintenance*

Because of its structural homology to PCNA, which interacts with polymerase δ and ε, as well as, translesion synthesis polymerases, the 9-1-1 complex has been examined for roles as docking platform for translesion synthesis polymerases (Navadgi-Patil and Burgers, 2009). HUS1, specifically, has been shown to physically

interact with POL-K, a protein involved in translesion synthesis that is upregulated in a checkpoint activation-dependent manner (Kai and Wang, 2003). 9-1-1 clamp may physically regulate POL-ζ-dependent mutagenesis by controlling the access of POL-ζ to damaged DNA (Sabbioneda et al., 2005).

The 9-1-1 complex has been shown to directly act in DNA repair through interactions with components of BER machinery. The 9-1-1 complex interacts with and has a stimulatory effect on DNA POL-b, an essential repair polymerase for BER. This suggests that the 9-1-1 complex might attract DNA POL-β to DNA damage sites, thus directly connecting checkpoints and DNA repair (Toueille et al., 2004). The 9-1-1 complex has been shown to interact with the apurinic/apyrimidinic endonuclease 1 (APE 1), an early component of BER, and can stimulate its AP-endonuclease activity. 9-1-1 also plays a role in the final steps of BER through recruitment and stimulation of ligase I (Smirnova et al., 2005; Wang et al., 2006). Moreover, it has also been suggested that the 9-1-1 complex is a damage-specific activator of FEN1, which cleaves the remaining flap following repair (Friedrich-Heineken et al., 2005; Wang et al., 2004c). Overall, this indicates that the 9-1-1 complex is directly involved in long-patch BER (LP-BER), thus providing a possible link between DNA damage checkpoints and BER. Additionally, the 9-1-1 complex has also been shown to be a component of the mismatch repair involved in MNNG-induced damage response (Bai et al., 2010) and may directly interact with human MYH to repair misincorporated bases opposite DNA damage (Shi et al., 2006). Clearly, the 9-1-1 complex is involved in a broad range of genomic maintenance mechanisms and the extent of its functions is not yet fully understood.

The 9-1-1 complex has also been shown to play direct, evolutionarily conserved roles in telomere maintenance in yeast, worms, and mammals (Ahmed and Hodgkin, 2000; Hofmann et al., 2002; Nakamura et al., 2002). Severe telomeric

shortening has been observed in both *Hus1*-deficient mouse embryonic fibroblasts and thymocytes from conditional *Hus1*-knockout mice (Francia et al., 2006). RAD9 has also been shown to preserve telomere integrity and prevent chromosomal fusions in mouse and human cells (Pandita et al., 2006). Also, 9-1-1 is found in association with catalytically competent telomerase in cell lysates. These findings identify an unanticipated function for the 9-1-1 checkpoint complex at telomeres in mammals and provide a mechanistic link between the activity of DNA-damage-checkpoint proteins and the telomere-maintenance machinery (Francia et al., 2006).

**1.3 Defects in the Atr pathway result in genomic instability.**

Given its essential role in responding to DNA damage, it is not surprising that defects in the ATR pathway result in genomic instability, which can have a severe physiological impact. ATR knockout cells fail to proliferate, rapidly accumulate chromosomal breaks, and ultimately undergo caspase-dependent apoptosis due to loss of genomic integrity (Brown and Baltimore, 2000). Cells expressing greatly reduced levels of ATR show hypersensitivity to genotoxic stress, increased chromosomal aberrations and DNA damage, delayed checkpoint induction, and an increase in replication stress induced apoptosis (Murga et al., 2009; Ragland et al., 2009). ATR has also been shown to act at common fragile sites, areas that are difficult to replicate, to stabilize forks and prevent breaks and resulting chromosomal rearrangements (Arlt et al., 2006; Casper et al., 2002; Cha and Kleckner, 2002). Further supporting a role for the ATR pathway in chromosomal stability, depletion of CHK1, but not CHK2, in human cells results in increased chromosomal instability and breaks at common fragile sites, resulting in chromosomal fragmentation and cell death (Durkin et al., 2006).

Individual components of the 9-1-1 complex are also important for the maintenance of genomic integrity. Decrease in expression of any component of the 9-

1-1 complex results in disruption of the 9-1-1 complex as a whole, suggesting an interdependence on the stability of each component for the stability of the complex (Bao et al., 2004; Roos-Mattjus et al., 2003; Zou et al., 2002). This disrupted complex then results in defects in repairing S-phase DNA damage (Bao et al., 2004). For example, loss of RAD1 causes disintegration of the 9-1-1 complex, and disruption of sliding-clamp function causes major defects in S-phase control. A deficiency in RAD1 results in defects in sustained cell proliferation and affects the efficiency of replication recovery from DNA synthesis blockage, resulting in chromosomal abnormalities and prolonged S phase (Bao et al., 2004). Complete loss of RAD9, another component of the 9-1-1 complex, in cells also shows a marked increase in spontaneous chromosomal aberrations and HPRT mutations (Hopkins et al., 2004). Mice with $Rad9^{+/-}$ or $Rad9^{-/-}$ keratinocytes show no overt, spontaneous morphologic defects and seem similar to wild-type controls, suggesting a decreased dependence on the 9-1-1 complex of unstressed, non-proliferating cells *in vivo*. However, $Rad9^{-/-}$ keratinocytes incur more spontaneous and carcinogen-induced DNA double strand breaks than $Rad9^{+/+}$ keratinocytes (Hu et al., 2008). Likewise, complete inactivation of *Hus1* results in chromosomal instability, genotoxin hypersensitivity, and embryonic lethality (Weiss et al., 2000). MEFs with only partial *Hus1* expression exhibit spontaneous chromosomal abnormalities and undergo premature senescence due to an impaired response to oxidative genomic stress (Levitt et al., 2007). Conditional *Hus1* loss leads to chromosomal instability, particularly at fragile sites, during DNA replication. This causes increased apoptosis and impaired proliferation (Zhu and Weiss, 2007). The 9-1-1 complex has also been shown to play roles directly in DNA repair through interaction with components of base excision repair and mismatch repair (Helt et al., 2005b). Moreover, mouse ES cells that lack RAD17, the clamp loader of the 9-1-1 complex, show hypersensitivity to various DNA damaging agents (Budzowska et al.,

2004). Additionally, ATR, HUS1, and RAD9 have been shown to play roles in telomere maintenance in mice (Francia et al., 2006; McNees et al., 2010; Pandita et al., 2006), a process which is important for both tissue homeostasis and cancer prevention; ATR and RAD9 has been shown to play a critical role in human telomere maintenance as well (Pandita et al., 2006; Pennarun et al., 2010). Taken together, these results show the importance of the ATR pathway in maintaining genomic integrity in normal cellular homeostasis and replication as well as under stressed conditions.

## 1.4 The Atr pathway plays critical roles in development and tissue homeostasis.

### *1.4.1 Roles for Atr in development and tissue homeostasis*

In contrast to the ATM pathway, inactivation of any component of the ATR pathway results in embryonic lethality, suggesting the ATR pathway is essential to survive embryonic replication stress induced DNA damage (Brown and Baltimore, 2000; Budzowska et al., 2004; Han et al., 2010; Hopkins et al., 2004; Liu et al., 2000; Takai et al., 2000; Weiss et al., 2000). Conditional inactivation of components of the ATR pathway in adult mice has provided an avenue to identify roles for the ATR pathway in adult tissue homeostasis and tumor development. Mosaic *Atr* deletion in adult mice leads to defects in tissue regeneration and the rapid appearance of age-related phenotypes, such as hair graying, alopecia, kyphosis, osteoporosis, thymic involution, fibrosis, and other abnormalities due to acute cellular loss in tissues in which continuous cell proliferation is required for maintenance. This loss causes a dramatic reduction in tissue-specific stem and progenitor cell populations and exhausts tissue renewal and homeostatic capacity (Ruzankina et al., 2007), suggesting that ATR directly plays a role in stem cell maintenance.

*1.4.2 Mouse models of Seckel syndrome*

In humans, the disease Seckel syndrome can be caused by a point mutation in *Atr*, resulting in a hypomorphic allele with severely reduced, leaky expression of wild-type *Atr* (O'Driscoll et al., 2003) or by mutations in other proteins that result in reduced ATR signaling (Alderton et al., 2004; Griffith et al., 2008). Individuals homozygous for the Seckel Syndrome-1 (SCKL1) allele of *Atr* express reduced levels of ATR resulting in severe phenotypes, including intrauterine growth retardation, profound microcephaly, a 'bird-like' facial profile with receding forehead and chin, a 'beak-like' protruding nose, and mental retardation, characteristic of Seckel syndrome (O'Driscoll et al., 2003; Seckel, 1960). Because this disease has severe clinical characteristics and ultimately reduced lifespan, mouse modes of Seckel syndrome have recently been developed in order to better understand the underlying mechanism of this disease. In one model, homozygous SCKL1 mice that retain the neo cassette used for targeting a point mutation to the endogenous *Atr* allele have an estimated 66-82% reduction in total Atr protein levels due to missplicing into the neo cassette (Ragland et al., 2009). In a second model, the exons 8, 9, and 10 of mouse *Atr* sequence are exchanged for the mutated human sequence of a Seckel patients, including intergenic regions, resulting in $Atr^{s/s}$ mice. In this model, splicing is altered as is seen in human Seckel syndrome, resulting in decreased ATR expression. The $Atr^{s/s}$ mice recapitulate the phenotypes seen in Seckel syndrome, including premature aging, dwarfism, and microcephaly (Murga et al., 2009). Deletion mutations in *Atr*, *Rpa*, or *Rfc2*, which results in decreased ATR signalling, have been linked to Seckel-like diseases with similar phenotypes, including microcephaly and growth delay (O'Driscoll et al., 2007).

*1.4.3 Downstream components of the Atr pathway also play a role in development and tissue homeostasis*

Other components of the ATR pathway have been shown to be critical for tissue homeostasis. For example, CHK1 has been implicated in maintaining the balance between cell populations during differentiation in red blood cell production, and disruptions in CHK1 levels can lead to anemia in mice (Boles et al., 2010). CHK1 is also involved in hematopoietic stem cell differentiation in umbilical cord blood in humans (Carrassa et al., 2010). Combined inactivation of ATR or HUS1 with p53 results in an increased accumulation of damaged and dying cells associated with failed proliferation of surrounding cells resulting in loss of tissue homeostasis (Ruzankina et al., 2009; Yazinski et al., 2009). Additionally, clearance of chromosomal instable cells from the intestine of telomere-dysfunctional mice requires p53 (Begus-Nahrmann et al., 2009). Taken together, these results show that DNA damage checkpoint proteins play a critical role in maintaining genomic integrity throughout development. Furthermore, checkpoint proteins play a role in initiating cell death and clearance of aberrant cells in order to maintain tissue homeostasis.

## 1.5 Defects in the Atr pathway may contribute to tumorigenesis.

*1.5.1 Defects in the Atr pathway correlate with incidence of some human cancers*

Genomic instability is a classic hallmark of cancer. Since defects in Atr result in chromosomal aberrations, it is not surprising that mutations and misexpression of members of the Atr pathway have also been implicated in cancer development. Increased mutation frequencies in DNA damage response pathway genes, including Atr and Chk1, have been found to correlate significantly with advanced tumor grade (Vassileva et al., 2002). Specifically, *Atr* mutations in exon 10 have been seen in cancers with microsatellite instability, such as endometrial, stomach, and colon

cancers (Fang et al., 2004; Lewis et al., 2007; Lewis et al., 2005; Menoyo et al., 2001; Zighelboim et al., 2009). Additionally, endometrial cancers with *Atr* mutations have a poor prognosis (Zighelboim et al., 2009), while colon cancers harboring *Atr* mutations showed an improved disease-free survival compared with those with wild-type *Atr* (Lewis et al., 2007). This difference in prognosis may be due to tissue-specific differences in the requirement for ATR function. Additionally, lower levels of RAD9 are found in some prostate cancers, suggesting decreased *Rad9* expression is selected for in tumor development, and that RAD9 normally acts to prevent tumor development (Wang et al., 2004a). However, complete loss of any component of the ATR pathway has not been found in any human tumor.

### *1.5.2 Some mouse models suggest that the Atr pathway may play a role in tumor suppression*

Several mouse models and tissue culture systems were developed expressing reduced levels of components of the pathway in order to further understand the role of the ATR pathway in tumor development. $Atr^{+/-}$ mice also show a haploinsufficient tumor suppressor function on a mismatch repair deficient background, as these mice exhibit increased tumor formation and are prone to embryonic lethality (Fang et al., 2004). Upon chemical carcinogen exposure, mice with $Rad9^{-/-}$ keratinocytes develop tumors and senile skin plaques earlier and with greater severity than do $Rad9^{+/-}$ and $Rad9^{+/+}$ littermates, suggesting that RAD9 plays an important role in preventing tumor development in mice as well (Hu et al., 2008). Decreased levels of down stream effectors of the ATR pathway may also contribute to tumorigenesis. *Chk1* heterozygosity results in inappropriate S phase entry, accumulation of DNA damage during replication, and failure to restrain mitotic entry, all of which can contribute to tumorigenesis (Lam et al., 2004). Additionally, *Chk1* heterozygosity modestly

accelerates the tumorigenesis seen in *Wnt1* transgenic mice, further supporting CHK1 may act as a haploinsufficient tumor suppressor (Liu et al., 2000). Taken together, these reports suggest that components of the ATR pathway may act as tumor suppressors.

## 1.6 Defects in the Atr pathway may result in decreased tumor development due to non-oncogene addiction.

### *1.6.1 Increased expression of components of the Atr pathway in human tumors*

Since defects in DNA damage checkpoints cause genomic instability and can lead to cancer development, the checkpoint functionality of many cancers has been studied. However, contrary to expectation, many tumors show increases in checkpoint protein expression, due to aberrant methylation or gene amplification, relative to the surrounding normal tissue. The initial increase in the expression of DNA damage checkpoint proteins may be due to replication stress of neoplastic proliferation and act as a barrier to cancer formation (Bartkova et al., 2005; Gorgoulis et al., 2005); however, sustained increased expression of these genes may function as a mechanism for cancer cells to survive the increased stress of neoplastic proliferation and hyper-replication, and act to promote tumor growth. Overexpression of RAD9, for example, is seen in many human breast tumors, and this up-regulation correlates with both tumor size and local recurrence (Cheng et al., 2005). Similarly, elevated RAD9 levels are seen in some prostate cancer cells. Not only is there a strong correlation between RAD9 protein abundance and cancer stage, but also the effectiveness of small interfering RNA to lower RAD9 protein levels is correlated with reduction of tumorigenicity, indicating that RAD9 actively contributes to the disease (Zhu et al., 2008). Similarly, HUS1 expression levels in ovarian cancer correlate significantly with the clinicopathologic factors of poor prognosis (de la Torre et al., 2008).

Interestingly, a majority of tumors are deficient in the $G_1$-DNA damage checkpoint pathway while *Chk1* loss is rarely seen in human tumors (Bartek and Lukas, 2003). And in fact, CHK1 is found to be upregulated in colorectal cancers (Madoz-Gurpide et al., 2007) as well as certain types of breast cancers (Verlinden et al., 2007).

*1.6.2 Non-oncogene addiction to DNA damage checkpoint proteins in cancers*

These findings have lead to the hypothesis that transformed cells rely more heavily than normal cells on functional S and $G_2$ phase checkpoints for DNA repair and cell survival (Ashwell and Zabludoff, 2008). This phenomenon has been termed "non-oncogene addiction" since cancerous cells have higher requirements for proteins that compensate for increased cellular stress associated with neoplastic proliferation (Luo et al., 2009). Many tumors are defective in initiating $G_1$ arrest; therefore, they have an increased reliance on $S/G_2$ checkpoint pathway to maintain genomic integrity to survive. For this reason, inactivation of components of the ATR pathway, which responds primarily in signaling for cell cycle arrest and DNA repair $S/G_2$, results in increased tumor cell death, due to loss of genomic integrity, while surrounding normal cells, which retain an intact $G_1$ checkpoint, are able to survive this decreased levels of Atr signaling (Luo et al., 2001).

Further supporting a requirement for DNA damage checkpoint proteins in transformation and tumor growth is that inactivating mutations in any component of the Atr pathway have not yet been found in human tumors. Furthermore, conditional inactivation, partial inactivation, or mouse models heterozygous for any components of the Atr pathway alone does not result in spontaneous tumorigenesis (Greenow et al., 2009; Lam et al., 2004; Murga et al., 2009; Ruzankina et al., 2007; Ruzankina et al., 2009) (Han et al., 2010; Hu et al., 2008; Levitt et al., 2007; Yazinski et al., 2009).

*1.6.3 Inactivation of components of the Atr pathway sensitizes tumor cells to chemotherapeutics and induces cell death*

Supporting this idea, tumor-initiating cells of mammary tumors in mice show upregulation of several DNA damage response and repair proteins, including HUS1, suggesting these proteins are essential for the transformation process (Zhang et al., 2008). Down regulation of HUS1 enhances the sensitivity of human lung carcinoma cells to cisplatin (Kinzel et al., 2002) and loss of HUS1 or ATR in combination with loss of p53, a potent tumor suppressor, results in cell death, not tumorigenesis (Chapter 2) (Ruzankina et al., 2009; Yazinski et al., 2009). p53 deficient cancer cells can be sensitized to chemotherapeutics by CHK1 inhibitors (Chen et al., 2006), and knockdown of either ATR or CHK1 in mismatch repair defective colorectal cancer cells results in increased sensitivity to chemotherapeutics (Jardim et al., 2009). Since CHK1 is the major effecter of the S and $G_2$ checkpoints cascades, the inhibition of CHK1 signaling impairs DNA repair and increases tumor cell death, either through induction of apoptosis mediated by p53 signaling or through p53-independent signaling, such as through activation of caspase-2 (Sidi et al., 2008). CHK1 inhibition in tissue with a functional $G_1$ checkpoint, however, allows for DNA repair and cell survival (Ashwell and Zabludoff, 2008). Additionally, CHK1 is essential for tumor cell viability following activation of the replication checkpoint (Cho et al., 2005).

Additionally, checkpoint kinase inhibitors enhance the efficacy of several of the most commonly used chemotherapeutic compounds and radiotherapy, which act by damaging the genome of rapidly proliferating cells, impeding the progression of the cell cycle and preventing further proliferation, and reducing long-term cancer cell survival (Wilsker and Bunz, 2007). For example, significant cytotoxicity is observed in cancer cells when RAD9 expression is downregulated, probably due to the effects of inhibited CHK1 phosphorylation and the impairment of the ATR checkpoint

pathway (Yuki et al., 2008). Furthermore, cell lines deficient in the Fanconi Anemia (FA) DNA repair pathway are hypersensitive to CHK1 inhibition by siRNA or pharmacological agents which results in increased accumulation of DNA strand and chromosomal breakages (Chen et al., 2009). Taken together, these results suggest that the ATR pathway plays an essential role in maintaining cancer cell viability and can be exploited to sensitize cancer cells when abrogation of CHK1 or other pathway components is combined with DNA anti-metabolite chemotherapeutic drugs. Already, CHK1 inhibitors are being used in combination with common anticancer chemotherapies (Chen et al., 2006; Merry et al., 2010). This decreased level of CHK1 presumably drives cancer cells toward death due to increased fork stalling and DNA damage from chemotherapeutics, as cancer cells cannot recover from these insults without sufficient CHK1 levels.

### 1.7 Summary and remaining questions

In certain tissue types, reduced function of the ATR pathway may result in increased tumorigenesis on a tumor promoting background; however, impairment of the ATR pathway alone does not appear to induce tumorigenesis. Instead, decreased ATR function has been shown to inhibit transformation and tumor cell survival. In several cases, tumor cells display non-oncogene addiction to DNA damage checkpoints, and overexpression of these checkpoints actually enhances the growth and survival of tumor cells. Furthermore, there is evidence that inhibitors of checkpoint proteins in the ATR pathway may be effective in treatment of certain cancers that have a high dependence on DNA damage checkpoint function. In this case, an impairment of the ATR pathway results in cell death during the process of transformation.

Many questions still remain about the effect of reduced DNA damage checkpoint function on tumor development. It is not clear whether checkpoint inhibition has discrete effects on different cell types. In one cell type, defects in ATR signaling may promote tumor development, while in another cell type, the same defect may prevent transformation and tumor development. This difference may be related to the level of dependence of the tissue type on the ATR pathway in tissue homeostasis and cell maintenance. Also, the effect of the level of inhibition must be more clearly understood. Reduction of checkpoint function to half the wild-type level may promote tumorigenesis, while reduction to less than half may prevent transformation and tumor growth. Additionally, the consequences of inactivation of components of the ATR pathway on tissue homeostasis and other critical processes, such as meiosis, must be further examined to understand the effect of inhibitors, which are used to treat cancers, on the organism as a whole.

## 1.8 Use of HUS1 to understand the role of the Atr pathway in tissue homeostasis and tumor development

### *1.8.1 Conditional inactivation of Hus1 can be used to determine roles of Hus1 in adult tissue.*

In order to study the physiological functions of the ATR checkpoint pathway in tumor suppression and tissue homeostasis while bypassing the embryonic lethality of conventional knockout models, we previously developed a conditional loxP-flanked *Hus1* allele ($Hus1^{Flox}$) (Figure 1.2 A) (Levitt et al., 2005). $Hus1^{Flox}$ is a fully functional allele that expresses wild-type HUS1, but is converted to the null allele $Hus1^{\Delta 2,3}$ upon Cre-mediated recombination. $Hus1^{Flox/Flox}$ mice are bred to $Hus1^{+/\Delta 1}$ $Cre^{+}$ mice, which have one wild type ($Hus1^{+}$) and one *Hus1*-null allele ($Hus1^{\Delta 1}$), to generate control $Hus1^{Flox/\Delta 1}$ $Cre^{-}$ and $Hus1^{+/Flox}$ $Cre^{+}$ mice and experimental $Hus1^{Flox/\Delta 1}$ $Cre^{+}$ mice.

Hus1$^{+/Flox}$ Cre$^{+}$ mice serve as a reporter of the maximum amount of *Hus1* deletion achieved following Cre-mediated recombination, as these mice retain one wild-type *Hus1* allele, preventing selection against cells that have undergone recombination. However, these mice heterozygous for *Hus1*, and may have some heightened level of genomic instability. Experimental Hus1$^{Flox/\Delta 1}$ Cre$^{+}$ mice have no functional HUS1 expression in cells which have undergone recombination. Cre-recombinase can be expressed from a variety of tissue and developmentally specific promoters (Akagi et al., 1997) allowing for tissue specific inactivation of HUS1 in adult tissue.

*1.8.2 The Hus1 allelic series is an important tool used to study the roles of Hus1 and the Atr pathway.*

As previously mentioned, germline deletion of *Hus1* results in embryonic lethality. In order to bypass the severe effects of complete *Hus1* deletion, the Weiss Lab developed a *Hus1* allelic series in which expresses incrementally reduced levels of HUS1, while bypassing the embryonic lethality associated with complete germline inactivation of *Hus1* (Figure 1.2 A and B). The allelic series is created by combining a wild-type *Hus1*$^{+}$ allele, a *Hus1*$^{Neo}$ allele, which expresses reduced levels of HUS1 due to misplicing and exon skipping, or a null *Hus1*$^{\Delta 1}$ allele. Mice with the lowest level of HUS1, Hus1$^{Neo/\Delta 1}$, are grossly normal and are not prone to spontaneous tumor development; however, Hus1$^{Neo/\Delta 1}$ mice exhibit sensitivity to certain genotoxins, such as mitomycin C, and have increased genomic instability as measured by elevated micronucleus levels in erythrocytes. Primary Hus1$^{Neo/\Delta 1}$ embryonic fibroblasts exhibit spontaneous chromosomal abnormalities, undergo premature senescence associated with increase in oxidative stress, and show hypersensitivity to DNA damaging agents and replication inhibitors, such as 4NQO and aphidicolin. Together, these findings define a critical role for HUS1 in response to genome damage and replication stress.

***Figure 1.2*. Alleles used to construct the conditional Hus1 knockout and Hus1 allelic series, which expresses incremental reduced levels of Hus1. (**A) Alleles which make up conditional Hus1 knockout system and Hus1 allelic series. Notably, $Hus1^{Neo}$, an intermediate product in constructing the conditional $Hus1^{Flox}$ allele, has only partial Hus1 activity. (B) Northern blot demonstrating the incrementally reduced level of Hus1 in the Hus1 allelic series {Levitt, 2007 #199}. $Hus1^{+}$, $Hus1^{Neo}$, and $Hus1^{\Delta 1}$ alleles are combined to create the Hus1 allelic series, which ranges from $Hus1^{+/+}$, with wild-type levels of Hus1 expression, to $Hus1^{Neo/\Delta 1}$ which expresses the lowest level of Hus1.

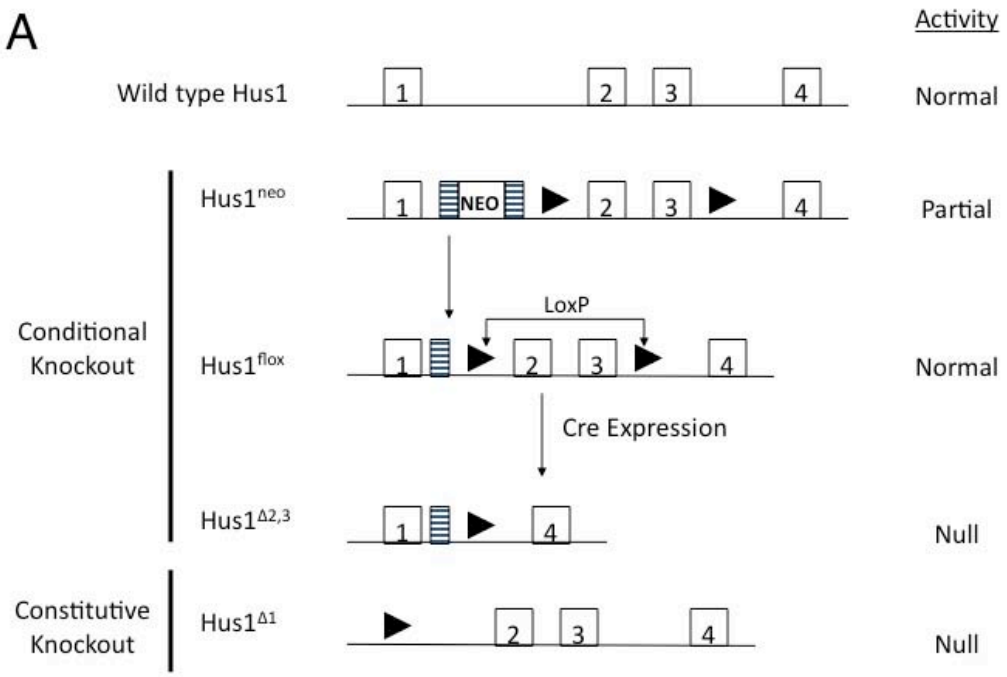


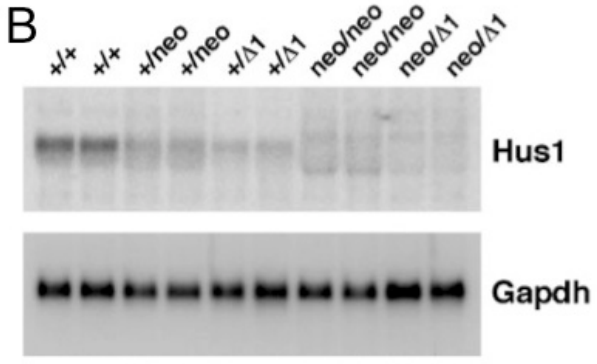


Levitt, PS., *et al.* MCB 27(6):2189-201, 2007.

Importantly, the *Hus1* allelic series provides an ideal tool to test the effect of reduced HUS1 on transformation and tumorigenesis (Levitt et al., 2007).

In the work presented here, I have made use of both the conditional allele of *Hus1* and the *Hus1* hypomorphic allele to study the role of HUS1 in tumorigenesis, and its response to antioxidant treatments. First, I have determined the effect of complete *Hus1* inactivation on tumorigenesis using the mouse mammary gland as a model. Secondly, I have made use of the *Hus1* allelic series in order to determine how reductions in HUS1 expression affect transformation ability, in both cell culture and *in vivo* using a two-step carcinogenesis scheme. Finally, I have determined the effect of antioxidant treatment in rescuing the severe phenotypes seen in cells expressing reduced levels of HUS1, as well as *Hus1*-null embryos. This body of work identifies HUS1 as key DNA damage and cellular stress response protein and a potential target for sensitizing cancer cells to chemotherapeutic treatment.

CHAPTER 2

# DUAL INACTIVATION OF HUS1 AND P53 IN THE MOUSE MAMMARY GLAND RESULTS IN ACCUMULATION OF DAMAGED CELLS AND IMPAIRED TISSUE REGENERATION[1]

## 2.1 ABSTRACT

In response to DNA damage, checkpoint proteins halt cell cycle progression and promote repair or apoptosis, thereby preventing mutation accumulation and suppressing tumor development. The DNA damage checkpoint protein HUS1 associates with RAD9 and RAD1 to form the 9-1-1 complex, which localizes to DNA lesions and promotes DNA damage signaling and repair. Because complete inactivation of mouse *Hus1* results in embryonic lethality, we developed a system for regulated *Hus1* inactivation in the mammary gland in order to examine roles for HUS1 in tissue homeostasis and tumor suppression. *Hus1* inactivation in the mammary epithelium resulted in genome damage that induced apoptosis and led to depletion of HUS1-null cells from the mammary gland. Conditional *Hus1* knockout females retained grossly normal mammary gland morphology, suggesting compensation by cells that failed to undergo Cre-mediated *Hus1* deletion. p53-deficiency delayed the clearance of *Hus1*-null cells from conditional *Hus1* knockout mice and caused the accumulation of damaged, dying cells in the mammary gland. Notably, compensatory responses were impaired following combined HUS1 and p53 loss, resulting in aberrant mammary gland morphology and lactation defects. Overall, these results establish an

[1] The data in this chapter has been published: Yazinski, S.A., Westcott, P.M., Ong, K., Pinkas, J., Peters, R.M., and Weiss, R.S. (2009). Dual inactivation of *Hus1* and *p53* in the mouse mammary gland results in accumulation of damage cells and impaired tissue regeneration. Proc Natl Acad Sci U S A *106*, 21282-21287

essential role for HUS1 in the survival and proliferation of mammary epithelium and identify a novel role for p53 in mammary gland tissue regeneration and homeostasis.

## 2.2 INTRODUCTION

DNA is constantly subjected to intrinsic and extrinsic genotoxins that may lead to mutations in growth regulatory genes, resulting in cancer formation (Hoeijmakers, 2001). To prevent mutation accumulation, evolutionarily conserved DNA damage checkpoint pathways survey the genome and respond to DNA lesions by halting the cell cycle, stabilizing replication forks, and inducing repair. In cases of extensive or unrepairable damage, checkpoints instead trigger apoptosis, which eliminates defective cells that are at risk for malignant transformation and stimulates regenerative proliferation that ensures tissue homeostasis.

Two primary checkpoint pathways, the ATM and ATR pathways, function in parallel to respond to DNA damage in mammals (Bartek and Lukas, 2007). The ATM pathway, which includes ATM, CHK2, p53, and additional components, responds to double-stranded DNA breaks (DSBs). Inactivating mutations in genes of the ATM pathway cause increased risk for a variety of malignancies, including breast cancers (Walsh and King, 2007). Notably, over half of all solid human tumors are estimated to have *p53* mutations (Soussi, 2007). In addition to its well-established functions in apoptosis induction, cell cycle control, and safeguarding of genome stability, p53 also plays a complex and incompletely understood role in tissue homeostasis. In some settings, p53 appears to impede regenerative processes (Maier et al., 2004; Rodier et al., 2007; Tyner et al., 2002), while in others it facilitates tissue renewal and recovery from cell loss (Matheu et al., 2007; Valentin-Vega et al., 2008; Wells et al., 2006).

The ATR pathway, which includes ATR, CHK1, and the RAD9-RAD1-HUS1 (9-1-1) complex, responds to stalled replication forks and a broad array of DNA

lesions (Bartek and Lukas, 2007). Because the ATR pathway is essential for embryonic development in mammals, many of its physiological roles have not been fully characterized. Although CHK1 activation is known to occur in response to oncogenic signals (Bartek et al., 2007), there is limited direct evidence indicating that ATR pathway defects are strongly tumor predisposing. Monoallelic *Atr* and *Chk1* mutations, as well as misexpression of *Chk1* and 9-1-1 complex components, have been reported in human cancers (Bertoni et al., 1999; Menoyo et al., 2001; Vassileva et al., 2002). In mouse models, *Atr* heterozygosity causes a slight increase in tumor incidence (Brown and Baltimore, 2000). *Chk1* haploinsufficiency is associated with defects suggestive of cell transformation in the mammary gland (Lam et al., 2004) and modestly accelerates mammary tumorigenesis in *Wnt-1* transgenic mice (Liu et al., 2000). These data suggest a possible role for the ATR pathway in tumor suppression; however, heterozygosity for these genes in mice results in relatively mild phenotypes.

As a member of the 9-1-1 complex, HUS1 shows predicted structural homology to proliferating cell nuclear antigen (Parrilla-Castellar et al., 2004), the sliding clamp that serves as a processivity factor during DNA replication. 9-1-1 is loaded onto DNA in response to damage and functions as a scaffold that facilitates the formation of checkpoint signaling complexes, leading to efficient phosphorylation and activation of downstream effectors in response to DNA damage. Notably, 9-1-1 promotes the ATR-dependent phosphorylation of CHK1 through the recruitment of the checkpoint mediator TOPBP1, which stimulates ATR kinase activity (Burrows and Elledge, 2008). Targeted deletion of *Hus1* (Weiss et al., 2000) or *Rad9* (Hopkins et al., 2004) results in severe genomic instability, profound hypersensitivity to genotoxic stress, and mid-gestational embryonic lethality.

In order to study the physiological functions of the ATR checkpoint pathway in tumor suppression and tissue homeostasis while bypassing the embryonic lethality

of conventional knockout models, we previously developed a conditional loxP-flanked *Hus1* allele ($Hus1^{Flox}$) (Levitt et al., 2005). $Hus1^{Flox}$ is a fully functional allele that expresses wild-type HUS1, but is converted to the null allele $Hus1^{\Delta 2,3}$ upon Cre-mediated recombination. In this study, we generated conditional *Hus1* knockout mice that express Cre from the beta-lactoglobulin (Blg) promoter in order to inactivate *Hus1* selectively in the mammary glands of pregnant and lactating mice (Selbert et al., 1998). The mammary gland was targeted because this tissue expresses HUS1 (Weiss et al., 1999), has a well-characterized developmental pattern (Silberstein, 2001), and is susceptible to tumor development due to defects in DNA damage response factors (Walsh and King, 2007). Complete *Hus1* inactivation was not associated with increased mammary tumor predisposition; instead HUS1 was found to be essential for genome maintenance and cell survival in mammary epithelium. Unexpectedly, *p53* loss exacerbated the deleterious effects of *Hus1* inactivation and impaired a compensatory response that in p53-proficient animals promoted tissue regeneration by cells that failed to delete *Hus1*. These data identify a novel role for p53 in tissue homeostasis in the mammary gland and additionally suggest that inhibition of ATR signaling may be an effective tool for the treatment of p53-deficient cancers.

## 2.3 MATERIALS AND METHODS

*Mice.* Previously described $Hus1^{Flox}$ (Levitt et al., 2005) and $Hus1^{\Delta 1}$ (Weiss et al., 2000) mice were maintained on a 129S6 inbred genetic background. $p53^{+/-}$ mice with the *Trp53*$^{tm1Tyj}$ allele were maintained on a C57BL/6J background (Jacks et al., 1994). Blg-Cre mice were maintained on a mixed background (Selbert et al., 1998). $Hus1^{Flox/Flox}$ mice were bred to Blg-Cre transgenic ($Cre^{+}$) mice that also were heterozygous for the null *Hus1*$^{\Delta 1}$ allele to produce $Hus1^{Flox/\Delta 1}$ $Cre^{+}$ conditional *Hus1* knockout mice, as well as $Hus1^{+/Flox}$ $Cre^{+}$ and $Hus1^{Flox/\Delta 1}$ $Cre^{-}$ control animals. All animals were genotyped by PCR analysis of DNA extracted from tail tip biopsies. Mice were housed in accordance with institutional animal care and use guidelines.

*Southern blot.* Genomic DNA for Southern blotting was isolated from fourth mammary gland or spleen tissue using Proteinase K digestion and ethanol precipitation. DNA was digested with *Nhe*I, run through a 0.8% agarose gel, transferred to a nylon membrane, and hybridized with a $^{32}$P-labeled 190-base pair *Eag*I fragment from plasmid pCR2.1-5'UTR-Δ2,3, as previously described (Levitt et al., 2005). The extent of deletion of the conditional *Hus1* allele was quantified using a PhosphorImager (GE Healthcare, Piscataway, NJ, USA). Statistical analysis was by one-way ANOVA.

*Whole mounts and histology.* Conditional *Hus1* knockout mice ($Hus1^{Flox/\Delta 1}$ $Cre^{+}$) or control mice ($Hus1^{+/Flox}$ $Cre^{+}$ or $Hus1^{Flox/\Delta 1}$ $Cre^{-}$), either on $p53^{+/+}$ or $p53^{-/-}$ backgrounds, were mated with wild-type males overnight, and checked for copulatory plugs the following morning. The fourth mammary glands were harvested on 18$^{th}$ day of pregnancy (P18), or the second (L2) or fourth (L4) day of lactation. For whole mount analysis, the fourth mammary gland was harvested, fixed in Carnoy's solution

for 6 hours, stained overnight in Carmine Alum solution at 4°C, dehydrated, and stored in xylenes. For histological analyses, the fourth mammary gland was fixed in 10% neutral-buffered formalin overnight, dehydrated, embedded in paraffin, and sectioned at 5-8 μm. Sections were deparaffinized in xylenes, rehydrated, and stained with Hematoxylin and Eosin or subjected to immunohistochemical analysis. The relative area of each mammary gland occupied by epithelial or adipose tissue was measured using ImageJ (National Institutes of Health) and Canvas 8 (ACD Systems) software applications.

*Ki67 and γ-H2AX immunohistochemistry.* Mammary gland sections from at least three females of each genotype were stained for the presence of Ki67 antigen or γ-H2AX. Heat-mediated antigen retrieval was performed in 0.01M citrate buffer (for Ki67) or 25mM EDTA (for γ-H2AX) for 50 minutes. Sections were incubated with anti-Ki67 Clone MM1 (Vector Laboratories) or anti-γ-H2AX (Upstate Biotechnology) antibodies followed by biotinylated polyclonal rabbit anti-mouse (DAKO). Approximately 500 cells in at least two fields of vision at 40X magnification were counted per slide. Statistical analysis was by two-tailed Student's t-test.

*TUNEL staining*. Mammary gland sections from three different female mice for each genotype were prepared and analyzed using the ApopTag® peroxidase *In Situ* Apoptosis Detection Kit (Millipore) according to the manufacturer's directions. Approximately 500 cells in at least two fields of vision at 40X magnification were counted per slide. Statistical analysis was by two-tailed Student's t-test.

## 2.4 RESULTS

**2.4.1 Depletion of *Hus1*-null cells from the mouse mammary gland following conditional *Hus1* inactivation.** The conditional allele $Hus1^{Flox}$ (Levitt et al., 2005) was used in combination with Blg-Cre transgenic mice (Selbert et al., 1998) to produce mice in which *Hus1* was deleted selectively in mammary epithelium. $Hus1^{Flox/\Delta1}$ $Cre^{+}$ conditional *Hus1* knockout mice contained the conditional allele and one copy of the null allele $Hus1^{\Delta1}$ such that Cre-mediated recombination in the mammary gland upon pregnancy would generate *Hus1*-deficient cells. Control $Hus1^{+/Flox}$ $Cre^{+}$ mice served as an indicator of the maximum possible *Hus1* deletion in the absence of selection against *Hus1* loss, as the mammary glands of these mice retain one wild-type *Hus1* copy following recombination. $Hus1^{+/+}$ and $Hus1^{Flox/Flox}$ $Cre^{-}$ mice express wild-type levels of HUS1 and were used to establish baseline values in all assays.

Conditional *Hus1* knockout and control mice were born at expected frequencies and appeared grossly normal (Table 2.1). To determine the extent of Cre-mediated *Hus1* inactivation, we performed Southern blotting on DNA extracted from mammary glands from mice as virgins, at the eighteenth day of pregnancy (P18), or at the second day of lactation (L2) using a probe that can distinguish the unrecombined $Hus1^{Flox}$, wild-type $Hus1^{+}$, and inactivated $Hus1^{\Delta2,3}$ alleles (Figure 2.1 A and B). No *Hus1* deletion was seen in the $Cre^{-}$ control animals as expected, and only limited deletion was seen in virgin $Cre^{+}$ control mice, likely due to basal Blg promoter activity as reported previously (Selbert et al., 1998). Blg-Cre expression increases during pregnancy and lactation, and accordingly, control $Hus1^{+/Flox}$ $Cre^{+}$ mammary glands showed an average of 43% *Hus1* deletion at P18 and 50% at L2. Notably, the extent of $Hus1^{Flox}$ deletion was substantially reduced in $Hus1^{Flox/\Delta1}$ $Cre^{+}$ mice relative to $Hus1^{+/Flox}$ $Cre^{+}$ mice at every developmental stage. $Hus1^{Flox/\Delta1}$ $Cre^{+}$ mammary glands

Table 2.1. Genotyping results for weanlings from $Hus1^{Flox/Flox}$ X $Hus1^{+/\Delta 1}$ $Cre^{+}$ breedings[a]

| Genotype | Expected | Observed |
|---|---|---|
| **$Hus1^{+/Flox}$ $Cre^{-}$** | 104 (25%) | 98 (26.2%) |
| **$Hus1^{+/Flox}$ $Cre^{+}$** | 104 (25%) | 115 (22.6%) |
| **$Hus1^{Flox/\Delta 1}$ $Cre^{-}$** | 104 (25%) | 94 (27.6%) |
| **$Hus1^{Flox/\Delta 1}$ $Cre^{+}$** | 104 (25%) | 109 (23.6%) |

[a] Genomic DNA was isolated from tail biopsies from weanlings and then genotyped by PCR as described in Materials and Methods. *[Table by P.Westcott]*

***Figure 2.1*. Depletion of Hus1-deficient cells from mammary glands of conditional Hus1 knockout mice.** (***A***) DNA was isolated from mammary glands of virgin mice, mice at the 18$^{th}$ day of pregnancy (P18) or mice at the second day of lactation (L2), and analyzed by Southern blotting. The position of the bands for Hus1$^{Flox}$, wild-type Hus1, and the recombined inactivated Hus1 allele, Hus1$^{\Delta 2,3}$, are indicated. The Hus1$^{\Delta 1}$ allele is not detected in this assay. Because there is variation in gel mobility between samples, the position of the band for wild-type Hus1 is additionally marked with a "<" symbol. "% deletion" refers to the extent of Cre-mediated conversion of Hus1$^{Flox}$ to Hus1$^{\Delta 2,3}$, as determined by quantification of Southern blot signal by PhosphorImager. (***B***) Bar graph shows the average percentage of Hus1 deletion at each developmental stage for mice of the indicated genotypes. Values are means derived from the Southern blots in Fig. 1*A* and S1*A*, with error bars denoting standard deviation. Hus1 deletion was significantly lower in Hus1$^{Flox/\Delta 1}$ Cre$^{+}$ mice relative to Hus1$^{+/Flox}$ Cre$^{+}$ controls at all stages except in virgins (virgin, $p=0.856$; P18, $p<0.001$; L2, $p<0.001$; Multiparous, $p<0.001$) as determined by one-way ANOVA. (***C***) Representative images of whole mount preparations and histological sections of mammary glands from conditional Hus1 knockout and control females are shown. Scale bar represents 400μm. *[Southern blot (A) by R.S. Weiss; Bar graph and whole mounts by S.A. Yazinski]*

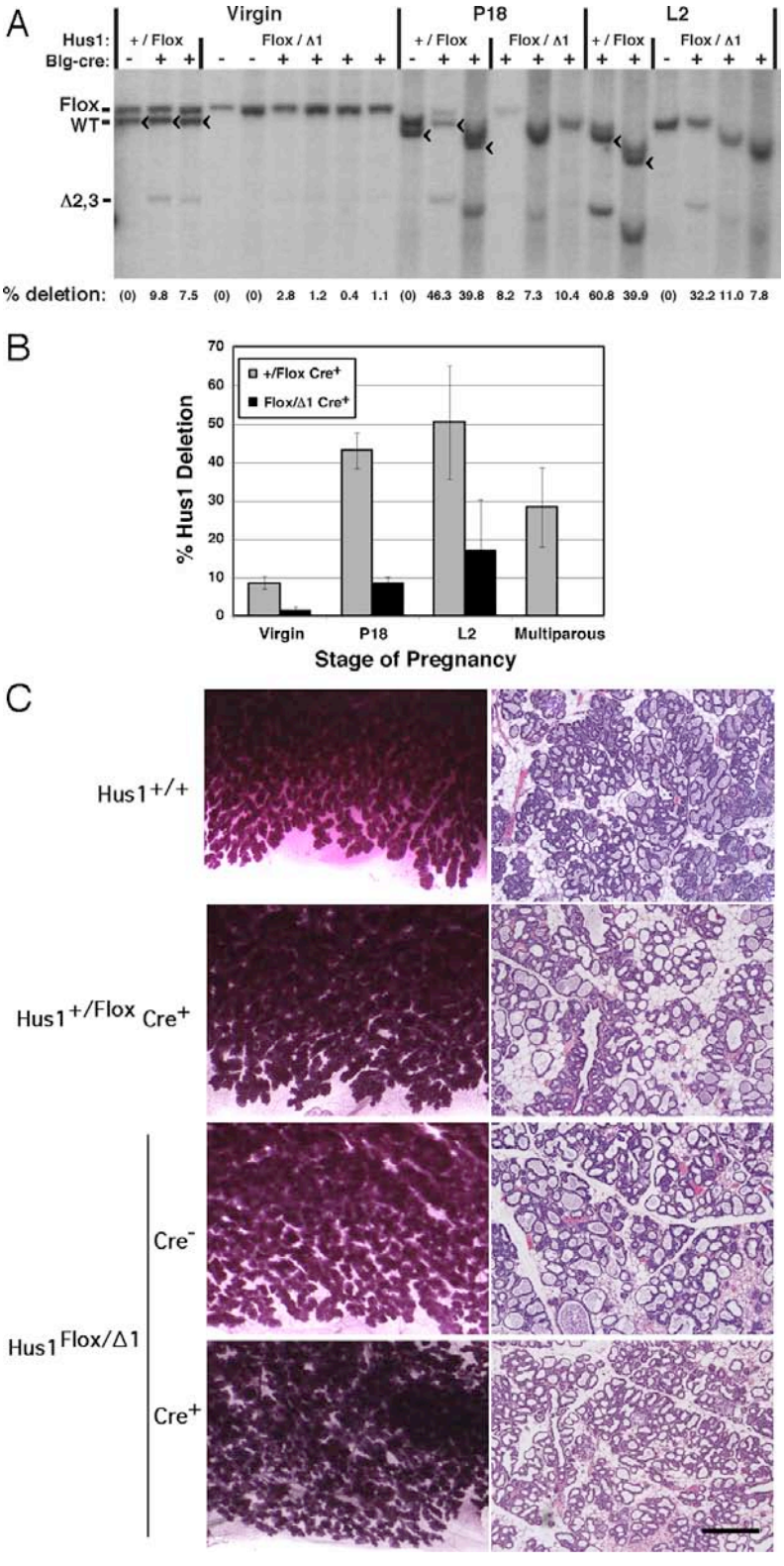
A
Virgin
P18
L2
Hus1:
Big-cre:
+ / Flox
Flox / Δ1
Flox
WT
Δ2,3
% deletion: (0) 9.8 7.5 (0) (0) 2.8 1.2 0.4 1.1 (0) 46.3 39.8 8.2 7.3 10.4 60.8 39.9 (0) 32.2 11.0 7.8
B
+/Flox Cre+
Flox/Δ1 Cre+
% Hus1 Deletion
Virgin
P18
L2
Multiparous
Stage of Pregnancy
C
Hus1+/+
Hus1+/Flox Cre+
Hus1Flox/Δ1
Cre-
Cre+

showed an average of 1.4% (virgin), 9% (P18), and 17% (L2) *Hus1* deletion. Relative to Hus1$^{+/Flox}$ Cre$^{+}$ controls, these values represent decreases in *Hus1* deletion of 84%, 80%, and 66% in virgin, P18, and L2 mice, respectively. These data suggest that *Hus1* loss puts cells at a selective disadvantage and results in their depletion from the mammary gland.

To determine whether *Hus1*-deficient cells would accumulate in the mammary glands of multiparous females, we continuously bred conditional *Hus1* knockout females to wild-type males. On average, Hus1$^{+/Flox}$ Cre$^{+}$ females gave birth to 10 litters, while Hus1$^{Flox/\Delta1}$ Cre$^{-}$ and Hus1$^{Flox/\Delta1}$ Cre$^{+}$ females gave birth to 11 litters. Mammary glands were harvested from these females several months after they gave birth to their final litter, and DNA was isolated and analyzed by Southern blot for *Hus1* deletion (Figure 2.1 B and Figure 2.2). Strikingly, there was a complete absence of *Hus1*-deficient cells in Hus1$^{Flox/\Delta1}$ Cre$^{+}$ multiparous mammary glands. By contrast, an average of 28% *Hus1* deletion was observed in Hus1$^{+/Flox}$ Cre$^{+}$ multiparous mammary glands; this *Hus1* deletion level is lower than that seen in control females at L2 of their first pregnancy because of reduced epithelial cell content following involution. Together, these data indicate that *Hus1*-deficient cells are selected against and, following multiple pregnancies, completely eliminated from mammary glands of conditional *Hus1* knockout mice.

**2.4.2 Grossly normal mammary gland morphology following Cre-mediated *Hus1* inactivation.** To determine the effects of *Hus1* deletion on mammary gland development and morphology, we performed histopathological analysis of mammary glands from conditional *Hus1* knockout and control mice at P18 (Figure 2.3), L2 (Figure 2.1 C), or following multiple rounds of pregnancy (Figure 2.2 B). Whole mounts and histological sections of Hus1$^{Flox/\Delta1}$ Cre$^{+}$ mammary glands were similar to

***Figure 2.2*. Mammary glands from conditional Hus1 knockout mice following multiple rounds of pregnancy show depletion of Hus1-deficient cells and grossly normal morphology.** (***A***) DNA was extracted from mammary glands of mice of multiparous mice, and probed by Southern blot using a Hus1-specific probe. Southern blot analysis of spleen DNA was included to confirm mammary gland-specific Cre expression. (***B***) Hus1-deficient cells are not detectable in mammary tumors from multiparous conditional Hus1 knockout mice. DNA was isolated from mammary gland tumors from conditional Hus1 knockout and control multiparous females and probed by Southern blot using a Hus1-specific probe. The position of the bands for $Hus1^{Flox}$ (**<**), wild-type Hus1, and the recombined inactivated Hus1 allele, $Hus1^{\Delta 2,3}$, are indicated. (***C***) Representative images of histological sections of involuted mammary glands from multiparous conditional Hus1 knockout and control females are shown. At approximately five months following the weaning of the final litter, the fourth mammary glands from females of the indicated genotypes were harvested, fixed, embedded, sectioned, and stained with H&E. Scale bar represents 400μm. (***D***) Representative images of mammary tumors from multiparous females of the indicated genotypes were taken at low (left) or high (right) magnification. Scale bars represent 500μm and 100μm, respectively. The tumor incidence in multiparous conditional Hus1 knockout (2 of 22) and control (1 of 16) females was not significantly different (p=1.000; Chi-square test). Tumor incidence values also were not significantly different when including a third multiparous $Hus1^{Flox/\Delta 1}$ $Cre^{+}$ female with a palpable mammary mass that subsequently regressed (p=0.624; Chi-square test). *[Multiparious Southern blot by R.S. Weiss; tumor Southern blot, multiparous histology, tumor histology by S.A. Yazinski]*

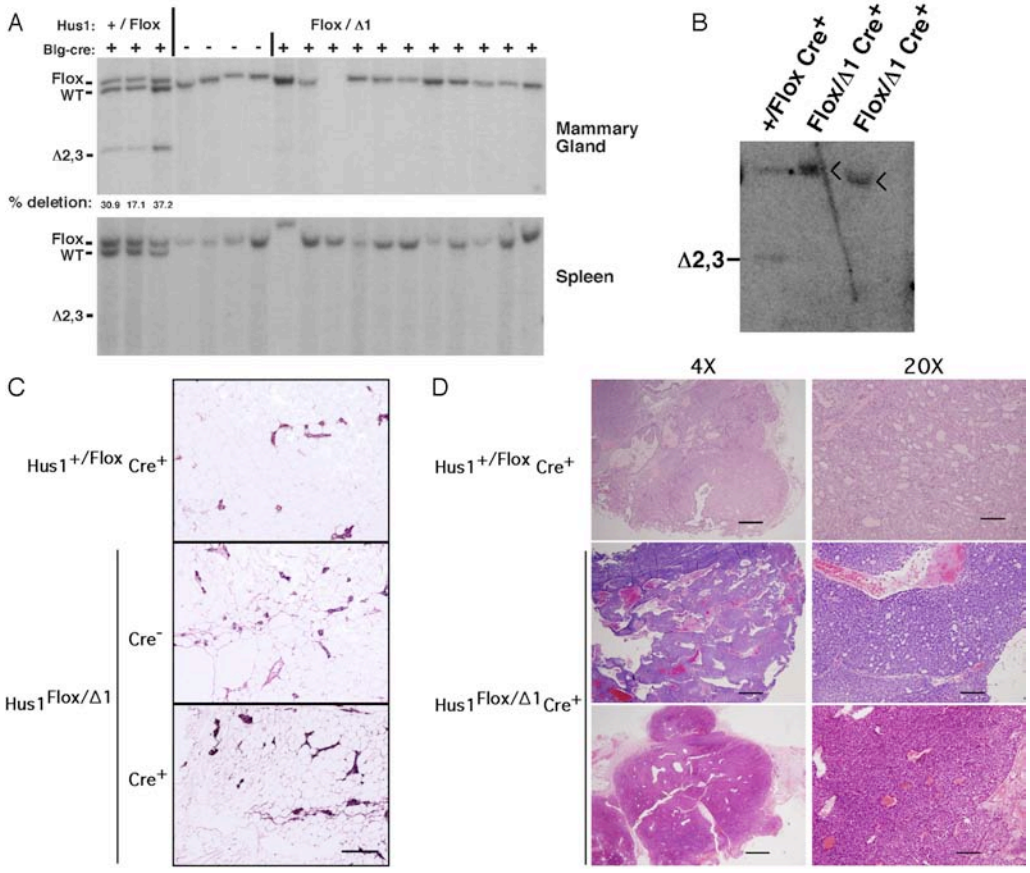
A
Hus1: + / Flox
Flox / Δ1
Big-cre: + + + - - - - + + + + + + + + + +
Flox
WT
Δ2,3
Mammary Gland
% deletion: 30.9 17.1 37.2
Flox
WT
Δ2,3
Spleen
B
+/Flox Cre+
Flox/Δ1 Cre+
Flox/Δ1 Cre+
Δ2,3
C
Hus1+/Flox Cre+
Hus1Flox/Δ1
Cre-
Cre+
D
4X
20X
Hus1+/Flox Cre+
Hus1Flox/Δ1 Cre+

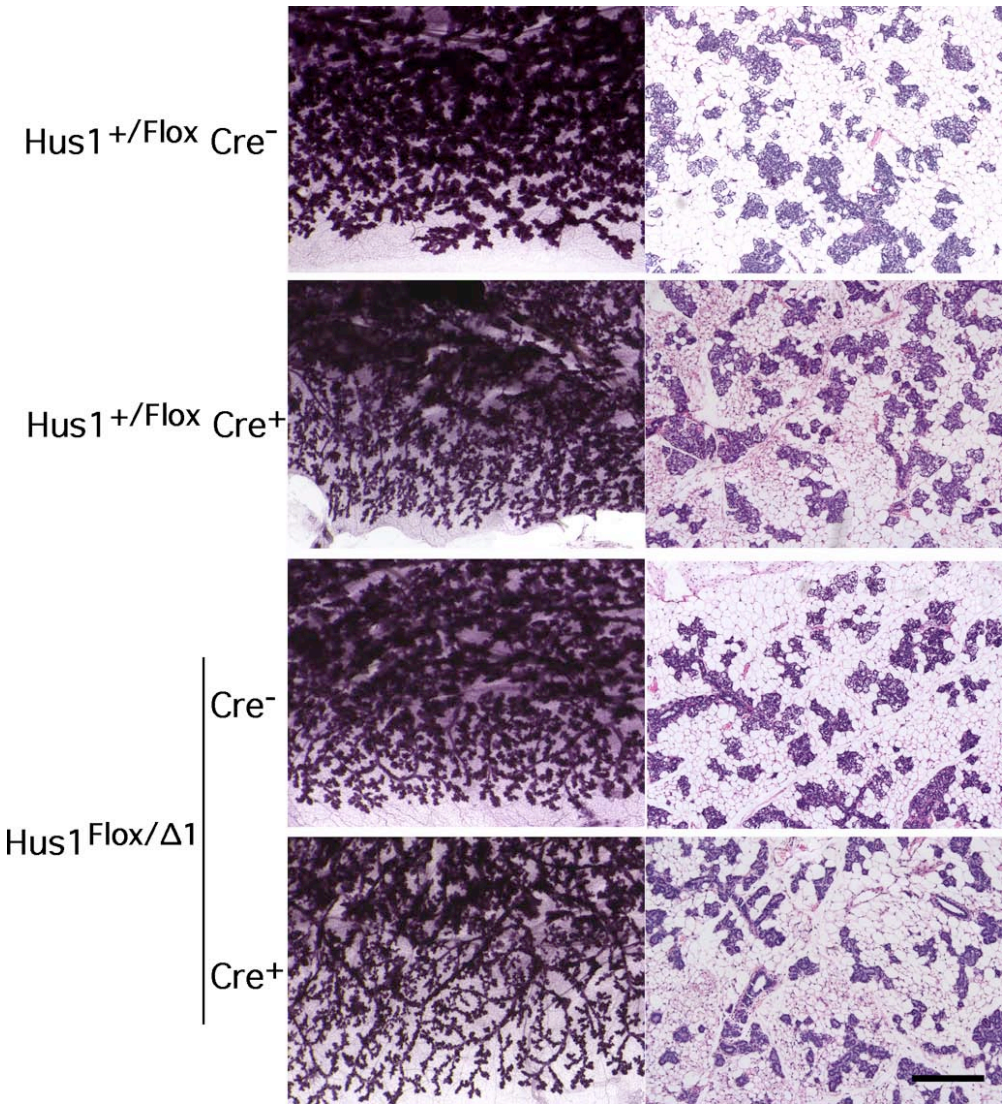


***Figure 2.3.*** **Grossly normal mammary gland morphology in conditional Hus1 knockout mice.** Representative images of whole mounts and histological sections of mammary glands from conditional Hus1 knockout and control females are shown. The fourth mammary glands of mice of the indicated genotype at P18 were harvested, fixed, and stained with Carmine Alum. The contralateral mammary glands were harvested, fixed, embedded, sectioned, and stained with H&E. Scale bar represents 400μm. *[Experiment and figure by S.A. Yazinski]*

those prepared from control Hus1$^{+/Flox}$ Cre$^{+}$, Hus1$^{Flox/\Delta1}$ Cre$^{-}$, and wild-type females at all developmental stages. Normal mammary gland development was observed during pregnancy and lactation in mammary glands of all genotypes (Figure 2.1 C), including similar densities of epithelial and adipose cells as well as typical patterns of side branching, ductal epithelial expansion, and terminal differentiation of milk-producing alveoli (Silberstein, 2001). These findings suggest that cells that failed to undergo Cre-mediated recombination were able to compensate for the loss of *Hus1*-deficient cells from the mammary gland and promote normal development.

Consistent with these observations of normal mammary gland architecture, Hus1$^{Flox/\Delta1}$ Cre$^{+}$ mice were capable of lactating and nursing offspring. Both Hus1$^{Flox/\Delta1}$ Cre$^{+}$ and control multiparous females had an average of 7 pups per litter at weaning, suggesting that multiparous Hus1$^{Flox/\Delta1}$ Cre$^{+}$ females were capable of nourishing their offspring. In addition, conditional *Hus1* inactivation had no significant effect on mammary tumor incidence. Mammary epithelial tumors were found in 2 of 22 (9.1%) multiparous Hus1$^{Flox/\Delta1}$ Cre$^{+}$ females, and 1 of 16 (6.25%) multiparous Hus1$^{+/Flox}$ Cre$^{+}$ and Hus1$^{Flox/\Delta1}$ Cre$^{-}$ control females. The mammary tumors were composed of cuboidal cells arranged in solid to cystic lobules with variable amounts of glandular formation and scant supporting stroma (Figure 2.2 D). The cells had small to moderate amounts of eosinophilic cytoplasm and round to oval nuclei with few (<5) mitotic figures in ten 400x fields. A third Hus1$^{Flox/\Delta1}$ Cre$^{+}$ mouse developed a palpable mammary mass that fully regressed prior to euthanasia. Southern blot analysis further indicated that *Hus1* loss did not directly contribute to tumor formation in multiparous Hus1$^{Flox/\Delta1}$ Cre$^{+}$ mice, as these tumors showed no *Hus1* deletion, whereas complete recombination of the *Hus1$^{Flox}$* allele was observed in the neoplasm from the multiparous Hus1$^{+/Flox}$ Cre$^{+}$ control female (Figure 2.2 C). The tumors arose in mice that were on average 14 months old and had delivered multiple litters each, suggesting

that these were spontaneous background neoplasms in aged mice. Overall, the analysis of conditional *Hus1* knockout mice indicates that *Hus1*-deleted cells are cleared from the mammary gland and do not cause increased cancer risk. Moreover, remaining *Hus1*-expressing cells compensate for the loss of *Hus1*-deficient cells and regenerate a morphologically normal, functional mammary gland.

**2.4.3 Increased genome damage and apoptosis in *Hus1*-deficient mammary epithelium.** Checkpoint dysfunction can cause increased cell death or impaired cell cycle progression (Bartek and Lukas, 2007). In order to determine if the depletion of *Hus1*-deficient cells from the developing mammary gland was due to apoptosis or defective proliferation, we performed terminal uridine deoxynucleotidyl transferase dUTP nick end labeling (TUNEL) and Ki67 antigen staining. TUNEL staining detects extensive DNA fragmentation, a characteristic feature of apoptotic cells (Heatwole, 1999), while Ki67 antigen is expressed in actively dividing but not quiescent cells and therefore is commonly used as a proliferation marker (Scholzen and Gerdes, 2000). At L2, control $Hus1^{+/Flox}$ $Cre^{+}$ mammary glands contained an average of 0.44% apoptotic cells, whereas $Hus1^{Flox/\Delta 1}$ $Cre^{+}$ glands contained an average of 0.85% apoptotic cells, indicating that *Hus1* deficiency led to a moderate but significant increase in apoptosis in the developing mammary gland ($p=0.049$; Figure 2.4 B). The increased apoptosis was not associated with a significant change in cellular proliferation ($p=0.265$; Figure 2.4 A).

To determine the basis for the increased apoptosis, we performed immunohistochemistry against γ-H2AX, the phosphorylated histone variant that accumulates at DSB sites and serves as a robust marker for genome damage (Vidanes et al., 2005). Control $Hus1^{+/Flox}$ $Cre^{+}$ mammary glands showed low levels of γ-H2AX staining, whereas $Hus1^{Flox/\Delta 1}$ $Cre^{+}$ mammary glands showed significantly elevated

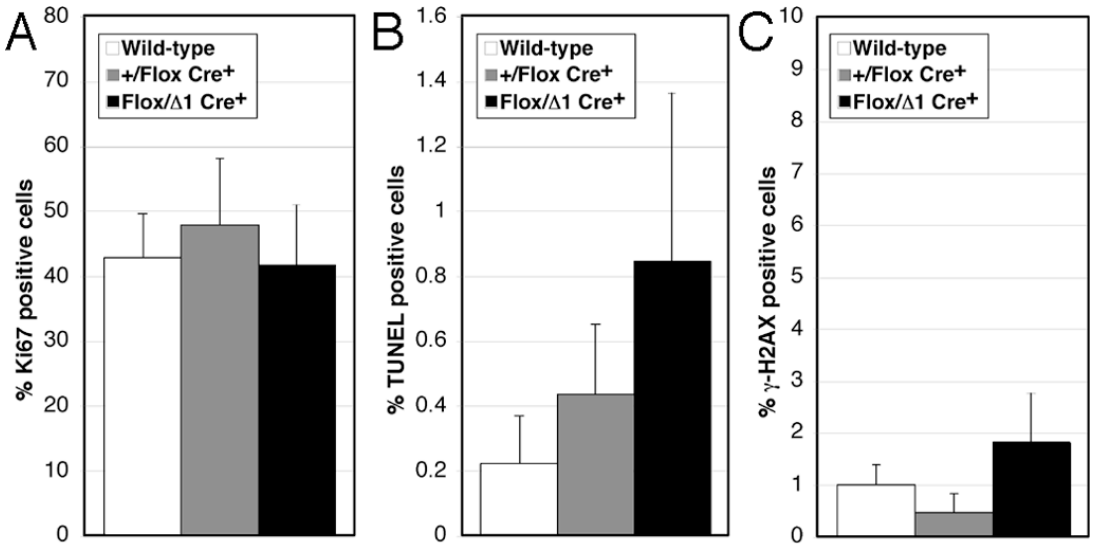


***Figure 2.4.*** **Significantly increased apoptosis and genome damage in mammary glands from conditional Hus1 knockout mice.** Sections from the fourth mammary gland of conditional Hus1 knockout mice at L2 were stained for Ki67 to assess proliferation, by TUNEL assay to detect apoptosis, or for γ-H2AX to detect DNA damage. The percentage of **(*A*)** Ki67, **(*B*)** TUNEL, or (***C***) γ-H2AX positive cells was quantified. Values are means of at least 6 fields per genotype, with error bars denoting standard deviation. The respective number of wild-type ($Hus1^{+/+}$ or $Hus1^{Flox/Flox}$ $Cre^{-}$), $Hus1^{+/Flox}$ $Cre^{+}$, and $Hus1^{Flox/\Delta1}$ $Cre^{+}$ mice analyzed was 4, 2, and 3 in panel (***A***); 4, 4, and 5 in panel (***B***); and 4, 2, and 2 in panel (***C***). *[Experiments and figure by S.A.Yazinski]*

levels of DNA damage (p=0.016; Figure 2.4 C). Overall, these histological analyses suggest that *Hus1* deficiency in the mammary gland results in genome damage that impairs cell viability, while cells that escape recombination and retain wild-type *Hus1* compensate to maintain the structure of the developing mammary gland.

**2.4.4 p53 loss delays the clearance of *Hus1*-deficient cells from the mammary gland but impairs mammary gland structure and function**. *Hus1* loss results in genome damage that can trigger HUS1-independent DNA damage responses (Weiss et al., 2000; Zhu and Weiss, 2007). Because p53 induction is observed following *Hus1* inactivation in embryos and cultured fibroblasts (Weiss et al., 2002), we hypothesized that the increased apoptosis in *Hus1*-deficient mammary tissue may be due to a p53-dependent checkpoint response to genome damage that occurs following *Hus1* loss. We therefore tested whether *Hus1*-deficient cells would be retained in the mammary gland in the absence of *p53* by crossing conditional *Hus1* knockout mice onto a *p53*-deficient background. Southern blot analysis of mammary glands from control $Hus1^{+/Flox}$ $Cre^{+}$ mice on $p53^{-/-}$ and $p53^{+/-}$ backgrounds revealed levels of *Hus1* deletion similar to those in $Hus1^{+/Flox}$ $Cre^{+}$ $p53^{+/+}$ controls (Figure 2.5 A and B, Figure 2.6). Notably, $Hus1^{Flox/\Delta 1}$ $Cre^{+}$ mice on $p53^{-/-}$ and $p53^{+/-}$ backgrounds showed deletion levels similar to those of $Hus1^{+/Flox}$ $Cre^{+}$ controls, suggesting that inactivation of even one *p53* allele reduced the loss of *Hus1*-deficient cells from the mammary gland. At L2, $p53^{-/-}$ conditional *Hus1* knockout mammary glands showed an average of 41% deletion, a 2.3-fold increase in *Hus1* deletion as compared to that in $p53^{+/+}$ conditional *Hus1* knockouts. Likewise, *p53*-deficiency caused a 2.2-fold increase in *Hus1* deletion in the *p53*-deficient conditional knockout glands at P18 (Figure 2.6), and similar results also were observed at L4 (Figure 2.7 A).

To determine the effects of combined *Hus1* and *p53* loss on mammary gland

***Figure 2.5.*** **Increased retention of Hus1-null cells in mammary glands from p53-deficient conditional Hus1 knockout mice.** (***A***) Southern blot analysis was performed to determine the extent of Hus1 deletion in mammary glands of conditional Hus1 knockout mice that differ in p53 status. DNA was extracted from mammary glands of mice of the indicated genotypes at L2 and probed by Southern blot as described in Fig. 1. (***B***) The percentage of Hus1 deletion for each genotype was calculated as the average from the following number of mice: $Hus1^{+/Flox}$ $p53^{+/+}$ $Cre^{+}$ (n=2), $Hus1^{Flox/\Delta 1}$ $p53^{+/+}$ $Cre^{+}$ (n=4), $Hus1^{+/Flox}$ $p53^{+/-}$ $Cre^{+}$ (n=1), $Hus1^{Flox/\Delta 1}$ $p53^{+/-}$ $Cre^{+}$ (n=2), $Hus1^{+/Flox}$ $p53^{-/-}$ $Cre^{+}$ (n=4), $Hus1^{Flox/\Delta 1}$ $p53^{-/-}$ $Cre^{+}$ (n=2). Error bars denote the standard deviation. Hus1 deletion was significantly lower in $Hus1^{Flox/\Delta 1}$ $Cre^{+}$ mice relative to $Hus1^{+/Flox}$ $Cre^{+}$ controls in the $p53^{+/+}$ background (p=0.006) but not in the $p53^{-/-}$ background (p=0.839) as determined by one-way ANOVA. (***C***) Representative histological sections of mammary glands from p53-deficient conditional Hus1 knockout and control mice are shown. Scale bars represent 400μm or 100μm for low (left panels) or high (right panels) magnification images, respectively. *[Experiments and figure by S.A.Yazinski]*

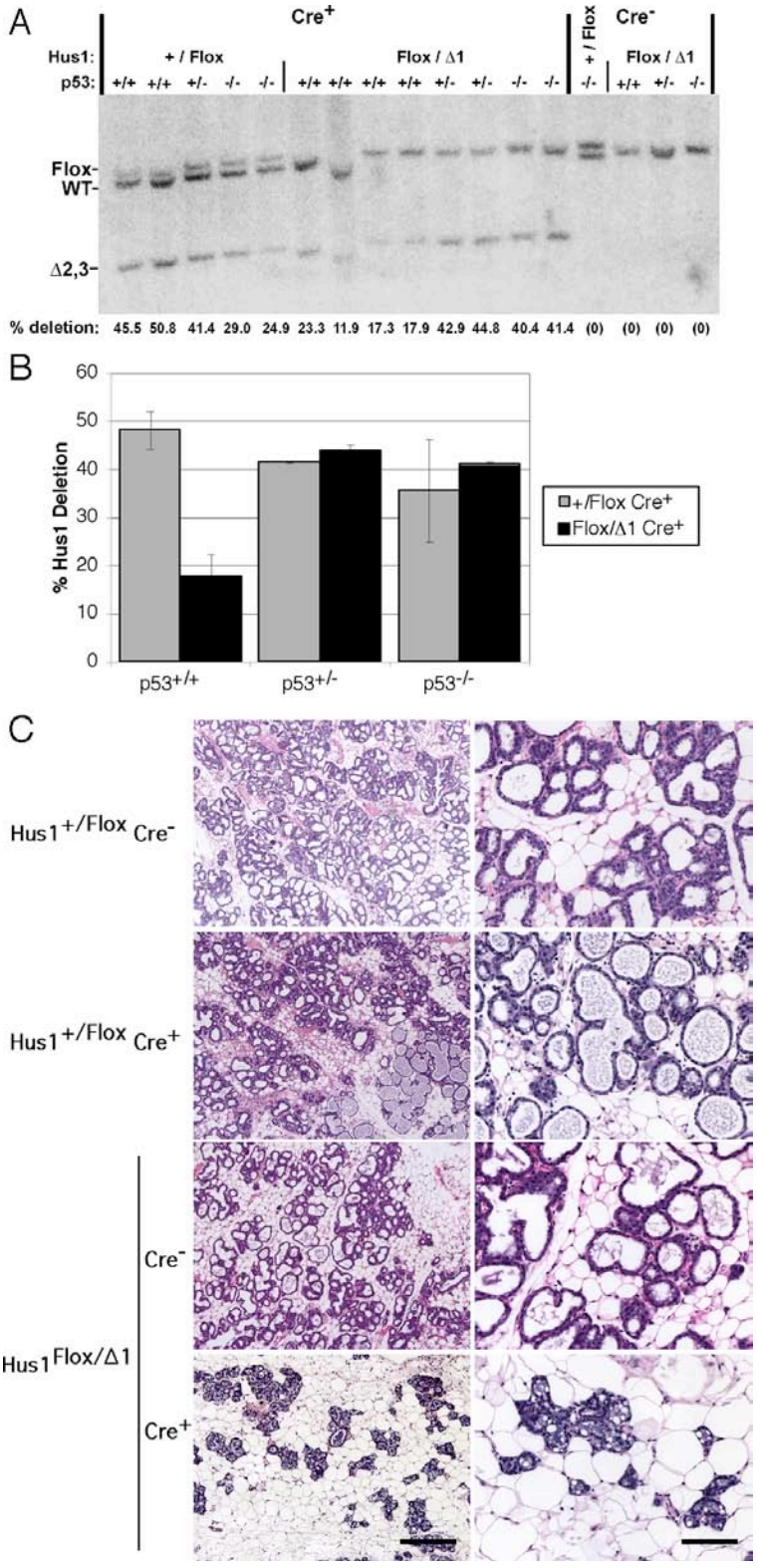
A
Cre+
Cre-
Hus1:
+ / Flox
Flox / Δ1
+ / Flox
Flox / Δ1
p53:
+/+ +/+ +/- -/- -/- +/+ +/+ +/+ +/+ +/- +/- -/- -/- -/- +/+ +/- -/-
Flox-
WT-
Δ2,3-
% deletion: 45.5 50.8 41.4 29.0 24.9 23.3 11.9 17.3 17.9 42.9 44.8 40.4 41.4 (0) (0) (0) (0)
B
% Hus1 Deletion
60
50
40
30
20
10
0
p53+/+
p53+/-
p53-/-
+/Flox Cre+
Flox/Δ1 Cre+
C
Hus1+/Flox Cre-
Hus1+/Flox Cre+
Hus1Flox/Δ1
Cre-
Cre+

***Figure 2.6.*** **Increased retention of Hus1-null cells in mammary glands from p53-deficient conditional Hus1 knockout mice at P18.** (***A***) Southern blot analysis was performed to measure Hus1 deletion in the mammary glands of conditional Hus1 knockout mice that differ in p53 status. DNA was extracted from mammary glands of mice of the indicated genotypes at P18 and probed by Southern blot as described in the legend of Fig. 1. (***B***) Representative histological sections of mammary glands from p53-deficient conditional Hus1 knockout and control mice are shown. The fourth mammary glands of mice of the indicated genotype at P18 were harvested, fixed, embedded, sectioned, and stained with H&E. Scale bars represent 400μm for the low magnification images (middle panels) and 100μm for the higher magnification images (right panels). (***C***) Representative images of whole mounts from p53-deficient conditional Hus1 knockout and control mice are shown. The fourth mammary glands of mice of the indicated genotype at P18 or L2 were harvested, fixed, and stained with Carmine Alum. *[Experiments and figure by S.A. Yazinski]*

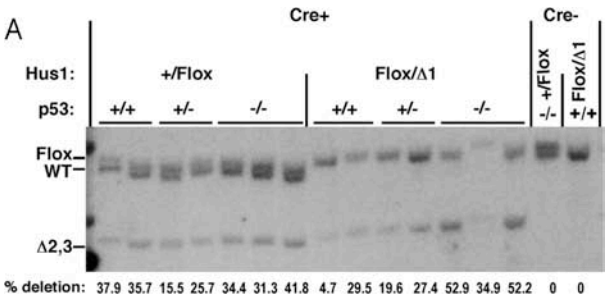
A
Cre+
Cre-
Hus1:
+/Flox
Flox/Δ1
+/Flox
Flox/Δ1
p53:
+/+
+/-
-/-
+/+
+/-
-/-
-/-
+/+
Flox
WT
Δ2,3
% deletion: 37.9 35.7 15.5 25.7 34.4 31.3 41.8 4.7 29.5 19.6 27.4 52.9 34.9 52.2 0 0

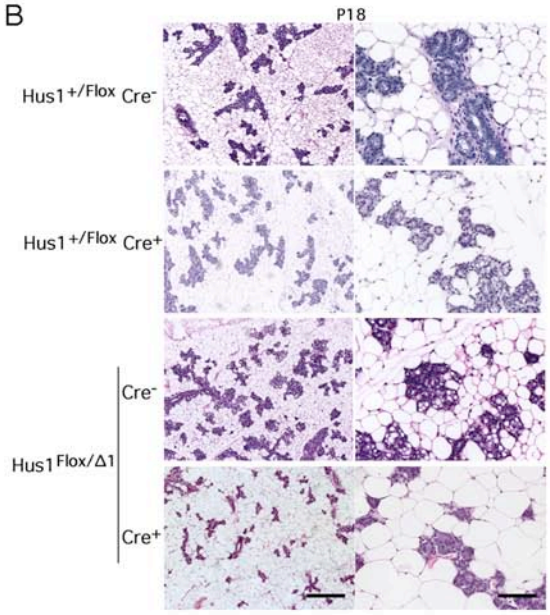
B
P18
Hus1+/Flox Cre-
Hus1+/Flox Cre+
Hus1Flox/Δ1
Cre-
Cre+

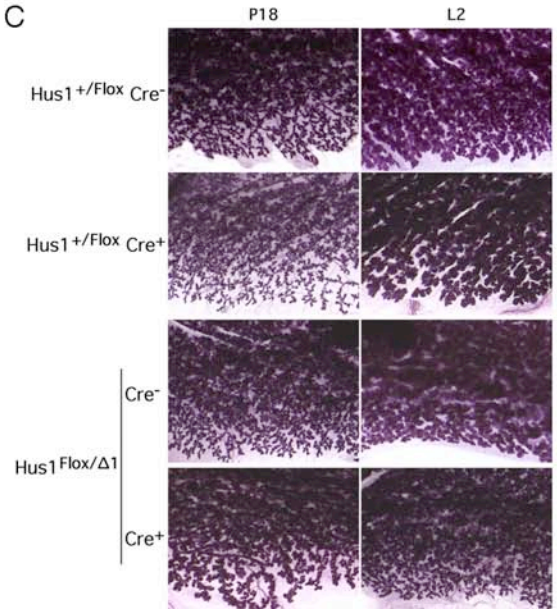
C
P18
L2
Hus1+/Flox Cre-
Hus1+/Flox Cre+
Hus1Flox/Δ1
Cre-
Cre+

***Figure 2.7.*** **Aberrant morphology and increased frequency of damaged and dying cells in L4 mammary glands from p53-null conditional Hus1 knockout mice.** (***A***) Hus1 deletion in the mammary glands of conditional Hus1 knockout mice at L4 was measured by extracting DNA from mammary tissue from mice of the indicated genotypes and probing by Southern blot as described in the legend of Fig. 1. The position of the band for $Hus1^{Flox}$ is marked with a "<" symbol. (***B***) Representative histological sections of mammary glands from p53-deficient conditional Hus1 knockout and control mice are shown. The fourth mammary glands of mice of the indicated genotype at L4 were harvested, fixed, embedded, sectioned, and stained with H&E. Scale bars represent 400μm for the 10X images (left panels), 100μm for the 40X images (middle panels), or 40μm for the 100X images (right panels). (***C-E***) Sections from the fourth mammary gland of p53-deficient conditional Hus1 knockout mice at L4 were stained for Ki67 to assess proliferation, by TUNEL assay to detect apoptosis, or for γ-H2AX to detect DNA damage. Bar graphs show the average percentage of cells positive for (***C***) Ki67, (***D***) TUNEL, or (***E***) γ-H2AX staining. Values are the mean for three independent mammary gland regions from a single mouse of each genotype, with error bars denoting standard deviation. *[Experiments and figure by S.A. Yazinski]*

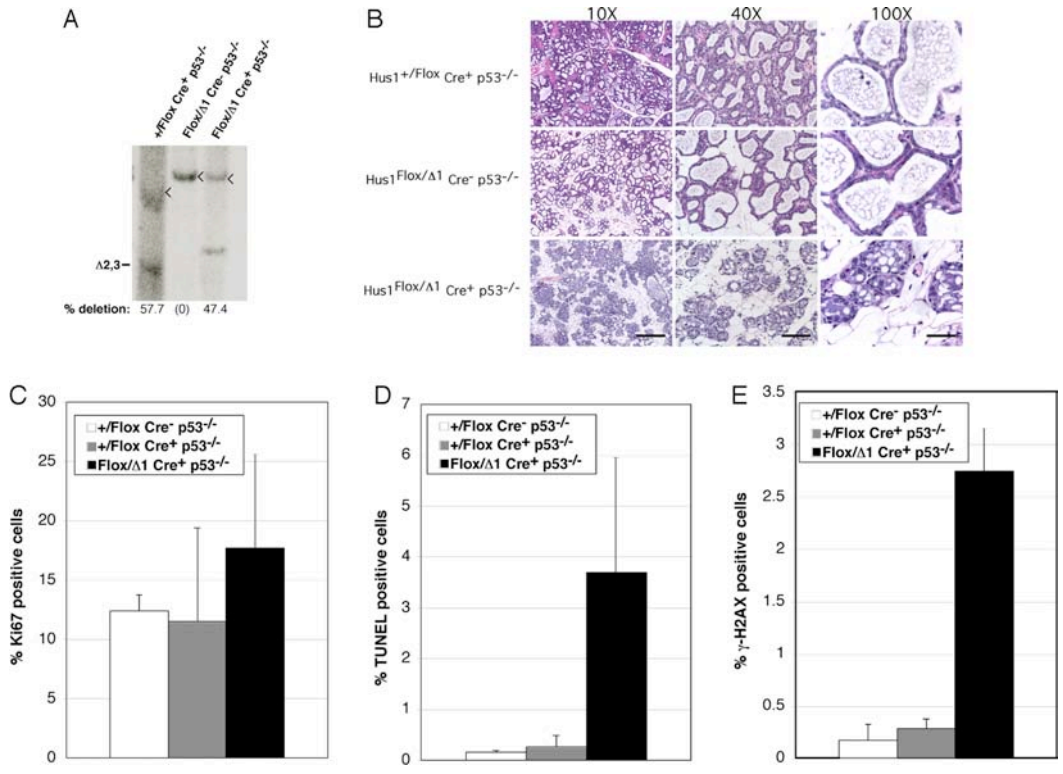
A
+/Flox Cre+ p53-/-
Flox/Δ1 Cre- p53-/-
Flox/Δ1 Cre+ p53-/-
Δ2,3
% deletion: 57.7 (0) 47.4
B
10X
40X
100X
Hus1+/Flox Cre+ p53-/-
Hus1Flox/Δ1 Cre- p53-/-
Hus1Flox/Δ1 Cre+ p53-/-
C
% Ki67 positive cells
+/Flox Cre- p53-/-
+/Flox Cre+ p53-/-
Flox/Δ1 Cre+ p53-/-
D
% TUNEL positive cells
E
% γ-H2AX positive cells

development and morphology, we prepared whole mounts and histological sections from the mammary glands of these mice at P18 and L2. Germline $p53^{-/-}$ mice exhibit normal mammary gland growth and morphogenesis during pregnancy and lactation (Jerry et al., 1998). These mice typically do not develop mammary neoplasms, but succumb to other malignancies. In agreement with these previous findings, grossly normal mammary gland growth and morphogenesis was observed at P18 and L2 in $Hus1^{+/Flox}$ $Cre^{-}$ $p53^{-/-}$, $Hus1^{+/Flox}$ $Cre^{+}$ $p53^{-/-}$ and $Hus1^{Flox/\Delta1}$ $Cre^{-}$ $p53^{-/-}$ control mice (Figure 2.5 *C*, Figure 2.6 B and C). However, histological analysis of $Hus1^{Flox/\Delta1}$ $Cre^{+}$ $p53^{-/-}$ mammary glands at P18 unexpectedly showed delayed lobuloalveolar development and fewer lipid vacuoles (Figure 2.5 B). These defects were even more striking at L2 (Figure 2.5 C and Figure 2.6 C) and L4 (Figure 2.7 B), at which point the mammary epithelium appeared sparser and the formation of milk-filled alveoli was impaired. Quantification of epithelial content revealed that $Hus1^{Flox/\Delta1}$ $Cre^{+}$ $p53^{-/-}$ mammary glands contained 2.2-fold less epithelium than those from $Hus1^{+/Flox}$ $Cre^{+}$ $p53^{-/-}$ control mice ($p<0.001$; Figure 2.8). Consistent with these findings, offspring from four $Hus1^{Flox/\Delta1}$ $Cre^{+}$ $p53^{-/-}$ females showed delayed growth relative to cross-fostered littermates and in three of four cases failed to survive to weaning age, suggesting that these females were incapable of normal lactation. Subsequent litters from these females showed less severe phenotypes, and in one case, apparently normal pups were obtained, presumably because the involution defects of *p53*-deficient mice (Jerry et al., 1998) resulted in retention of mammary epithelium into subsequent pregnancies.

To determine how *p53* loss affected the proliferation and survival of mammary epithelium, we performed TUNEL and Ki67 staining on histological sections from *p53*-deficient conditional *Hus1* knockout mice at L2 (Figure 2.9). There was no significant difference in proliferation between conditional *Hus1* knockout and control

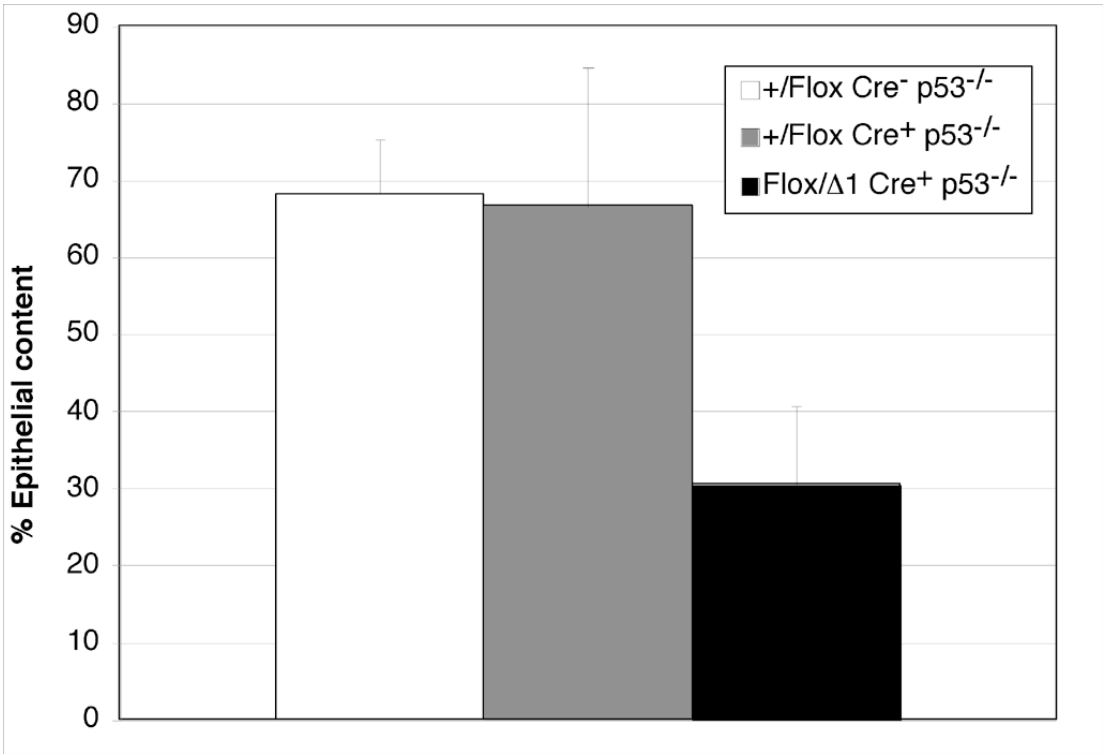


***Figure 2.8.*** **Significantly reduced epithelial content in mammary glands from p53-null conditional Hus1 knockout mice.** Digital images of H&E-stained L2 mammary gland tissue were analyzed using ImageJ and Canvas 8 software applications to determine the total area occupied by epithelial or adipose tissue. At least three independent 40X fields were analyzed from each animal, including $Hus1^{+/Flox}$ $Cre^{-}$ $p53^{-/-}$ (2 mice), $Hus1^{+/Flox}$ $Cre^{+}$ $p53^{-/-}$ (3 mice), and $Hus1^{Flox/\Delta 1}$ $Cre^{+}$ $p53^{-/-}$ (2 mice). The difference in epithelial content between $Hus1^{Flox/\Delta 1}$ $Cre^{+}$ $p53^{-/-}$ and control $Hus1^{+/Flox/}$ $Cre^{+}$ $p53^{-/-}$ mammary glands was significantly different ($p<0.001$) as determined by Student's t-test. *[Experiment and figure by S.A. Yazinski]*

***Figure 2.9.*** **Increased genome damage and apoptosis in mammary glands from p53-deficient conditional Hus1 knockout mice.** Sections from the fourth mammary gland of p53-deficient conditional Hus1 knockout mice at L2 were stained for Ki67 to assess proliferation, by TUNEL assay to detect apoptosis, or for γ-H2AX to detect DNA damage. Representative images of mammary glands stained for (***A***) Ki67, (***C***) TUNEL, or (***E***) γ-H2AX are shown. Arrows highlight positively-stained cells. Scale bars represent 40μm. Bar graphs show the average percentage of cells positive for (***B***) Ki67, (***D***) TUNEL, or (***F***) γ-H2AX staining. Wild-type refers to $Hus1^{+/+}$ $Cre^{-}$ $p53^{+/+}$ and $Hus1^{Flox/Flox}$ $Cre^{-}$ $p53^{+/+}$ or $Hus1^{+/Flox}$ $Cre^{-}$ $p53^{-/-}$. Values for $p53^{-/-}$ mice are the mean of at least 6 fields from two animals, with error bars denoting standard deviation. Data for Ki67, TUNEL, and γ-H2AX staining on sections from $p53^{+/+}$ mice are the same as those shown in Fig. 2. The difference between the frequency of positively stained cells in $Hus1^{Flox/\Delta 1}$ $Cre^{+}$ $p53^{-/-}$ and $Hus1^{+/Flox}$ $Cre^{+}$ $p53^{-/-}$ mice was significant for TUNEL ($p=0.021$) and H2AX ($p<0.001$) but not Ki67 ($p=0.059$) assays as determined by Student's t-test. *[Experiments and figures by S.A.Yazinski]*

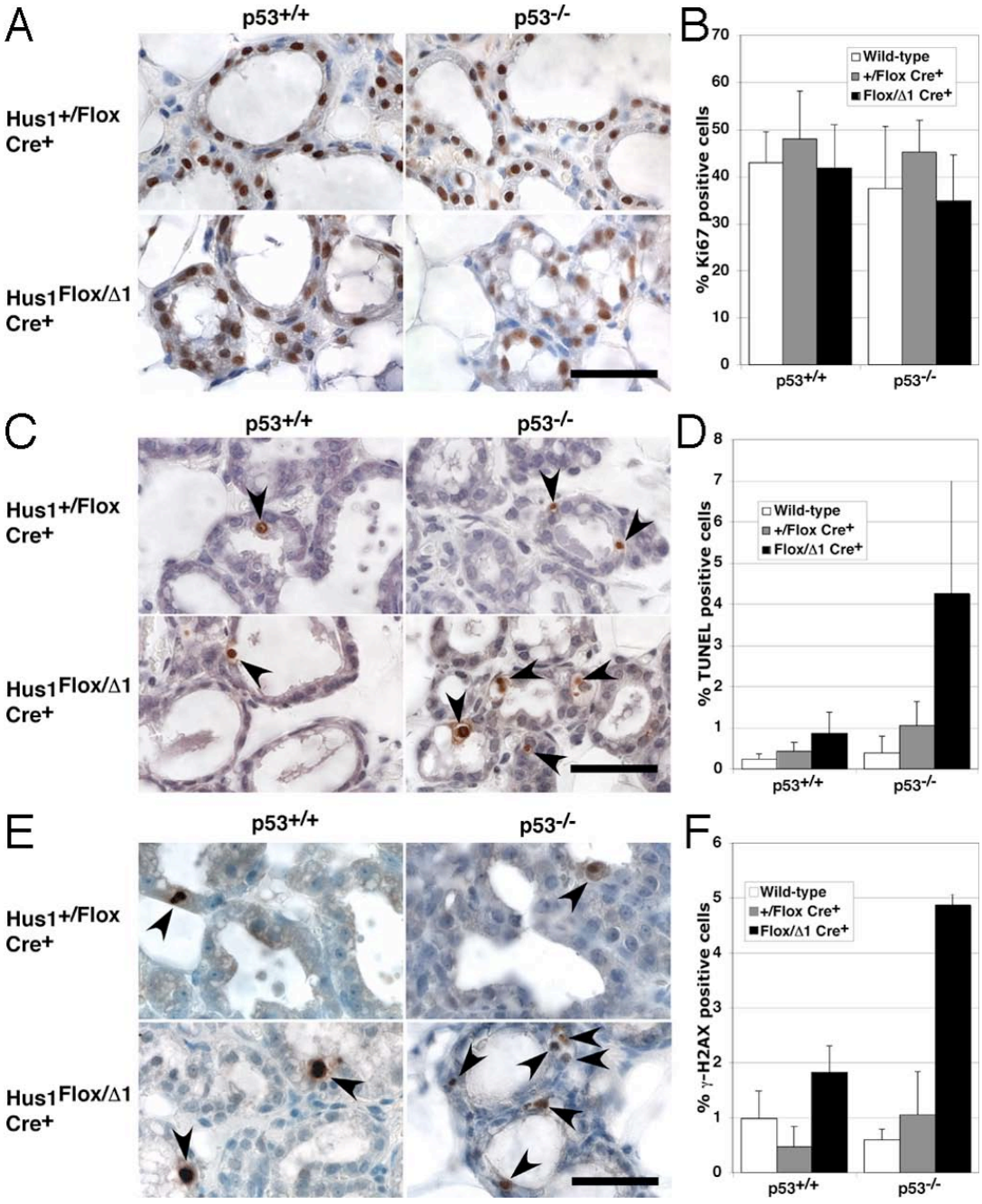
A
p53+/+
p53-/-
Hus1+/Flox Cre+
Hus1Flox/Δ1 Cre+
B
Wild-type
+/Flox Cre+
Flox/Δ1 Cre+
% Ki67 positive cells
0
10
20
30
40
50
60
70
p53+/+
p53-/-
C
p53+/+
p53-/-
Hus1+/Flox Cre+
Hus1Flox/Δ1 Cre+
D
Wild-type
+/Flox Cre+
Flox/Δ1 Cre+
% TUNEL positive cells
0
1
2
3
4
5
6
7
8
p53+/+
p53-/-
E
p53+/+
p53-/-
Hus1+/Flox Cre+
Hus1Flox/Δ1 Cre+
F
Wild-type
+/Flox Cre+
Flox/Δ1 Cre+
% γ-H2AX positive cells
0
1
2
3
4
5
6
p53+/+
p53-/-

mice on either $p53^{+/+}$ or $p53^{-/-}$ backgrounds (Figure 2.9 A and B). Interestingly, the 2-fold increase in apoptosis observed in $p53^{+/+}$ conditional *Hus1* knockout mammary glands as seen in Figure 2.4 was elevated to a 4-fold increase in the absence of *p53* (Figure 2.9 C and D). The significantly increased apoptosis in the *p53*-deficient conditional *Hus1* knockout as compared to p53-deficient $Hus1^{+/Flox}$ $Cre^{+}$ control mice ($p=0.021$) also was associated with a significantly greater level of H2AX phosphorylation ($p<0.001$) (Figure 2.9 E and F). Similar results were observed in mammary glands at L4 (Figure 2.7 C-E). Together, the data suggest that while *p53* loss delays the clearance of *Hus1*-deficient cells from the mammary gland, these cells do undergo apoptosis through a p53-independent pathway that responds to unrepaired DNA damage. In contrast to what happens in $p53^{+/+}$ conditional *Hus1* knockout mammary glands, tissue regeneration by cells that have not undergone *Hus1* deletion is limited in the absence of *p53*, resulting in impaired mammary gland development and function.

## 2.5 DISCUSSION

*Hus1* is an essential checkpoint gene, inactivation of which results in spontaneous chromosomal aberrations and embryonic lethality in mice. The ability to conditionally delete *Hus1* in adult mice using Cre-loxP recombination allowed us to circumvent this lethality and investigate the physiological consequences of checkpoint dysfunction specifically in the mammary gland. Southern blot analysis revealed that *Hus1*-deficient cells were under-represented in mammary glands from $Hus1^{Flox/\Delta 1}$ $Cre^{+}$ mice at all developmental stages and, instead of accumulating over multiple rounds of pregnancy and repeated Cre induction, were entirely absent from multiparous females. Mammary glands from conditional *Hus1* knockout mice exhibited increased DNA damage and apoptosis, suggesting that *Hus1*-null cells were selected against due to impaired genome maintenance. Together with previous observations that *Hus1* inactivation has severe consequences on genomic integrity in embryos and embryonic fibroblasts (Weiss et al., 2000; Zhu and Weiss, 2007), these data further establish a fundamental requirement for HUS1 in responding to spontaneous genome damage, even in the absence of extrinsic genotoxic stresses.

Importantly, conditional *Hus1* knockout females were not predisposed to mammary tumor formation. This finding is consistent with the fact that complete inactivation of ATR pathway components has not been observed in human cancers. In mice, nullizygous mutations in *Atr*, *Chk1*, *Hus1*, or *Rad9* cause embryonic lethality (Brown and Baltimore, 2000; Hopkins et al., 2004; Liu et al., 2000; Weiss et al., 2000). Conditional inactivation of these genes also has not been reported to result in tumor predisposition. *Chk1* deletion in the mammary glands of $Chk1^{Flox/Flox}$ Wap-$Cre^{+}$ mice leads to loss of proliferative potential and clearance of *Chk1*-deficient epithelium by apoptosis (Lam et al., 2004), similar to the effects of *Hus1* deficiency we observed. In thymocytes, *Chk1* deletion causes apoptosis and cell loss, but is not associated with

spontaneous tumorigenesis or leukemogenesis (Zaugg et al., 2007). *Atr* adult mosaic knockout mice similarly are not tumor prone (Ruzankina et al., 2007). Partial inactivation of the ATR pathway, however, may have tumor-promoting effects. Deletion of one *Chk1* allele causes inappropriate S-phase entry and other features common to cancer cells (Lam et al., 2004), and also moderately enhances mammary tumor predisposition in *Wnt-1* transgenic mice (Liu et al., 2000). In addition, $Atr^{+/-}$ mice develop various neoplasms at a low frequency (Brown and Baltimore, 2000). On the other hand, mice with a partial reduction in HUS1 expression are not prone to spontaneous tumor development, despite increased genomic instability (Levitt et al., 2007). Clearly, additional studies are required to fully resolve the importance of HUS1 and the ATR checkpoint pathway in tumorigenesis.

50-60% of cells in the mammary glands of control $Hus1^{+/Flox}$ $Cre^{+}$ mice underwent Cre-mediated *Hus1* deletion. Depletion of an equivalent number of cells from the mammary glands of conditional *Hus1* knockout mice would be predicted to result in significant morphological defects. Yet, $Hus1^{Flox/\Delta 1}$ $Cre^{+}$ mammary glands were morphologically indistinguishable from controls, suggesting that cells that failed to undergo *Hus1* deletion compensated for the loss of *Hus1*-deficient cells and promoted normal mammary gland development. Similarly, *Atr* deletion in adult mice by Cre-loxP recombination leads to widespread cell loss, followed by the recovery of cellularity in most tissues due to expansion of cells retaining Atr expression (Ruzankina et al., 2007). Apoptosis-induced compensatory proliferation is a well-established phenomenon known to occur in *Drosophila* and mammals (Fan and Bergmann, 2008; Valentin-Vega et al., 2008; Vandivier et al., 2006; Wells et al., 2006). Dying cells, as well as the phagocytes that clear them, signal to surrounding cells via mitogens and immune modulators (Fan and Bergmann, 2008; Shi et al., 2003; Vandivier et al., 2006). The relatively normal mammary gland architecture in

conditional *Hus1* knockout mice reflects the action of powerful homeostatic mechanisms that are capable of regenerating a functional mammary gland following extensive cell loss.

Based on the central role of p53 in the apoptotic response to DNA damage (Rodier et al., 2007), we hypothesized that p53 was responsible for the elimination of *Hus1*-deficient cells from the mammary gland. In mouse embryos, *Hus1* deficiency triggers p53-dependent induction of p21 and Perp, indicating that p53 is activated by genome damage induced by *Hus1* loss (Weiss et al., 2002). In this study, *Hus1*-deficient cells were retained in the mammary gland longer in the absence of *p53*, suggesting that p53 normally contributes to the death and/or clearance of *Hus1*-deficient cells. Although *p53* loss did reduce the clearance of *Hus1*-deficient cells from the mammary gland at P18, L2, and L4, the combined loss of *p53* and *Hus1* ultimately resulted in significantly increased DNA damage and apoptosis in the mammary gland. The increased TUNEL staining observed in *p53*-deficient conditional *Hus1* knockout mice may occur because cell death becomes restricted to a narrower time frame, or because dying cells accumulate due to inefficient clearance. Alternatively, *p53* deficiency may cause an even greater amount of genome damage in *Hus1*-null mammary epithelial cells, resulting in elevated apoptosis. The latter possibility is supported by the prior observation that *p53* loss increases genomic instability in primary conditional *Hus1* knockout fibroblasts (Zhu and Weiss, 2007).

These results add to the emerging picture that dysfunction of the ATR checkpoint pathway triggers p53-independent apoptotic responses. For instance, *Chk1*-deficient embryos undergo p53-independent apoptosis (Liu et al., 2000). Similarly, IR or replication stress in the absence of CHK1 trigger apoptosis through p53-independent pathways that are dependent on Caspase-2 or Caspase-3, respectively (Myers et al., 2009; Sidi et al., 2008). Here we show that *Hus1* loss sensitizes *p53*-

deficient cells to apoptosis *in vivo*, without additional exogenous stresses. Altogether, the data presented here suggest that *Hus1*-deficient cells in the developing mammary gland are targeted for apoptosis even when p53 is absent, a process that eliminates cells that are at risk for malignant transformation due to increased genomic instability. While this manuscript was in preparation, Greenow and colleagues published similar results indicating that conditional *Chk1* inactivation in the small intestine causes p53-independent apoptosis followed by compensatory proliferation by remaining *Chk1*-proficient cells (Greenow et al., 2009).

It follows that HUS1 impairment also may reduce cancer cell viability. Interestingly, tumor-initiating cells from *p53*-null mammary tumors show upregulation of *Hus1* and other DNA damage response genes, suggesting that these cancer stem cells may be highly dependent upon checkpoint functions (Zhang et al., 2008). Inactivation of *Hus1* or other ATR checkpoint pathway components therefore represents a potential strategy to sensitize tumors, particularly those harboring *p53* mutations, to DNA-damaging chemotherapeutics. The CHK1 inhibitors currently undergoing clinical testing represent one promising means to accomplish this, and evidence from cell culture models suggests that these agents are indeed effective in cells with mutant *p53* (Ashwell and Zabludoff, 2008; Chen et al., 2006).

Among the most striking findings from this study was that *p53* deficiency greatly limited compensatory tissue regeneration by cells that escaped recombination of the conditional *Hus1* allele, resulting in substantial morphological defects in the mammary glands of $p53^{-/-}$ conditional *Hus1* knockout mice. In $p53^{+/+}$ conditional *Hus1* knockout mice, p53-induced apoptosis and clearance of *Hus1*-deleted cells during mammary development may signal surrounding cells to regenerate a functional mammary gland. This could be a physical cue, such as the creation of space for the expansion of neighboring cells, or a biochemical signal, such as the production of a

secreted mitogen, that is lacking in the *p53*-deficient genetic background. Such a mechanism has been elucidated in *Drosophila*, where p53 is required for compensatory proliferation in damaged tissues containing dying cells (Wells et al., 2006). An alternative model is that the damaged *Hus1*-deficient cells that accumulate in the absence of p53 secrete a dominant inhibitory signal that acts on surrounding cells. Cells that are induced to senesce by genotoxic stress are known to produce various secreted factors, some of which are growth inhibitory, and a recent study indicates that the senescence-associated secretory phenotype is more vigorous in the absence of p53 (Coppe et al., 2008). These mechanisms are not mutually exclusive; in *p53*-deficient conditional *Hus1* knockout mammary glands, compensatory growth may be prevented through a combination of the absence of a regenerative signal and the presence of a dominant inhibitory signal. The conditional *Hus1* knockout mouse model described here will be a valuable tool for deciphering the precise molecular mechanism underlying the novel role for p53 in mammary gland tissue regeneration and homeostasis.

**2.6 Acknowledgements**

The authors thank Phil Leder for support during the early stages of this project, Eric Brown for helpful discussions and sharing unpublished results, Alex Nikitin, Yves Boisclair, Joe Wakshlag, and members of the Weiss lab for valuable suggestions and comments on the manuscript, and the staff of the Cornell Center for Animal Resources and Education (CARE) and Lab Animal Services for excellent animal care. This work was supported by NIH grant R01 CA108773 and an American Cancer Society Institutional Exploratory Research Grant (RSW). SAY was supported through a DOD Breast Cancer Research Program predoctoral fellowship.

# CHAPTER 3

# A PARTIAL DEFECT IN THE CHECKPOINT PROTEIN HUS1 IMPAIRS CELLULAR TRANSFORMATION AND TUMOR DEVELOPMENT

## 3.1 ABSTRACT

DNA damage checkpoint proteins act to protect genomic integrity. In some contexts, this may function as a tumor suppressor by preventing mutations that can result in activation of oncogenes or inactivation of tumor suppressors. However, checkpoints also may act to promote tumor initiation and development by providing the tools to cope with the genomic stress of oncogene-induced proliferation. Our lab previously developed an allelic series in which mice express incrementally reduced levels of HUS1, an essential component of the ATR DNA damage checkpoint pathway, allowing us to investigate how partial HUS1 impairment effects transformation and oncogene-induced proliferation. Cell culture transformation assays revealed that more immortalized embryonic fibroblasts cell lines with reduced HUS1 levels showed reduced focus formation and anchorage-independent growth as compared to control cell lines, suggesting impaired transformation ability. We further tested the effect of reduced levels of HUS1 on skin papilloma formation following chemical carcinogenesis. A subset of mice with reduced *Hus1* expression initially developed papillomas at an accelerated rate compared to control animals, suggesting that genomic instability and checkpoint failure in initiated cells with reduced *Hus1* expression results in shorter latency for papilloma development. However, at late stages of the experiment, mice expressing reduced levels of HUS1 showed a decreased risk of papilloma development and, by the conclusion of the experiment, they showed significant decreases in papilloma size and number, which correlated with the level of HUS1 reduction. These effects were not associated with increased cell death or

decreased cellular proliferation following carcinogen exposure, suggesting that the decrease in papilloma formation may be because of an inability of cells with reduced *Hus1* expression to survive the stresses of neoplastic proliferation due to insufficient genome maintenance. Taken together, these results suggest that the HUS1-dependent ATR pathway may be exploited as a drug target to sensitize tumors to anti-cancer therapies that act by causing genome damage.

## 3.2 INTRODUCTION

Cancer is aberrant, uncontrolled cellular proliferation that arises due to an accumulation of mutations in cell growth regulatory genes. DNA damage checkpoint proteins act to protect genomic integrity against such mutations. Additionally, DNA damage checkpoint proteins act in response to oncogene-induced proliferation to promote senescence (Bartek et al., 2007). In these two ways, checkpoint proteins can suppress tumorigenesis. On the other hand, checkpoints may also aid tumor development by playing a critical role promoting survival and growth following transformation (Luo et al., 2009). Checkpoint proteins may protect the genome of transformed cells from chromosomal instability, oxidative stress, and replication stress associated rapid proliferation. The roles of checkpoint pathways in tumorigenesis and tumor maintenance is yet unresolved, and an important area of research.

There are two main DNA damage checkpoint pathways, the ATR pathway and the ATM pathway. Roles for the ATM pathway have been well established, and mutations in many of the components have been shown to increase tumor incidence in both mouse models as well as human disease (Bartek et al., 2007). For example, mutations of ATM itself results in the human disease Ataxia Talangiectasia, which has a predisposition to lymphoma. *Atm* mutant mouse models also show an increased tumor incidence of lymphoma (Shiloh, 2003). Additionally, mutations of several ATM

pathway components are also associated with an increased risk of breast cancer development (Ahmed and Rahman, 2006). The role of the ATR checkpoint pathway in tumor suppression is not well understood, as deletion of any component of this pathway results in embryonic lethality (Brown and Baltimore, 2000; de Klein et al., 2000; Han et al., 2010; Hopkins et al., 2004; Liu et al., 2000; Takai et al., 2000; Weiss et al., 2000). Some studies have suggested that the ATR pathway may play a critical role in tumor suppression, while others suggest that inactivation of the ATR pathway may instead inhibit tumor growth. For example, heterozygous mutations in *Chk1*, *Atr*, and *Rad1* slightly elevate tumor incidence when these mutations are crossed onto a tumor prone background (Fang et al., 2004; Han et al., 2010; Lam et al., 2004; Lewis et al., 2005). Additionally, ATR pathway mutations have been found in human tumors (Fang et al., 2004; Lewis et al., 2007; Lewis et al., 2005; Menoyo et al., 2001; Vassileva et al., 2002); though, tumors retain at least partial function of the mutated protein. On the other hand, heterozygous mutants or conditional knockout mice for *Chk1*, *Atr*, *Rad9*, *Rad1*, and *Hus1* mice are not prone to spontaneous tumor development (Boles et al., 2010; Greenow et al., 2009; Han et al., 2010; Hu et al., 2008; Lam et al., 2004). Furthermore, mutations in the ATR pathway that result in complete inactivation of any component have not been found in human tumors. This, together with recent studies that show some components of the ATR pathway up-regulated in human tumors (Maniwa et al., 2005; Zhu et al., 2008), suggests that the ATR pathway may not play a role in tumor suppression, but rather may be necessary or beneficial for tumor development.

HUS1 is an essential component of the ATR pathway, that, along with RAD9 and RAD1, forms the 9-1-1 complex, a heterotrimeric sliding clamp which is loaded onto DNA in response to damage, acting as a scaffold to allow docking of checkpoint and repair proteins. To determine the role of HUS1 in tumor suppression, we made use

of the previously described *Hus1* allelic series, which expresses incrementally reduced levels of HUS1, while bypassing the embryonic lethality associated with complete germline inactivation of *Hus1*. Mice with the lowest level of *Hus1*, $Hus1^{Neo/\Delta 1}$, are grossly normal, are not prone to spontaneous tumor development, but show sensitivity to certain genotoxins; while, primary $Hus1^{Neo/\Delta 1}$ embryonic fibroblasts exhibit spontaneous chromosomal abnormalities and undergo premature senescence associated with increase in oxidative stress. Treatment of $Hus1^{Neo/Neo}$, with ~40% *Hus1* expression, and $Hus1^{Neo/\Delta 1}$, with ~20% *Hus1* expression, cells with DNA adducting agents results in a loss of cell viability associated with S-phase DNA damage checkpoint failure (Levitt et al., 2007). Together, these findings define a critical role for HUS1 in response to genome damage and replication stress. Importantly, the *Hus1* allelic series also provides an ideal tool to test the effect of reduced HUS1 on transformation and tumorigenesis.

In this study, we show that reduced levels of HUS1 results in decreased transformation ability. Cells with decreased *Hus1* expression showed a slight defect in transformation by a less stringent focus formation assays, and showed a more obvious defect in transformation ability by the more stringent soft agar assays. Furthermore, we found that, following a two-step chemical carcinogen treatment to induce papilloma formation in the skin, mice expressing reduced levels of HUS1 showed a decreased risk of papilloma development and, ultimately developed fewer and smaller papillomas. Furthermore, the decrease in papilloma number and size was dependent on the level of *Hus1* expression. These data suggest that cells with reduced *Hus1* expression are not able to survive the stresses of neoplastic proliferation due to insufficient genome maintenance.

## 3.3 MATERIALS AND METHODS

*Mice:* Previously described $Hus1^{+/\Delta 1}$ and $Hus1^{+/Neo}$ mice (Levitt, 2007 #31) were maintained on a 129S6 inbred genetic background. To generate experimental $Hus1^{Neo/\Delta 1}$ mice, as well as littermate control $Hus1^{+/+}$, $Hus1^{+/Neo}$, and $Hus1^{+/\Delta 1}$ mice, $Hus1^{+/\Delta 1}$ and $Hus1^{+/Neo}$ mice were bred, and first generation offspring were used for DMBA/TPA experiments. To generate $Hus1^{Neo/Neo}$ and control littermates, $Hus1^{+/Neo}$ mice were intercrossed. All animals were genotyped by PCR analysis of DNA extracted from tail tip biopsies. Mice were housed in accordance with institutional animal care and use guidelines.

*Generation of mouse embryonic fibroblasts (MEFs):* Timed matings were performed with $Hus1^{+/Neo}$ females by $Hus1^{Neo/\Delta 1}$ males. Embryos from pregnant females were harvested at 13.5dpc, as previously described (Levitt et al., 2007). After differentiated tissues (head, liver, and spleen) were removed, the remaining cells were plated in DMEM + 10% FBS, 1% non-essential amino acids, 1% l-glutamine, 1% penicillin-streptomycin. Cells were maintained on a 3T3 protocol (Todaro and Green, 1963), and passed every three days. Cells were immortalized spontaneously following at least 20 passages when cells overcame senescence, as measured by population doublings, by spontaneous immortalization.

*Large-T antigen immortalization assay:* Primary MEFs were prepared, grown at low oxygen, and transfected at passage 1 using Fugene 6 transfection agent (Roche) with pSG5-Large-T (Addgene plasmid 9053) (Zalvide and DeCaprio, 1995) or eGFP-C2 (GenBank Accession #: U57606) (BD Biosciences) as a control for transfection efficiency. The transfected cells were passed after 48 hours, plated at low density ($1\times10^3$ cells), and fed every three days. After two weeks, plates were fixed with

methanol, and stained overnight with 0.01% crystal violet in 95% ethanol. Colonies were counted for each plate, and statistical analysis was performed by two-tailed Student's T-test.

*Focus formation assays:* Immortalized MEFs were transfected by the calcium phosphate precipitation method with 20μg total plasmid DNA (eGFP-C2 (Zhao et al., 1998), Ras (Tabin and Weinberg, 1985), E1A (Logan and Shenk, 1984), or 10μg of each Ras and E1A). Cells were fed every three days for two weeks, fixed with methanol, and stained with Giemsa overnight. Foci were quantified by ImageJ® software. Statistics were done by two-tailed Student's T-test.

*Virus production and infection:* Ecotropic viruses were generated from Phoenix-Eco packaging cells following transfection using Fugene 6 transfection reagent (Roche) with 6μg of DNA construct (pBabe-p-GFP, pBABE-p-HRas-V12 (Serrano et al., 1997), or pBABE-c-mycT58A+HRasG12V (Addgene plasmid 11130)(Kendall et al., 2005)) and 3μg p(Psi)2 packaging vector. 2 x $10^5$ immortalized MEFs were seeded to a single well of a gelatinized, 6-well plate and then were infected with 100ul of virus in 1ml of media containing heat inactivated serum and 1μl polybrene. Cells were passed after 48 hours and subsequently used for anchorage independent growth assays.

*Anchorage independent growth assays:* Immortalized MEFs were infected with equal volumes of packaged retroviruses (pBabe-p-GFP, pBABE-p-HRas-V12 (Serrano et al., 1997), or pBABE-c-mycT58A+HRasG12V (Addgene plasmid 11130))(Kendall et al., 2005). 48 hours after infection, 1 X $10^5$ cells were passed to 0.4% top agar, plated over 0.6% base agar in 60mm dishes, and fed once a week with fresh top agar. Plates

were imaged after two weeks of growth, and colony number and size were analyzed using ImageJ® software. Statistics were performed by two-tailed Student's T-test.

*Transplantation assay:* Immortalized MEFs were infected with equal volumes of packaged retroviruses (pBabe-p-GFP or pBABE-c-mycT58A+HRasG12V (Addgene plasmid 11130))(Kendall et al., 2005). Cells were passed for amplification 48 hours after infection. Cells were collected by gentle trypsinization, and resuspended at $10^7$ cells/ml of serum free media. $10^6$ cells were injected subcutaneously into the flanks of wild-type 129 mice and tumors were permitted to grow for 4 weeks. Tumors were harvested, measured, fixed, and processed for histological evaluation.

*Cell sensitivity to puromycin:* Immortalized MEFs were treated media containing the indicated concentration of puromycin for 2 weeks. Surviving colonies of cells were fixed with methanol overnight and stained with 0.01% crystal violet in 95% ethanol.

*Sensitivity to DMBA and TPA in cell culture:* Primary MEFs were given a single treatment of either DMBA or TPA dissolved in acetone or vehicle (acetone) alone added to cell culture media. The media was changed after 24 hours, and cell survival was determined after 48 hours using trypan blue exclusion staining to count surviving cells.

*Skin carcinogenesis experiments:* Mice were anesthetized with 2.5% Avertin and shaved on their back. Mice were determined not to be in anagen phase of the hair growth cycle by failure of hair to regrow after three days (Muller-Rover et al., 2001). Mice treated with a single dose of DMBA (200nmol in acetone). One week following DMBA treatment, mice were treated twice weekly with 5μg TPA for twenty weeks.

Papilloma development was monitored twice weekly, and tumor number and size were noted. Mice were euthanized 20 weeks post DMBA application following a 6 hour incubation with BrdU (50ug/g body weight) injected intraperitoneally, and skin was harvested, fixed, and processed for histopathological analysis. Statistical analysis were by a random coefficient model with random slope and intercept. The fixed effects are the genotype, days, and their interaction term. Tumor latency was plotted using a Kaplan-Meier survival curve and analyzed by log rank survival analysis using SPSS software.

*Sensitivity to DMBA and TPA in vivo:* To determine sensitivity of skin cells to DMBA or TPA, mice were anesthetized with 2.5% Avertin, shaved on their backs, and given a single treatment of DMBA or TPA. Twenty hours after initial treatment, mice were injected intraperitoneally with 50μg of BrdU per gram of body weight. Four hours later, mice were euthanized and skin samples were harvested, fixed in formalin, paraffin embedded, and sectioned. Tissue sections were stained using a TUNEL kit (ApopTag® Peroxidase In Situ Kit - Millipore) to assess apoptosis or using a BrdU kit (Zymed-Invitrogen) to assess proliferation. Approximately 500 cells in at least three fields of vision from at least three mice at 40X magnification were counted per slide. Statistical analysis was by a random coefficient model with random slope and intercept. The fixed effects were the genotype, dose, and their interaction term.

*3.4 RESULTS*

**3.4.1 Reduced *Hus1* expression results in a decreased ability to become immortalized.** Cells expressing reduced levels of *Hus1* have reduced DNA damage checkpoint function, which may affect the ability of cells to become immortalized and/or transformed. Decreased checkpoint function may allow cells to bypass senescence more easily and become transformed. Alternatively, decreased checkpoint function may decrease the ability of a cell to survive the transformation process, which is associated with hyper-replication and increased oxidative stress. In order to determine the effect of reduced levels of HUS1 on tumor development, we first tested the effect of reduced HUS1 on transformation capacity using a series of transformation assays in tissue culture models.

We tested the ability of primary MEFs expressing incrementally reduced levels of HUS1 to undergo immortalization by addition of a potent oncogene, Large-T antigen, which is singly capable of immortalizing cells by targeting the retinoblastoma (pRB) and p53 tumor suppressor proteins (Ali and DeCaprio, 2001). Primary $Hus1^{+}$ MEFs were more readily immortalized than $Hus1^{Neo/Neo}$ and $Hus1^{Neo/\Delta 1}$ MEFs upon exposure to Large-T antigen, as quantified by colony formation (Figure 3.1). On average, $Hus1^{+}$ MEFs formed more colonies (41.5) than either $Hus1^{Neo/Neo}$ (12.75) ($p=0.194$) or $Hus1^{Neo/\Delta 1}$ (13) ($p=0.194$) MEFs (Figure 3.1 A and B). This assay was repeated with two separate primary cultures for each genotype with consistent results. Importantly, there was equivalent transfection efficiency among all cell lines, as assessed by transfection using an equal amount of a GFP construct (Figure 3.1 C). Additionally, GFP transfected cells were not able to form colonies when plated at the same density. These data show that both $Hus1^{Neo/Neo}$ and $Hus1^{Neo/\Delta 1}$ cells are less able to become immortalized following addition of an oncogene. This suggests that a reduced level of HUS1 is not compatible with the continuous proliferation associated

***Figure 3.1*** **Cells with reduced Hus1 expression are resistant to Large-T antigen induced immortalization.** (A) Representative images of primary mouse embryonic fibroblasts (MEFs) of the indicated genotypes two weeks after transfection with Large-T Antigen. (B) Quantification of colony formation assay. Bars indicate the average of two independently derived averaged from colony formation at two densities ($1 \text{ X } 10^3$ and $1 \text{ X } 10^4$), with error bars indicating standard deviation. The number of colonies formed by $Hus1^{+}$ is not statistically different from $Hus1^{Neo/Neo}$ ($p=0.194$) or $Hus1^{Neo/\Delta 1}$ ($p=0.194$) by Students T-test. (C) Representative images of primary cells infected with GFP construct. Cultures showed equal transfection efficiency regardless of genotype. *[Experiment and figure by S. Yazinski and L. Gerwitz*

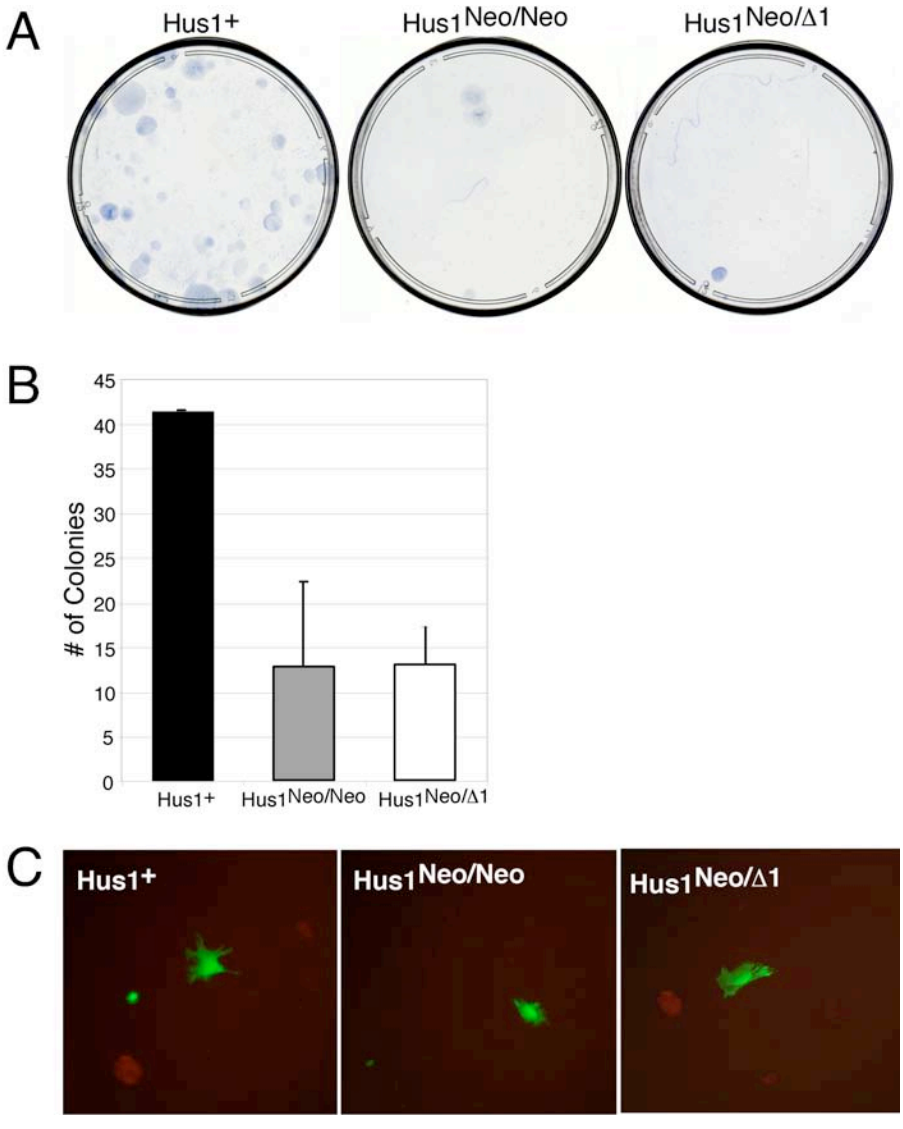
A
Hus1+
Hus1Neo/Neo
Hus1Neo/Δ1
B
# of Colonies
45
40
35
30
25
20
15
10
5
0
Hus1+
Hus1Neo/Neo
Hus1Neo/Δ1
C
Hus1+
Hus1Neo/Neo
Hus1Neo/Δ1

with immortalization, resulting in reduced colony numbers. This raises the possibility that cells with reduced HUS1 may also be more difficult to become transformed, as the process of transformation can involve increased proliferation due to an oncogenic stimulus.

**3.4.2 Reduced *Hus1* expression results in impaired focus formation in a transformation assay measuring loss of contact inhibition.** We next wanted to test the ability of cells with reduced levels of HUS1 to undergo transformation using the well-characterized focus formation assay. This assay assesses the ability of these cells to bypass contact inhibited growth by screening for focus formation, which results when cells continue to proliferate despite antagonistic signals from adjacent cells. Though transfection with a single oncogene alone is known to induce senescence in primary wild-type cells, transfection with two oncogenes simultaneously bypasses senescence and pushes a cell toward transformation (Knudson, 2001).

Three separately derived, spontaneously immortalized MEF cell lines for each genotype were tested at least twice (Figure 3.2). Immortalized cells are more readily transfected than primary cells; however, each line may have acquired additional mutations through the immortalization process. Because of this, there may be differences between cell lines of the same genotype in any given assay. It is important to note that the resulting monolayer from $Hus1^{Neo/\Delta 1}$ cells growing to confluence is more dense in all three independently derived cell lines. All nine spontaneously derived immortalized cell lines were transfected with plasmids expressing oncogenes, specifically, adenovirus E1A, activated H-Ras, or both simultaneously and assessed for focus formation (Figure 3.3). All MEF cell lines showed few to no foci following transfection with GFP or the E1A oncogene. Two $Hus1^{+}$ cell lines formed several foci after addition of activated Ras alone. All three cell lines formed a large number foci

***Figure 3.2*** **Three immortalized cell lines were derived independently for each genotype.** MEFs were prepared as described and were passed at least 25 times and had bypassed senescence before being used in transformation assays. Three separately derived immortalized cell lines were prepared from MEFs from two litters. The highlighted $Hus1^{+}$ cell line is morphologically distinct from the other 8 eight cell lines, grew slower, and was not able to form colonies in a soft agar assay.

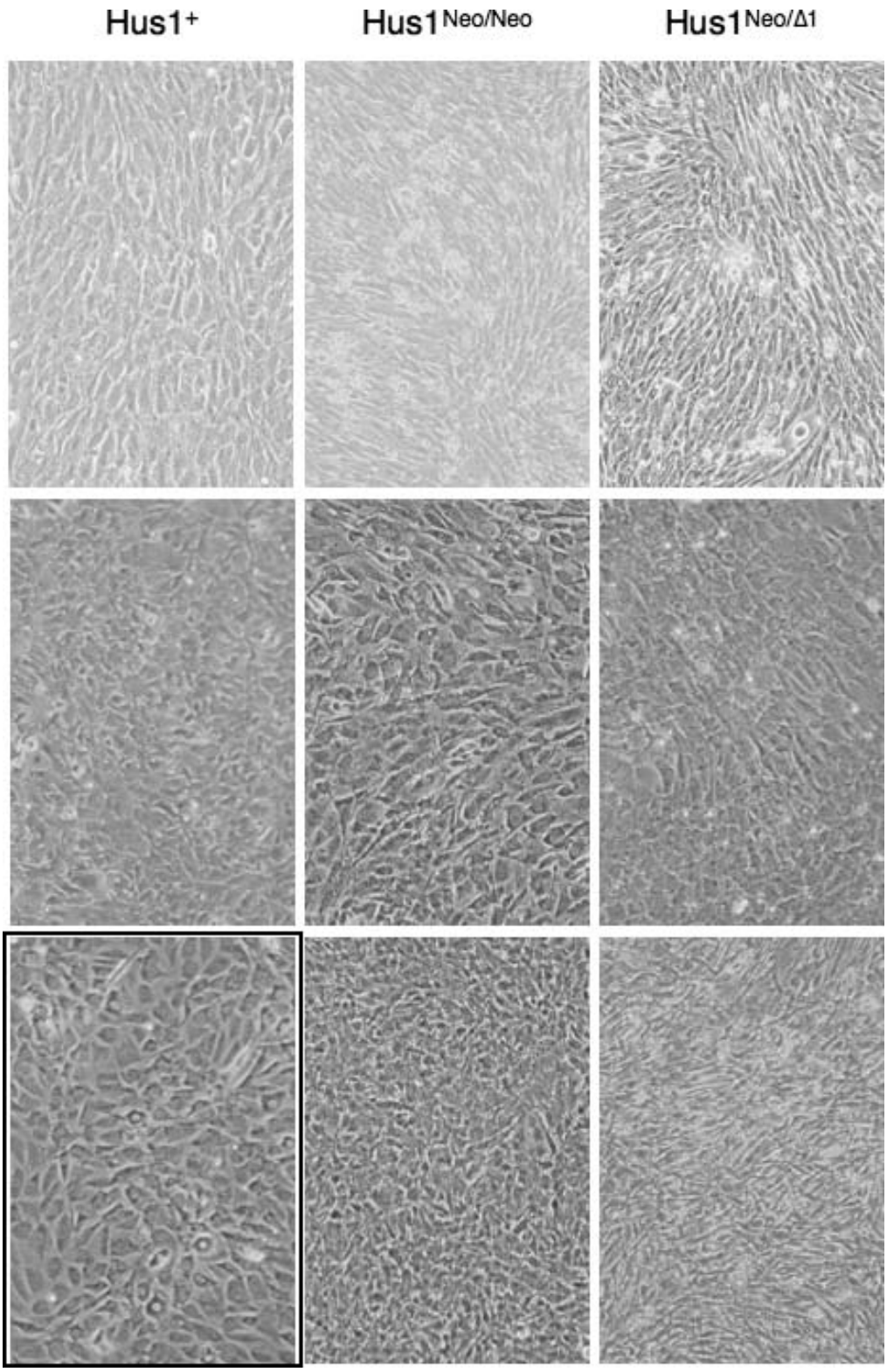
Hus1+
Hus1Neo/Neo
Hus1Neo/Δ1

***Figure 3.3*** **Cells with reduced Hus1 expression have a decreased probability of forming foci in a contact inhibition tranformation assay.** (A-C) Representative images of three independently derived immortalized MEF cultures of the indicated genotypes following transfection with (A) GFP, (B) a single activated oncogene (Ras or E1A), or (C) two activated oncogenes (Ras and E1A). Two weeks post transfection, cells were fixed with methanol and stained with Giemsa overnight. (D) Quantification of focus formation assays. Foci were counted using ImageJ software. Bars indicate the average of at least two independent experiments on each of three cell lines, with error bars indicating standard deviation. There was no statistically significant difference in the average focus formation across cell lines following transfection with plasmids expressing Ras and E1A between $Hus1^{+}$ and $Hus1^{Neo/Neo}$ ($p=0.727$) or $Hus1^{Neo/\Delta 1}$ ($p=0.232$) by Students two-tailed T-test. (E) Images of cells from each of the three independently derived cell line following transfection with GFP. Cells overall showed equivalent transfection efficiency within each experiment regardless of genotype. *[Experiment and figure by S. Yazinski and L. Gerwitz]*

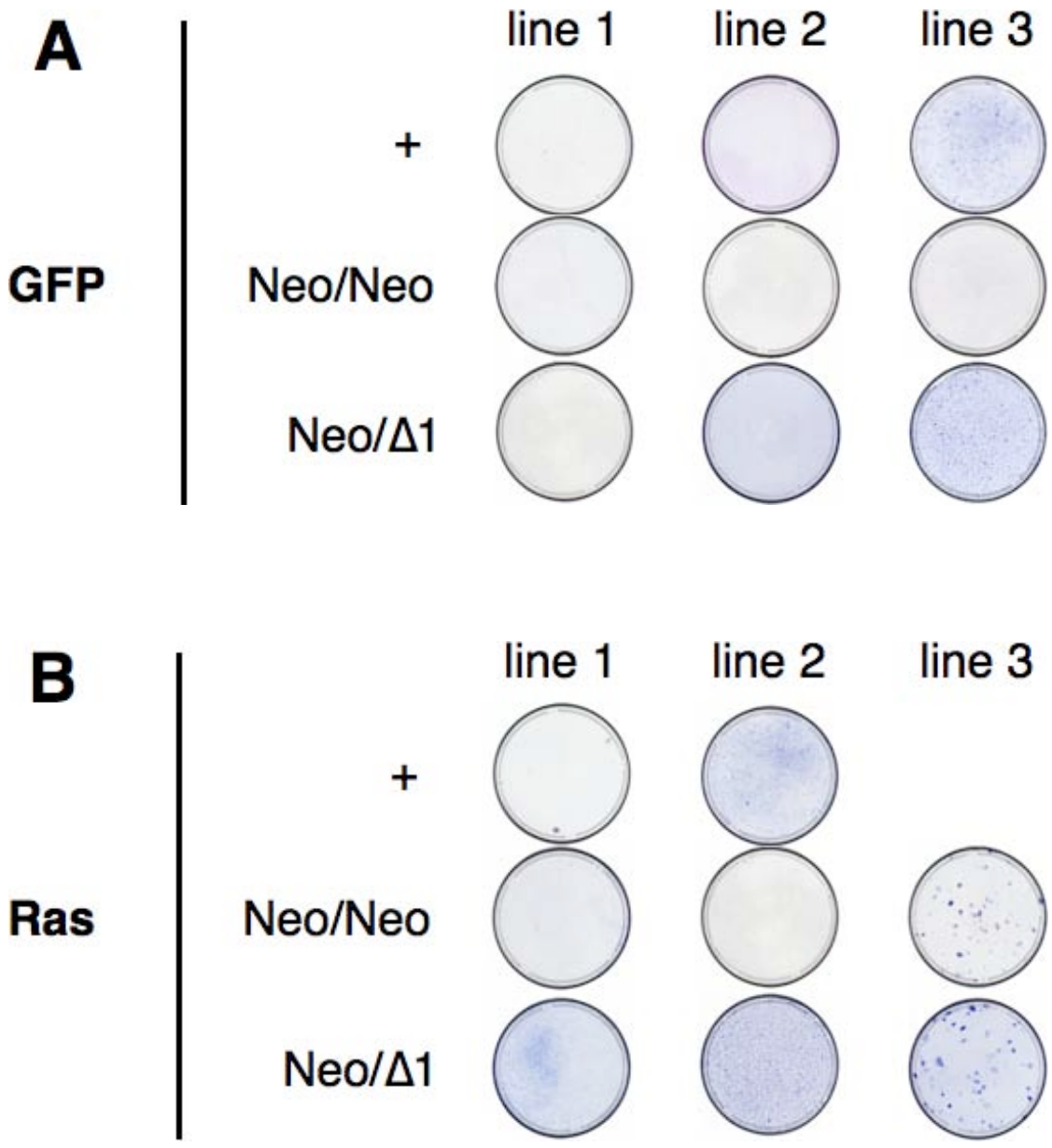
A
line 1
line 2
line 3
+
GFP
Neo/Neo
Neo/Δ1
B
line 1
line 2
line 3
+
Ras
Neo/Neo
Neo/Δ1

Figure 3.3 (Continued)

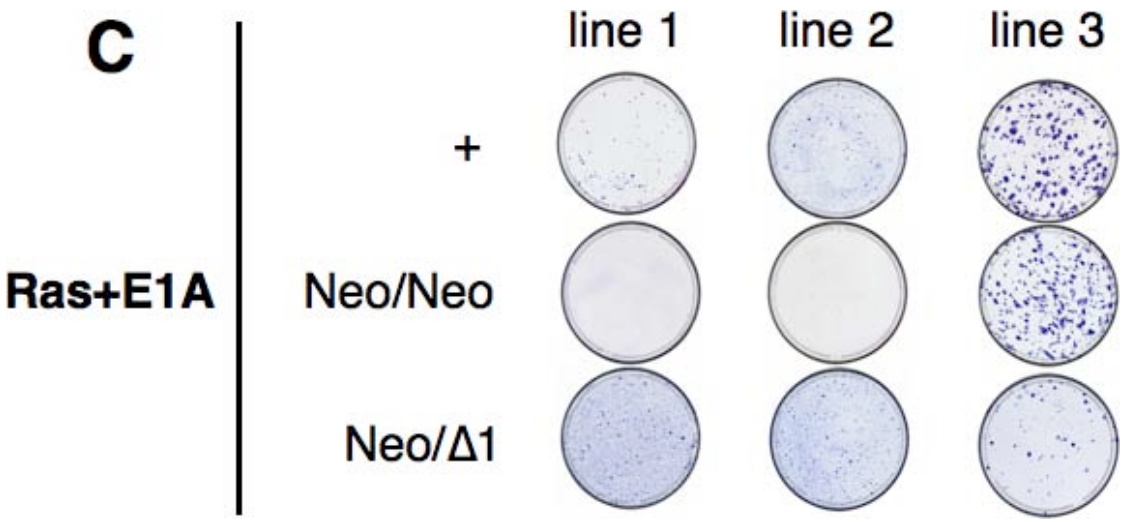


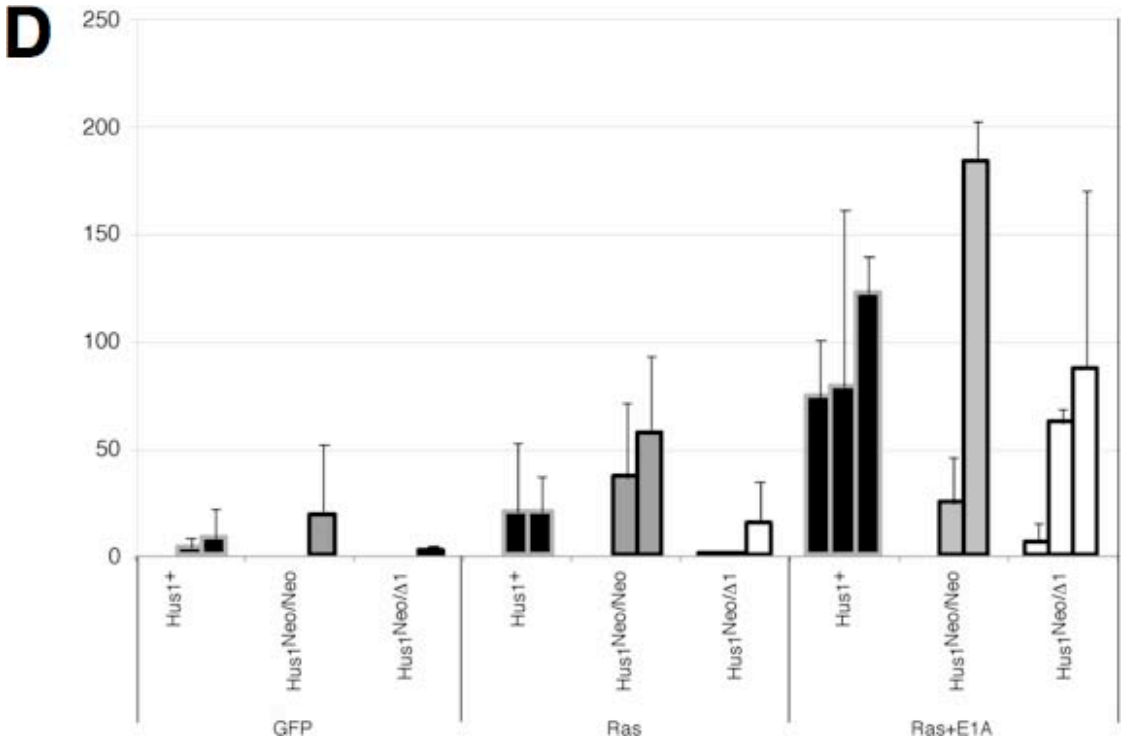

Figure 3.3 (Continued)

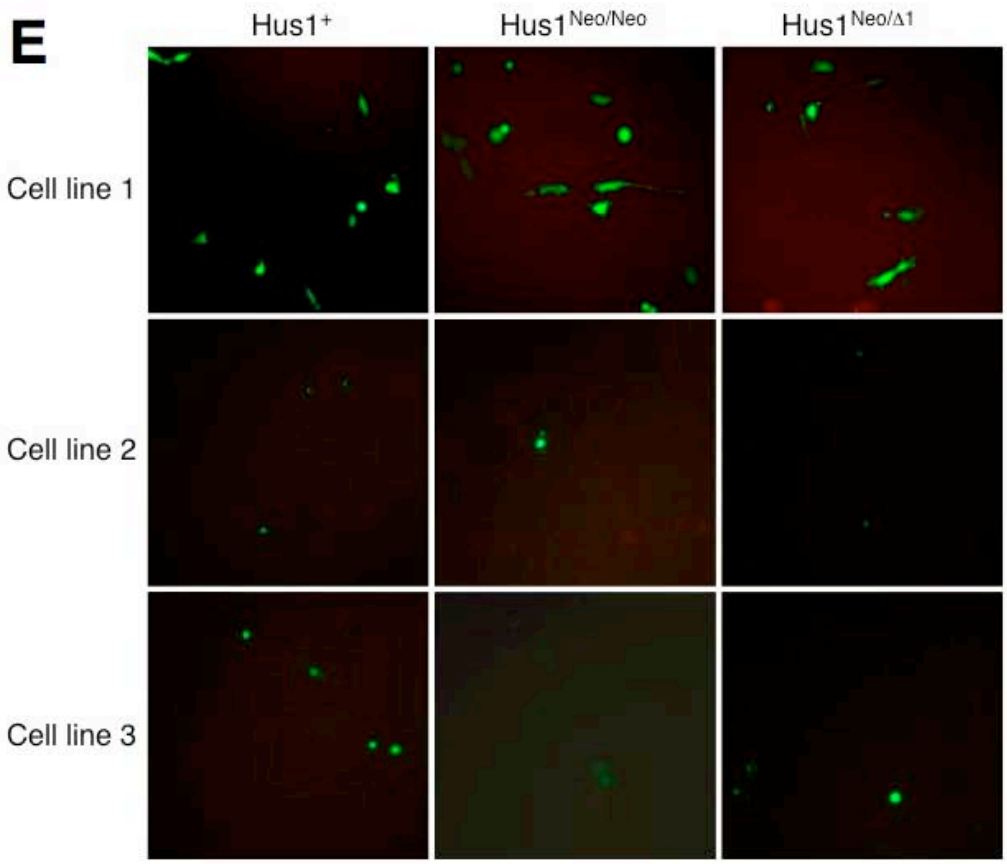

(74, 78, 122) following addition of Ras and E1A, which is expected, as two oncogenes in immortalized cells should efficiently transform cells.

Hus1$^{Neo/Neo}$ cells and Hus1$^{Neo/\Delta1}$ cells showed more variability between independent cell lines, though results were reproducible for each cell line. As with Hus1$^{+}$, only two Hus1$^{Neo/Neo}$ and one Hus1$^{Neo/\Delta1}$ cell lines formed few foci after transfection with activated Ras. This suggests that expression of a single activated oncogene in an immortalized cell line, regardless of genotype was not sufficient to induce efficient transformation. After addition of Ras and E1A, in two of three cell lines, Hus1$^{Neo/Neo}$ cells show very few foci (0 and 25), and the third cell line developed, on average, slightly more foci than Hus1$^{+}$ cells (183). This suggests that reduction of *Hus1* expression to about ~40% of wild-type levels, as is seen in Hus1$^{Neo/Neo}$ cells, results in a decreased probability of transformation, as two of three cell lines developed fewer foci. However, when a Hus1$^{Neo/Neo}$ cell line is able to undergo transformation, more foci form, suggesting that in some cases, these cells are more readily transformed.

Following addition of Ras and E1A, in the set of three Hus1$^{Neo/\Delta1}$ cell lines, two cell lines developed fewer foci than Hus1$^{+}$ on average (6.3 and 62), and one cell line grew a similar number of foci compared to Hus1$^{+}$ (87). Although the average number of foci formed by Hus1$^{Neo/Neo}$ or Hus1$^{Neo/\Delta1}$ cells was not significantly different from the number of foci formed by Hus1$^{+}$ cells ($p=0.727$ or $p=0.232$), there is a trend of decreased focus formation ability associated with decreased levels of HUS1 in some cells lines. This suggests that cells with severe reduction of *Hus1* expression are less prone to becoming transformed, although overcoming contact inhibition is still possible in certain cell lines. This variability between cell lines in Hus1$^{Neo/Neo}$ and Hus1$^{Neo/\Delta1}$ may be due to mutations that arise during immortalization and fixation of these mutations throughout the cell line. Despite the variability, these

data show that Hus1$^{Neo/Neo}$ and Hus1$^{Neo/\Delta 1}$ cells show decreased focus formation following addition of two oncogenes in a majority of cell lines, as compared to Hus1$^{+}$ cells.

**3.4.3 Reduced HUS1 levels result in impaired oncogene-induced anchorage independent growth.** In order to resolve the ambiguity seen in the focus formations assays (Figure 3.3) in Hus1$^{Neo/Neo}$ and Hus1$^{Neo/\Delta 1}$ MEFs, we next assessed the effect of reduced *Hus1* expression on transformation ability using anchorage independent growth, a more stringent test of transformation. Cell lines with reduced HUS1, which have an increased level of genomic instability, may be on the border of becoming transformed more readily or not being able to undergo transformation at all, and a more stringent assay may be a better indication of transformation ability and result in less variability between cell lines (Steele et al., 1996). Again, three independently derived, immortalized MEF cell lines were used for each genotype expressing incrementally reduced levels of HUS1. MEFs were infected with retroviruses carrying GFP, activated Ras, or activated Ras and Myc, and then grown in a suspension of soft agar. The number and size of macrocolonies, which directly related to the degree of transformation, was then determined (Freedman and Shin, 1974)(Figure 3.4). It was determined that cells of each genotype achieved similar levels of infection by evaluating percentage of cells expressing GFP 48 hours after infection (Figure 3.4 E).

When transduced with a vector expressing GFP, no cell lines formed colonies in soft agar, as expected. Two of three Hus1$^{+}$ MEF cell lines transduced with Ras alone formed many colonies (62 and 66). Whereas only one of three Hus1$^{Neo/Neo}$ cell lines and no Hus1$^{Neo/\Delta 1}$ cell lines were able to form colonies to the same extent when transduced with Ras alone, suggesting that reduced levels of *Hus1* expression decrease the probability of transformation after addition of a single oncogene (Figure 3.4 B and

***Figure 3.4*** **Cells with reduced Hus1 expression have a decreased capacity to form colonies in an anchorage independent growth transformation assay.** (A) Representative images of soft agar growth by three independently derived immortalized mouse embryonic fibroblasts (MEFs) of the indicated genotypes following infection with (two activated oncogenes (Ras and Myc). (B) Quantification of colony formation in soft agar. Foci were counted using ImageJ software. Bars indicate the average of at least two independent experiments on each of three cell lines, with dark shading indicating large colonies (>300 pixels) and light shading indicating small colonies (<300 pixels). (C) Images of immortalized cells following infection with a virus expressing GFP. All cell lines, regardless of genotype, showed similar infection efficiency. *[Experiment and figure by S. Yazinski and L. Gerwitz]*

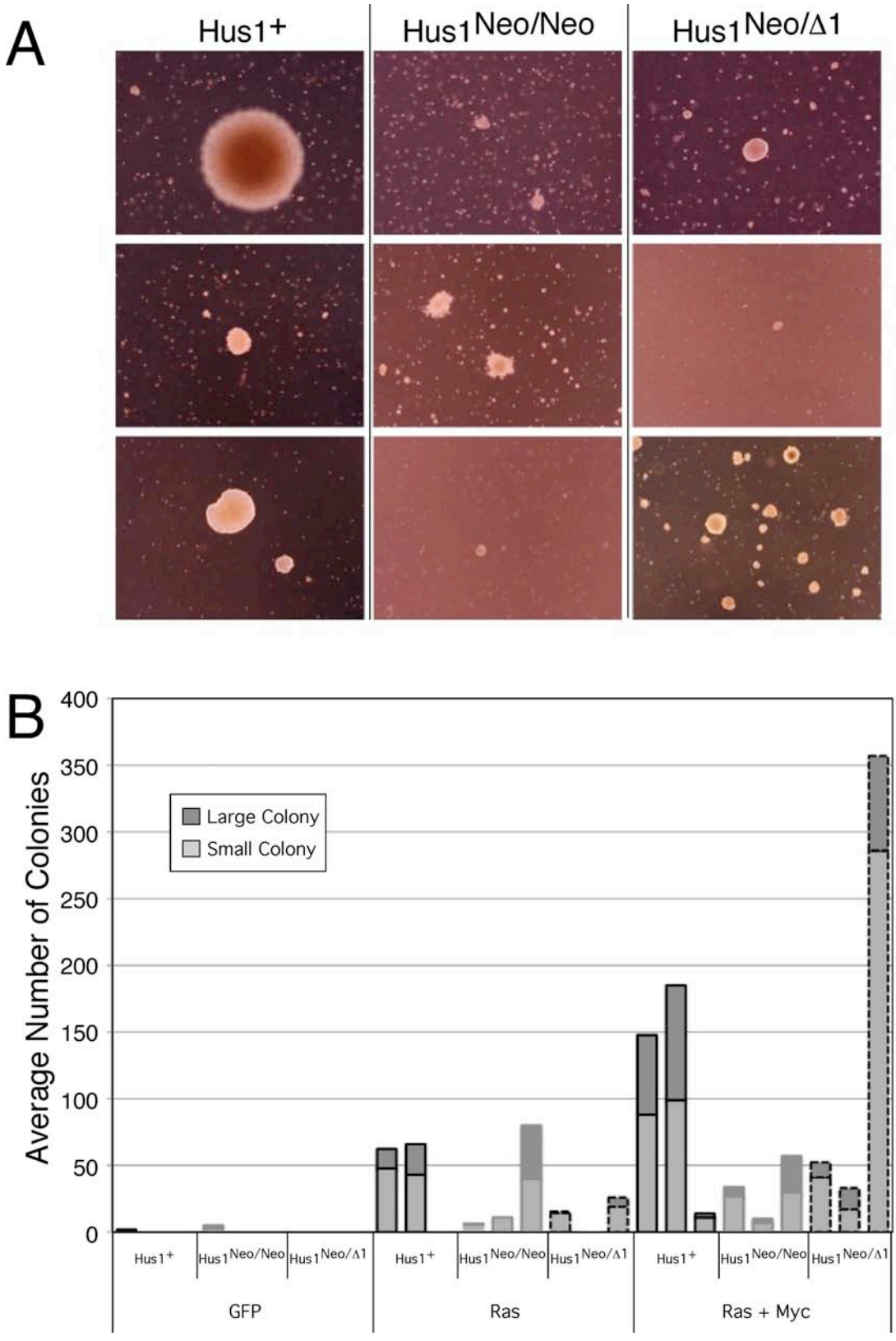
A
Hus1+
Hus1Neo/Neo
Hus1Neo/Δ1
B
Average Number of Colonies
400
350
300
250
200
150
100
50
0
Large Colony
Small Colony
Hus1+
Hus1Neo/Neo
Hus1Neo/Δ1
GFP
Ras
Ras + Myc

Figure 3.4 (Continuted)

C

D). Two of three Hus1$^{+}$ cell lines developed a large number of colonies following addition of Ras and Myc (148 and 185), while one Hus1$^{+}$ cell line developed very few colonies (14), suggesting, on average, Hus1$^{+}$ cells are readily transformed after addition of two active oncogenes (Figure 3.4 C and D). The cell line that was not able to form colonies is also morphologically distinct from the remaining 8 cell lines, in that it is more epithelial than fibroblastic, which may alter the behavior of this cell line in a colony formation assay (Figure 3.3). All three Hus1$^{Neo/Neo}$ cell lines showed reduced colony formation relative to Hus1$^{+}$ cells after infection with Ras and Myc (10, 33, 57). Two of three Hus1$^{Neo/\Delta 1}$ cell lines developed reduced colony numbers compared with Hus1$^{+}$ cell lines following infection with Ras and Myc (33 and 52) (Figure 3.4 C and D). The remaining Hus1$^{Neo/\Delta 1}$ cell line developed more than twice as many colonies (357) as the Hus1$^{+}$, however, the resulting colonies were smaller than the colonies of Hus1$^{+}$ cells (Figure 3.4 A and B). This suggests that cells with reduced levels of HUS1 that are able to be transformed are less able to proliferate to form large colonies in soft agar, as seen in Hus1$^{+}$ cells, following infection with activated oncogenes. Hus1$^{Neo/Neo}$ and Hus1$^{Neo/\Delta 1}$ cells more consistently show decreased transformation in comparison to Hus1$^{+}$ cells in this more stringent soft agar assay, as compared to a focus assay.

Taken together, these cell culture assays suggest that reduced levels of HUS1 may decrease the ability of cells to undergo transformation. Primary MEFs, that have not acquired any additional mutations from tissue culture, show that Hus1$^{Neo/Neo}$ cells and Hus1$^{Neo/\Delta 1}$ cells are less likely to be immortalized. Additionally, on average, cell lines with reduced HUS1, either Hus1$^{Neo/Neo}$ or Hus1$^{Neo/\Delta 1}$, were less likely to overcome contact inhibition and are less prone to undergo anchorage independent growth following oncogenic stimuli, both characteristics of transformation. This defect in proliferation following oncogenic-stimulation is not due to a universal decrease in

robustness in cells with reduced HUS1, as $Hus1^{Neo/\Delta 1}$ cells show resistance to treatment with puromycin, a translation inhibitor (Figure 3.5). This increased survival following treatment with puromycin shows that the inability of $Hus1^{Neo/\Delta 1}$ cells to proliferate to form either foci in a focus formation assay or colonies in an anchorage independent growth assay as a result of oncogene expression, not a general heightened sensitivity to stress. Taken together, these data indicate that reduced levels of HUS1 result in decreased transformation.

**3.4.4 Reduced *Hus1* expression results in decreased tumor size in a cell transplantation assay.** In order to determine the effect of reduced levels of *Hus1* expression on transformation in a more stringent assay, $Hus1^{+/Neo}$, $Hus1^{Neo/Neo}$, and $Hus1^{Neo/\Delta 1}$ MEFs were infected with an ecotropic virus expressing GFP or a virus expressing Ras and Myc from the same vector (Figure 3.6). An equal number of cells from each genotype were injected into the flanks of wild-type 129 mice, and tumors were allowed to grow for four weeks. Mice that were injected with $Hus1^{+}$ cells, $Hus1^{Neo/Neo}$ cells, or $Hus1^{Neo/\Delta 1}$ cells infected with virus expressing GFP formed no tumors. Mice injected with $Hus1^{+/+}$ cells infected with a virus expressing Ras and Myc grew the largest tumors, while mice that were injected with $Hus1^{Neo/Neo}$ cells or $Hus1^{Neo/\Delta 1}$ cells infected with a virus expressing Ras and Myc grew small tumors. These preliminary results show that cells expressing reduced levels of HUS1 are less able to become transformed as measured by this stringent assay of transformation, which agree with our previous cell culture data. This transplantation assay is a rigorous way to evaluate transformation abilities, which may reduce some variability seen between cell lines of the same genotype in other less stringent assays and this assay will need to be repeated with additional cell lines expressing reduced levels of HUS1. Additionally, this assay can be performed using host mice expressing

***Figure 3.5*** **Reduced Hus1 expression caused increased puromycin resistance treatment compared to a cell line with wild-type Hus1 expression.** (A-B) Three independently derived, immortalized MEF cell lines of the indicated genotypes were treated with the indicated dose of puromycin for ten days. The cells were fixed and stained with crystal violet overnight. (A) The first set of $Hus1^{Neo/\Delta 1}$ MEFs shows increased resistance to puromycin treatment at 0.5 and 1.0μg/ml compared to $Hus1^{+}$ MEFs. (B) A second and third set of $Hus1^{+}$, $Hus1^{Neo/Neo}$, and $Hus1^{Neo/\Delta 1}$ MEFs were tested for puromycin resistance. The second $Hus1^{Neo/\Delta 1}$ cell line and the second $Hus1^{Neo/Neo}$ cell line showed increased resistance to puromycin treatment at 1.0μg/ml compared to $Hus1^{+}$ MEFs, while a third $Hus1^{Neo/\Delta 1}$ cell line and a third $Hus1^{Neo/Neo}$ cell line showed similar sensitivity to puromycin treatment at 1.0μg/ml compared to $Hus1^{+}$ MEFs. *[Experiment by S. Yazinski; Figure by L. Gerwitz]*

A

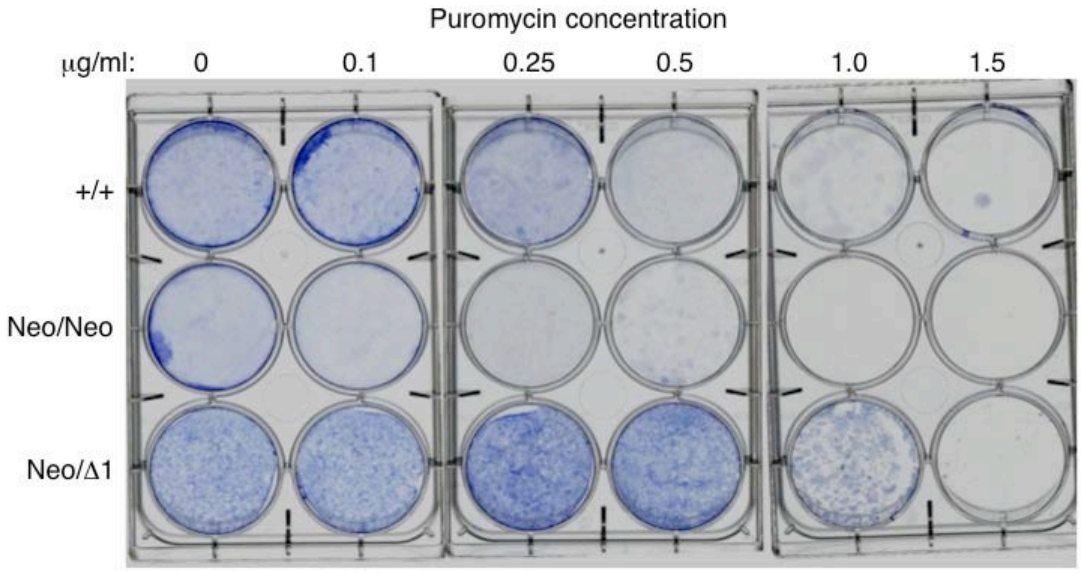

Figure 3.5 (Continued)

B

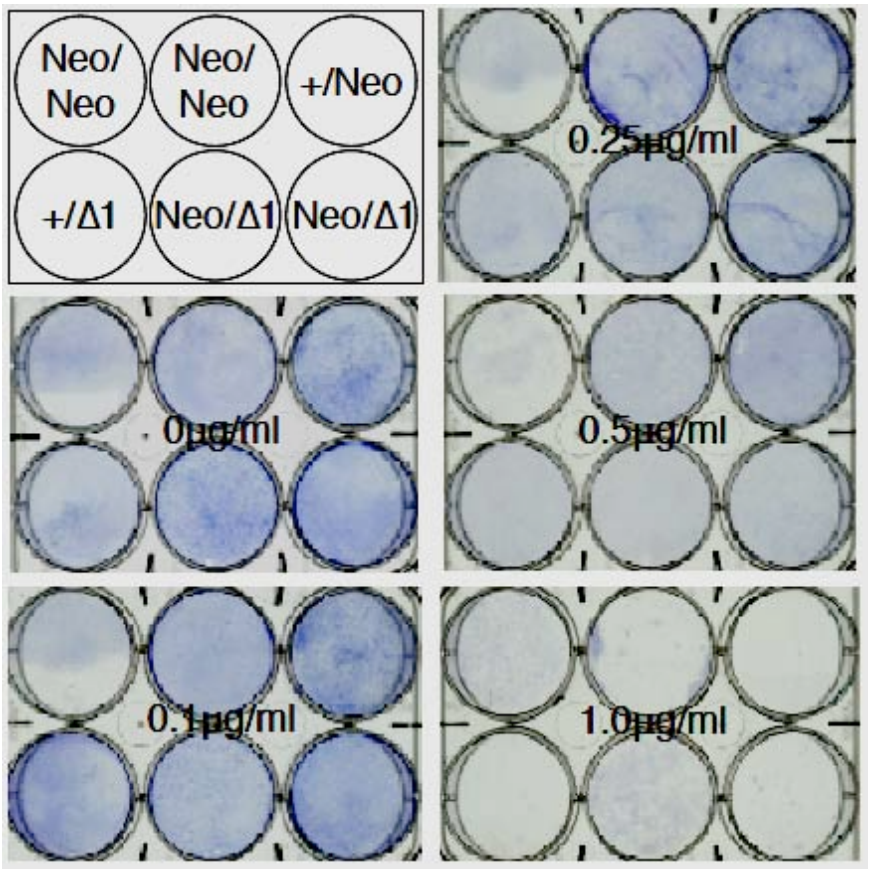

***Figure 3.6*** **Transplantation of Hus1$^{+}$ cells infected with a virus expressing Ras and Myc results in larger tumors than transplantation of Hus1$^{Neo/Neo}$ and Hus1$^{Neo/\Delta 1}$ cells infected with a virus expressing Ras and Myc.** (A) Images of mice injected with Hus1$^{+}$, Hus1$^{Neo/Neo}$, or Hus1$^{Neo/\Delta 1}$ cells that were infected with a virus expressing GFP or expressing Ras and Myc. (B) Images of tumors resulting from injection with Hus1$^{+}$, Hus1$^{Neo/Neo}$, or Hus1$^{Neo/\Delta 1}$ cells that were infected with a virus expressing Ras and Myc. No tumors developed from cells of any genotypes infected with a virus expressing GFP. Scale bar represents 1cm. (C and D) (C) Average size and (D) average weight of tumors resulting from injection with Hus1$^{+}$ (n = 3), Hus1$^{Neo/Neo}$ (n = 2), or Hus1$^{Neo/\Delta 1}$ (n = 2) cells that were infected with a virus expressing Ras and Myc. *[Experiment by S. Yazinski and L. Gerwitz]*

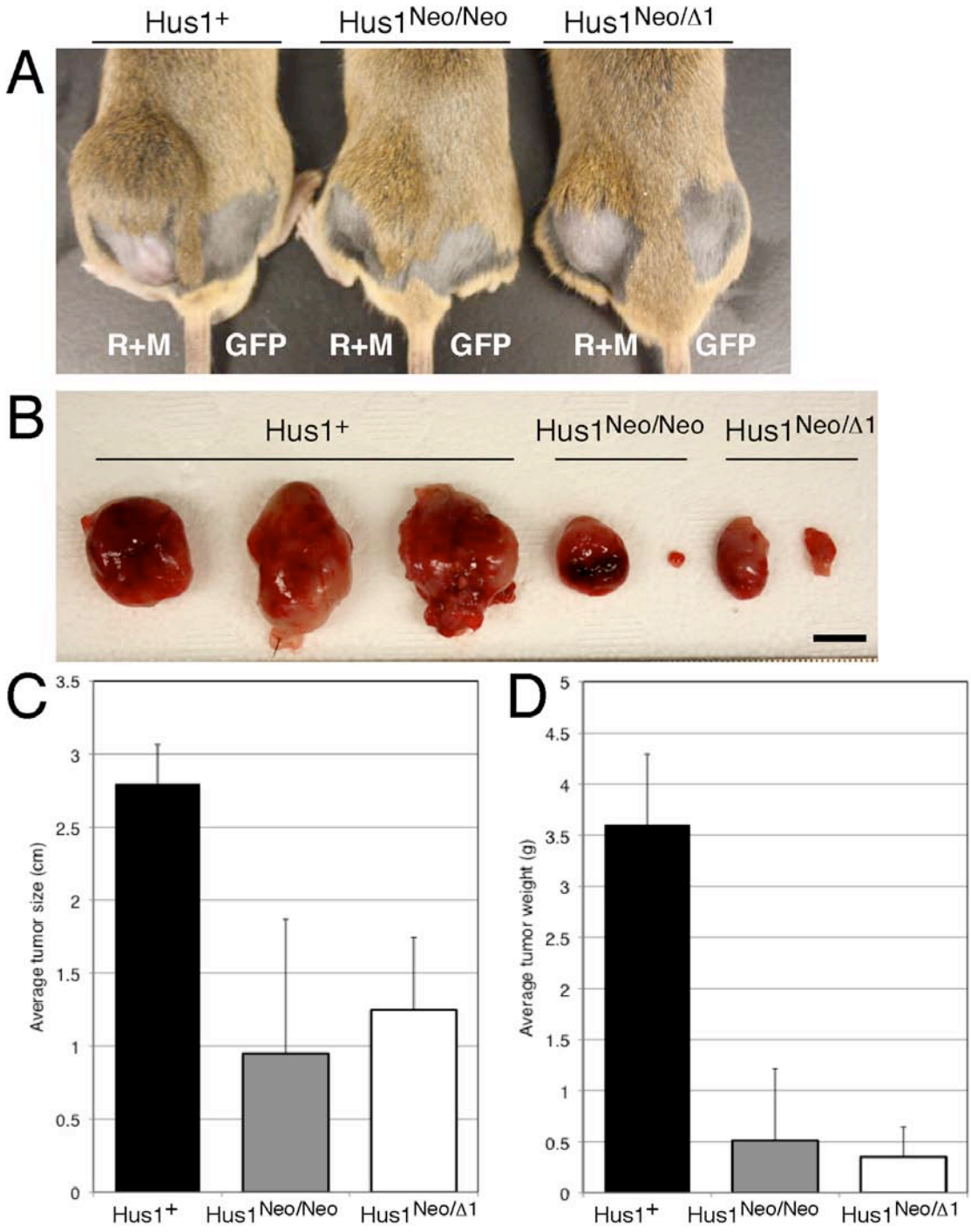
A
Hus1+
Hus1Neo/Neo
Hus1Neo/Δ1
R+M
GFP
R+M
GFP
R+M
GFP
B
Hus1+
Hus1Neo/Neo
Hus1Neo/Δ1
C
Average tumor size (cm)
3.5
3
2.5
2
1.5
1
0.5
0
Hus1+
Hus1Neo/Neo
Hus1Neo/Δ1
D
Average tumor weight (g)
5
4.5
4
3.5
3
2.5
2
1.5
1
0.5
0
Hus1+
Hus1Neo/Neo
Hus1Neo/Δ1

incrementally reduced levels of HUS1 in order to determine the effect of reduced HUS1 levels in surrounding cells on support of tumor development and growth.

**3.4.5 Mice with reduced levels of *Hus1* expression develop fewer and smaller papillomas than Hus1$^{+}$ mice in a two-step carcinogenesis model.** The cell culture results suggest that cells with reduced levels of HUS1 were resistant to transformation, and these results were more consistent in more stringent assays. We next tested the effect of reduced HUS1 on transformation using an *in vivo* animal model, by making use of the well-characterized carcinogen-induced skin papilloma model of tumorigenesis. In this experiment, mice with reduced levels of HUS1 were treated with 12-7-dimethylbenz(a)-anthracene (DMBA) and 12-O-tetradecanoylphorbol-13-acetate (TPA) to induce skin papillomas. DMBA causes specific A-T transversions at the second nucleotide of codon 61 of the Harvey-ras (H-ras) gene, resulting in H-ras activation, and is a well-characterized tumor initiator (Quintanilla et al., 1986). TPA is potent tumor promoter that acts through activation of protein kinase C (PKC) (Angel et al., 1987). DMBA is applied once to the skin, while TPA is applied twice weekly for twenty weeks, resulting in skin papilloma formation. Mice in anagen phase of the hair cycle were not used in the two-step skin carcinogenesis assay, as this phase features more stem cell proliferation. DMBA or TPA treatment of skin with an increased number of stem cells may result in altered papilloma numbers relative to treatment skin with fewer stem cells.

Based on the results of tissue culture assays, we anticipated that fewer tumors would develop on the back of Hus1$^{Neo/Neo}$ and Hus1$^{Neo/\Delta 1}$ mice, as the skin cells would be less prone to transformation. At each application of TPA, tumor latency, size, and number were measured. Hus1$^{+}$ mice developed the most and the largest papillomas, on average (Figure 3.7). Hus1$^{Neo/Neo}$ mice, with moderately reduced *Hus1* expression,

***Figure 3.7*** **Hus1$^{Neo/Neo}$ and Hus1$^{Neo/\Delta1}$ mice develop fewer and smaller average largest papillomas than Hus1$^{+}$controls.** Hus1$^{+}$ (n=18) and Hus1$^{Neo/\Delta1}$ (n=18), and Hus1$^{+}$ (n=19) and Hus1$^{Neo/Neo}$ (n=16), mice were treated with a single dose of DMBA and repeated applications of TPA to induce papilloma formation. Tumor development was monitored for 20 weeks. (A and B) The average number of papillomas per mouse was plotted for each day. (A) Hus1$^{Neo/\Delta1}$ and (B) Hus1$^{Neo/Neo}$ mice had significantly fewer papillomas when compared with control mice ($p<0.001$ and $p=0.004$, respectively, determined by mixed model analysis: linear regression with covariant structure using SPSS software). (C and D) The average size of the largest papilloma per mouse was plotted for each day. Hus1$^{Neo/\Delta1}$ mice had significantly smaller average largest papillomas than control mice ($p < 0.001$), while Hus1$^{Neo/Neo}$ papillomas were not significantly smaller ($p=0.605$). (E and F) Fraction of tumor free survival for (E) Hus1$^{+}$ compared to Hus1$^{Neo/\Delta1}$ mice and (F) Hus1$^{+}$ compared to Hus1$^{Neo/Neo}$ over 20 weeks is not significantly different between genotypes ($p=0.420$ and $p=0.077$, by Log Rank Comparison). Hus1$^{Neo/\Delta1}$ mice are the first to develop papillomas, but show a decreased risk for tumor development after 67 days ($p<0.05$ by Log Rank Hazard Analysis). (G and H) Representative images of (G) Hus1$^{+/+}$ (right) and Hus1$^{Neo/\Delta1}$ (left) and (H) Hus1$^{+/Neo}$ (right) and Hus1$^{Neo/Neo}$ (left) sex-matched littermates following DMBA/TPA treatment at 140 days after DMBA treatment. *[Experiment by L. Gerwitz and S. Yazinski, figure by S. Yazinski]*

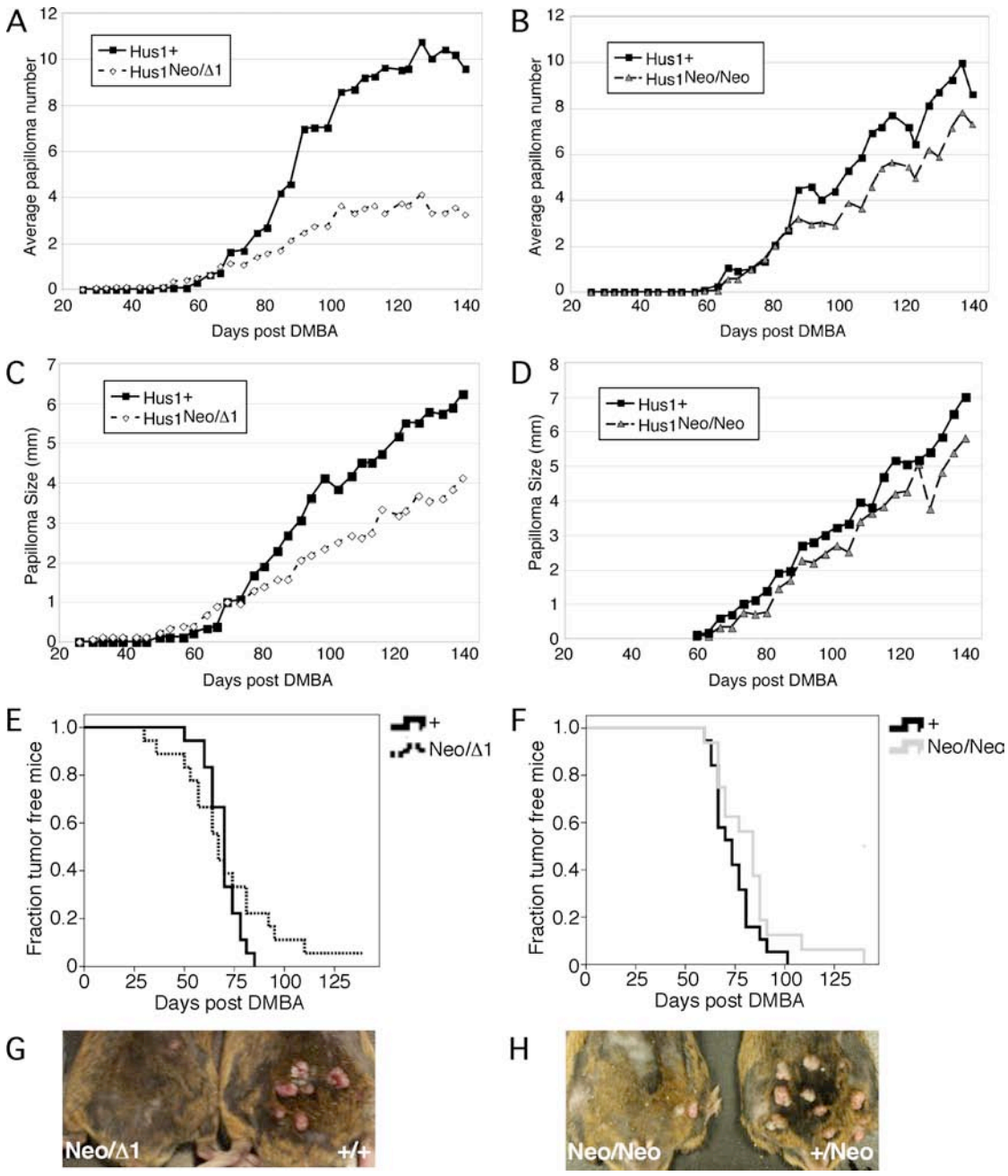
A
Average papilloma number
Hus1+
Hus1Neo/Δ1
Days post DMBA
B
Average papilloma number
Hus1+
Hus1Neo/Neo
Days post DMBA
C
Papilloma Size (mm)
Hus1+
Hus1Neo/Δ1
Days post DMBA
D
Papilloma Size (mm)
Hus1+
Hus1Neo/Neo
Days post DMBA
E
Fraction tumor free mice
+
Neo/Δ1
Days post DMBA
F
Fraction tumor free mice
+
Neo/Neo
Days post DMBA
G
Neo/Δ1
+/+
H
Neo/Neo
+/Neo

developed fewer papillomas than $Hus1^{+}$ mice (p=0.004) (Figure 3.7 B). Interestingly, a few $Hus1^{Neo/\Delta1}$ mice, with the lowest level of *Hus1* expression, developed papillomas with a slightly shorter latency than either $Hus1^{+}$ or $Hus1^{Neo/Neo}$ mice, though this difference in latency was not significant; however, overall tumor-free survival was not significantly different among genotypes (Figure 3.7 E and F). $Hus1^{Neo/\Delta1}$ mice had a reduced risk for papilloma development after 67 days when compared with $Hus1^{+}$ mice ($p < 0.05$ by Log Rank Hazard Analysis). Although $Hus1^{Neo/\Delta1}$ mice were the first to form papillomas, these mice ultimately developed the fewest ($p <0.001$ when compared with $Hus1^{+}$) and smallest papillomas ($p <0.001$ when compared with $Hus1^{+}$), on average (Figure 3.7 A and C). Although papillomas from $Hus1^{Neo/\Delta1}$ mice were significantly smaller than papillomas from $Hus1^{+}$ mice, the proliferation rate within papillomas of each genotype, as measured by BrdU incorporation, was not significantly different ($p = 0.97$) (Figure 3.8). Additonally, there was no change in malignancy between papillomas arising in $Hus1^{+}$ and $Hus1^{Neo/\Delta1}$, as only a single papilloma from $Hus1^{+}$ mice underwent malignant conversion, and no papillomas from a $Hus1^{Neo/\Delta1}$ mouse progressed to malignancy. These *in vivo* tumorigenesis data were consistent with the cell culture data, which suggested that $Hus1^{Neo/Neo}$ and $Hus1^{Neo/\Delta1}$ cells are less able to become transformed, though small number of $Hus1^{Neo/Neo}$ and $Hus1^{Neo/\Delta1}$ cells are able to undergo transformation and form papillomas. Furthermore, the *in vivo* data supports that a reduction in *Hus1* expression impairs transformed cell growth, as papillomas were smaller.

### 3.4.6 $Hus1^{Neo/\Delta1}$ mice are not sensitive to the initial treatments of DMBA or TPA.

There are at least two possible explanations for the correlation between reduced *Hus1* expression and the reductions in papilloma number and largest size. First, impaired

***Figure 3.8*** **Papillomas from Hus1$^{Neo/\Delta1}$ mice and Hus1$^{Neo/\Delta1}$ cells have similar proliferation rates.** (A) Papillomas from Hus1$^{+}$ and Hus1$^{Neo/\Delta1}$ mice were harvested, fixed, and stained for BrdU incorporation. Sections were counter stained by hematoxylin. (B) Quantification of BrdU positive cells in papillomas of Hus1$^{+}$ and Hus1$^{Neo/\Delta1}$ mice. There was no significant difference between BrdU staining of papillomas of Hus1$^{+}$ and Hus1$^{Neo/\Delta1}$ mice ($p = 0.972$, by Student's t-Test). Three 40X images were quantified for three mice of each genotype, with error bars denoting standard deviation. *[Experiment and figure by S. Yazinski]*

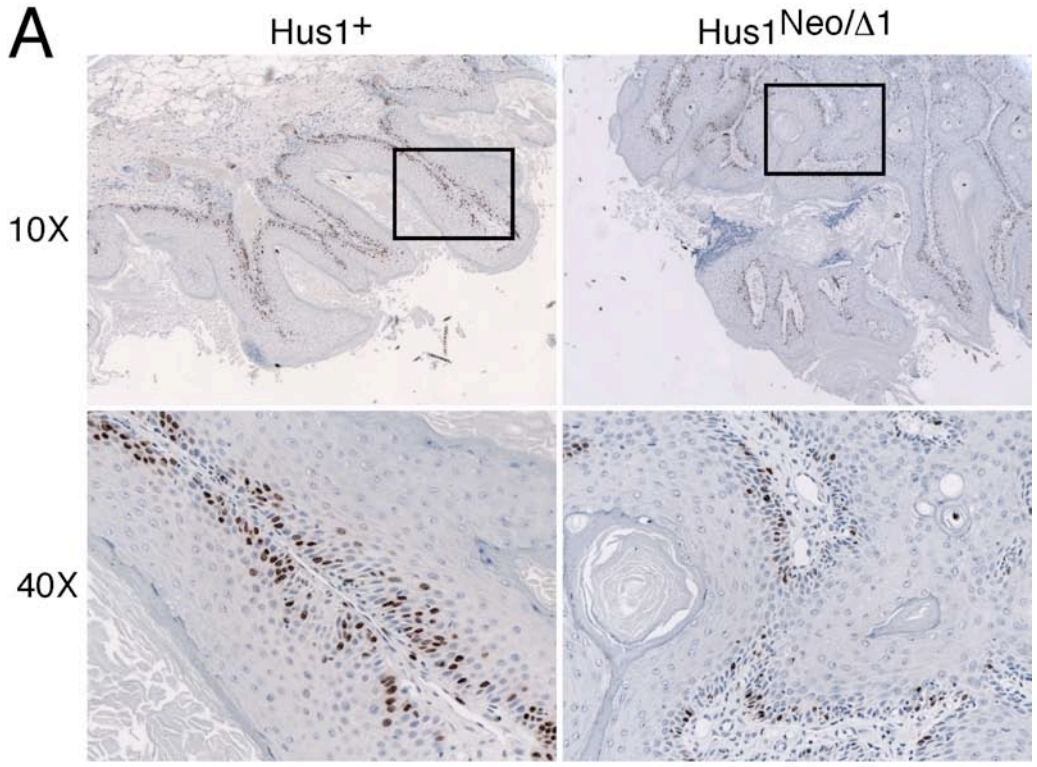
A
Hus1+
Hus1Neo/Δ1
10X
40X

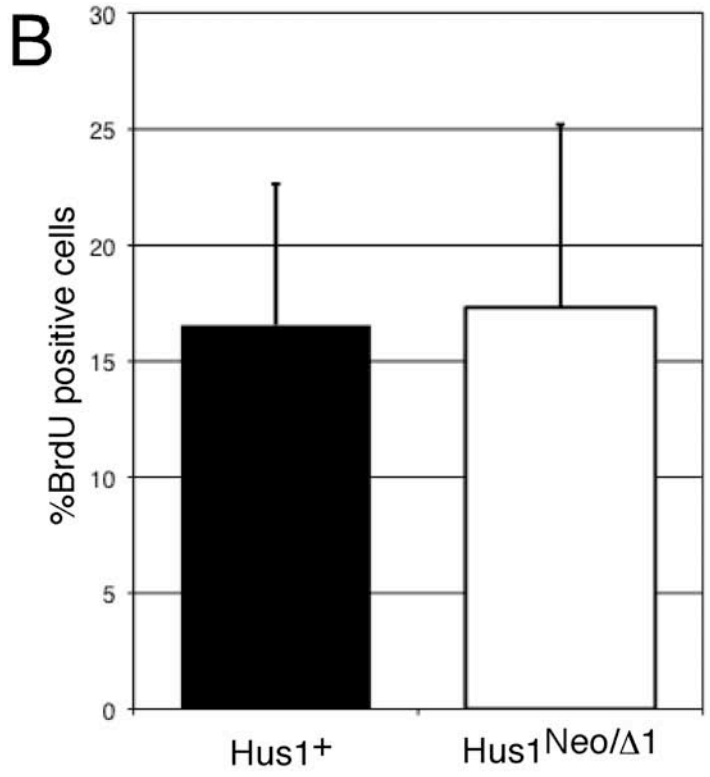
B
%BrdU positive cells
30
25
20
15
10
5
0
Hus1+
Hus1Neo/Δ1

checkpoint function due to reduced *Hus1* expression in Hus1$^{Neo/\Delta 1}$ cells may prevent transformation as these cells are unable to cope with the increased genomic stress associated with neoplastic proliferation, resulting in cell death. A second, more trivial, explanation maybe that a decreased ability to respond to genomic damage may sensitize Hus1$^{Neo/\Delta 1}$ cells to the initial treatments of DMBA or TPA, causing early cell death and few surviving cells capable of forming papillomas. To test whether cells with reduced *Hus1* expression were sensitive to the initial treatments of DMBA or TPA, we first treated primary MEFs with increasing doses of DMBA or TPA, and assessed for cell survival using a trypan blue exclusion assay (Figure 3.9 A and B). Hus1$^{Neo/\Delta 1}$ cells showed no increased sensitivity to either DMBA or TPA relative to Hus1$^{+}$ MEFs in cell culture, as both genotypes showed similar survival at each dose of DMBA or TPA.

While these results suggest that Hus1$^{Neo/\Delta 1}$ cells are not sensitive to DMBA or TPA treatment, we next wanted to test the sensitivity of the skin cells expressing reduced levels of HUS1 to the DMBA or TPA treatment *in vivo*. A single dose of DMBA or TPA was administered to the shaved skin of mice, and the skin was harvested 24 hours later. These mice were not in the anagen phase of hair cycle, reducing the probability that proliferation of stem cell pools at the hair follicle affected our results. Next, BrdU and TUNEL assays were performed to assess the rates of proliferation and apoptosis, respectively, by calculating the percentage of positively stained epithelial skin cells. Following DMBA treatment, the proliferation of cells was not significantly different from cells treated with acetone alone, regardless of the genotype or dose of DMBA ($p=0.777$) (Figure 3.10 A and C). Similarly, the percentage of cells undergoing apoptosis following each dose was similar to that of cells treated with acetone alone ($p=0.908$) (Figure 3.10 B and C). This indicates that acute treatment of DMBA at these doses does not affect proliferation or cell death.

***Figure 3.9*** **Hus1$^{Neo/\Delta1}$ cells do not show increased sensitivity to DMBA or TPA in culture.** Primary Hus1$^{+}$ or Hus1$^{Neo/\Delta1}$ MEFs were treated with a single dose of (A) TPA (0 ng/ml, 100 ng/ml, or 1,000 ng/ml) or (B) DMBA (0 μg/ml, 1 μg/ml, or 20 μg/ml). 24 hours after treatment, cells were harvested, stained with trypan blue, and counted to assess cell survival relative to untreated cells. Each assay was done in triplicate using three different primary cell lines. *[Experiment and figure by S. Yazinski]*

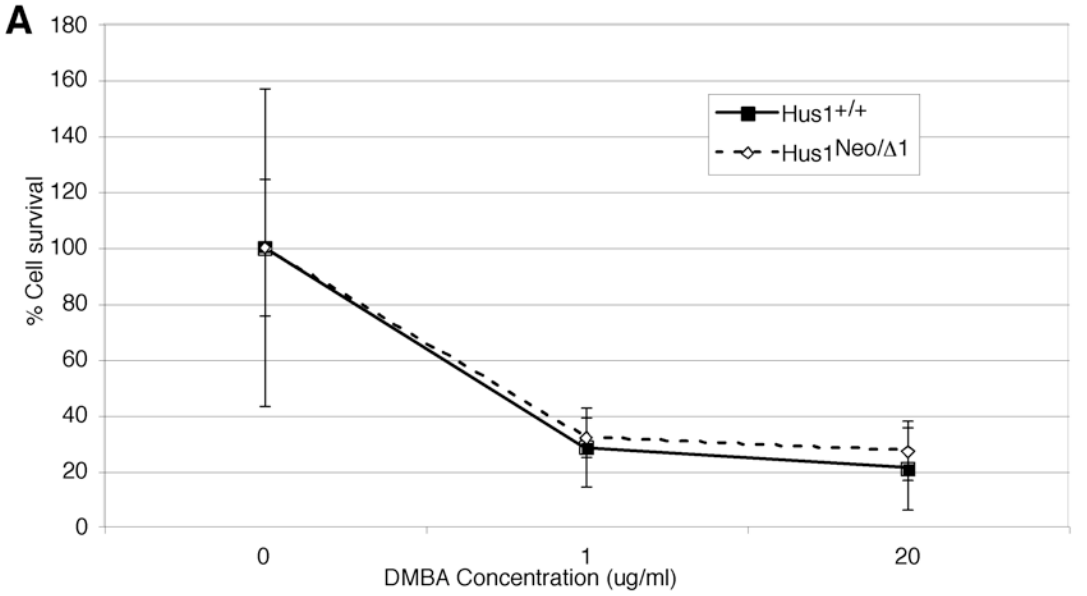
A
180
160
140
120
100
80
60
40
20
0
% Cell survival
Hus1+/+
Hus1Neo/Δ1
0
1
20
DMBA Concentration (ug/ml)

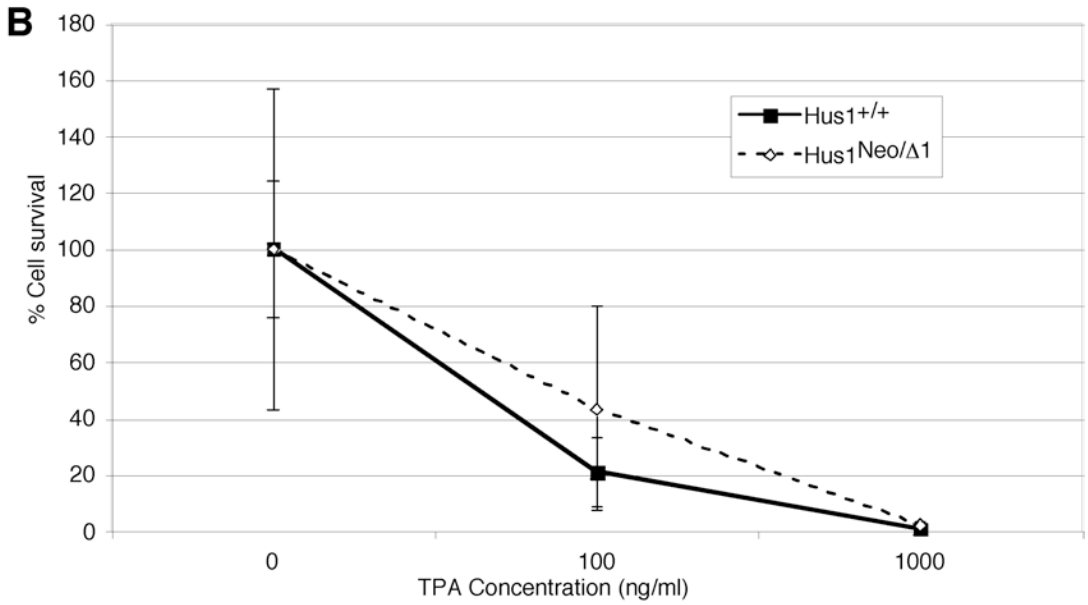
B
180
160
140
120
100
80
60
40
20
0
% Cell survival
Hus1+/+
Hus1Neo/Δ1
0
100
1000
TPA Concentration (ng/ml)

***Figure 3.10*** **Skin of Hus1$^{Neo/\Delta1}$ mice and Hus1$^{Neo/\Delta1}$ cells do not show increased sensitivity to DMBA or TPA.** Hus1$^{+}$ and Hus1$^{Neo/\Delta1}$ mice were shaved and treated with a single dose of DMBA or TPA. Skin was harvest and stained for apoptosis and BrdU. (A and B) Quantification of (A) BrdU positive and (B) TUNEL positive cells in skin sections from mice of the indicated genotype treated with a single dose of DMBA to determine the percentage of proliferating and apoptotic cells, respectively. (C) Skin sections from control and Hus1$^{Neo/\Delta1}$ mice treated with a 25nmol of DMBA stained by BrdU and TUNEL assay. Arrows point to brown, positive cells. Sections were counterstained with hematoxylin. (D and E) Quantification of (D) BrdU positive and (E) TUNEL positive cells in skin sections from mice of the indicated genotype treated with a single dose of TPA to determine the percentage of proliferating and apoptotic cells, respectively. (F) Representative skin sections from control and Hus1$^{Neo/\Delta1}$ mice treated with a 25μg/ml dose of TPA stained by BrdU and TUNEL assay. Arrows point to brown, positive cells. Sections were counterstained with hematoxylin. DMBA and TPA experiments were each performed on three mice of each genotype and three fields of view were counted to determine the rates of proliferation and apoptosis in each mouse. Error bars denote standard deviation. Statistical analysis was by a random coefficient model with random slope and intercept. The fixed effects were the genotype, dose, and their interaction term. *[Experiment and figure by L. Gerwitz, S. Yazinski, and T. Shand]*

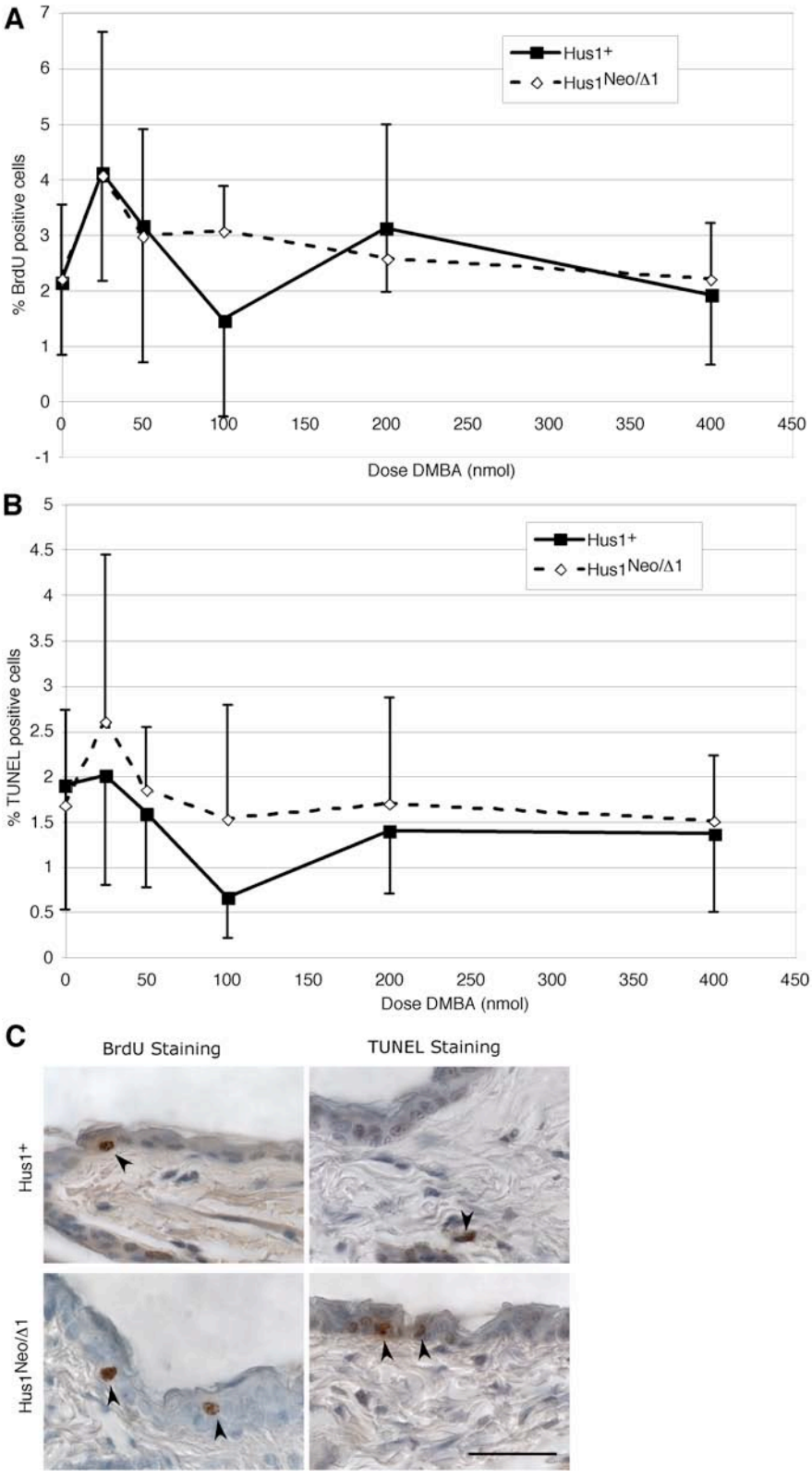
A
Hus1+
Hus1Neo/Δ1
% BrdU positive cells
Dose DMBA (nmol)
B
Hus1+
Hus1Neo/Δ1
% TUNEL positive cells
Dose DMBA (nmol)
C
BrdU Staining
TUNEL Staining
Hus1+
Hus1Neo/Δ1

Figure 3.10 (Continued)

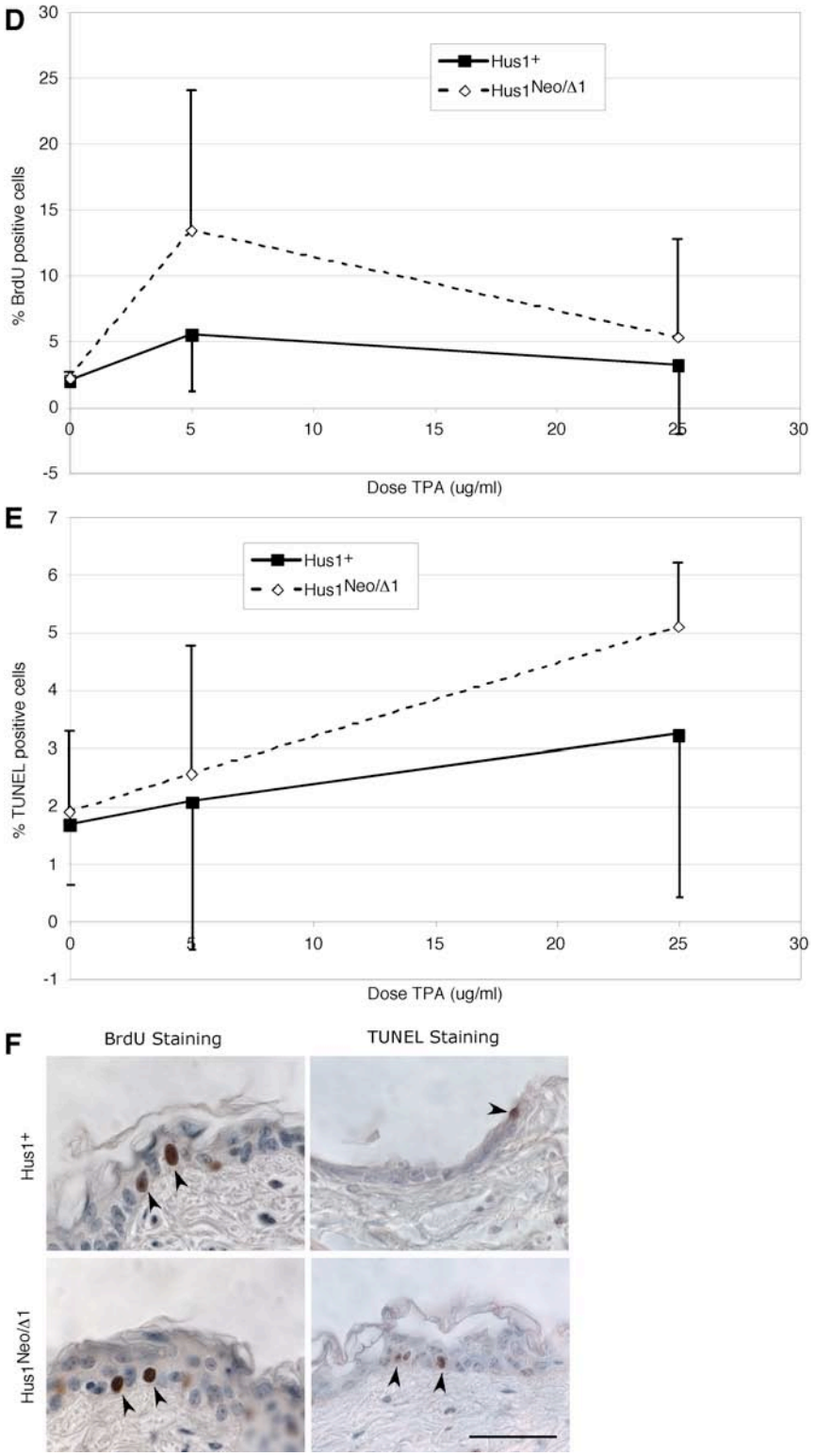

Following a low dose of TPA treatment (5μg), skin cells of both genotypes showed increased proliferation relative to acetone alone treated samples, and a moderate, but insignificant, increase in apoptosis (Figure 3.10 D - F). Following a higher dose of TPA (25μg), skin cells of both genotypes showed no change in proliferation relative to acetone alone treated samples, along with a larger increase in apoptosis (Figure 3.10 D – F). This increased cell death at the higher dose of TPA may account for the decreased proliferation levels compared to the lower dose of TPA. There was no difference in either cell death or proliferation between genotypes following TPA treatment ($p=0.696$ and $p=0.352$, respectively). Taken together, the rates of proliferation and apoptosis were not significantly different between the skin of $Hus1^{+}$ and $Hus1^{Neo/\Delta 1}$ mice among all doses of DMBA and TPA tested (Figure 3.10). These data suggest that decreased papilloma formation in $Hus1^{Neo/\Delta 1}$ mice is not due to a proliferation defect or increased sensitivity to either DMBA or TPA, but rather an inability of $Hus1^{Neo/\Delta 1}$ cells to survive the increased stress associated with transformation.

### *3.5 DISCUSSION*

Because defects in DNA damage checkpoints have been shown both to result in tumorigenesis and to inhibit tumor growth, we set out to determine how reduced levels of HUS1, a component of the ATR pathway, affects the process of transformation and tumor development. We have made use of the previously described *Hus1* allelic series, which genetically expresses incrementally reduced levels of wild-type HUS1 protein, allowing us to bypass the embryonic lethality associated with complete *Hus1* inactivation (Levitt et al., 2007). Primary cells with reduced levels of HUS1 exhibited a decreased propensity of becoming immortalized following transfection with large T antigen, a potent oncogene, suggesting that these cells may also be less likely to undergo transformation.

In order to test this, immortalized cell lines expressing reduced levels of HUS1 were then tested for transformation capability using two well-characterized assays, focus formation and anchorage independent growth. While all $Hus1^{+}$ cell lines were readily transformed after addition of two oncogenes, not all $Hus1^{Neo/Neo}$ and $Hus1^{Neo/\Delta1}$ cell lines were able to be transformed. Instead, in two of three $Hus1^{Neo/Neo}$ cell lines tested, transfected cells were not able to form foci in a contact inhibition assay, and in two of three cell lines, infected cells were not able to form colonies in soft agar. Similarly, in two of three $Hus1^{Neo/\Delta1}$ cell lines, fewer foci formed following addition of two oncogenes, and in two of three cell lines, a greatly reduced number of colonies form in soft agar. In the one set of cell lines tested, $Hus^{+}$ cells expressing two oncogenes were readily transformed forming large tumors in a transplantation assay, while $Hus1^{Neo/Neo}$ and $Hus1^{Neo/\Delta1}$ formed very small tumors. Importantly, these results were reproducible within each cell line, suggesting that the differences between cell lines were not due to technical difficulties, but rather genetic differences, perhaps due to an accumulation of mutations acquired during immortalization. Because $Hus1^{Neo/Neo}$

and Hus1$^{Neo/\Delta 1}$ cells show higher levels of genomic instability in cell culture, these cells may be less likely to survive the process of transformation, as seen in the more stringent anchorage independent growth and transplantation assays. However, this level of genomic instability may allow cells to overcome a less stringent test of transformation, such as contact inhibition. While these data suggest that reduced levels of *Hus1* expression may inhibit transformation ability, cell culture data may not recapitulate the effect of reduced HUS1 in an *in vivo* animal model.

In order to determine if cells with reduced HUS1 have reduced transformation ability in a mouse model, we made use of the well-characterized two-step skin carcinogenesis model of tumorigenesis using DMBA and TPA treatment. Because the resulting papillomas arise directly from clonal expansion of the initially transformed cells, the number of papillomas directly relates to the transformation potential of the cells (Yuspa, 1998). Initial time points reveal that a small number of Hus1$^{Neo/\Delta 1}$ mice developed tumors with a shorter latency than Hus1$^{Neo/Neo}$ or Hus1$^{+}$ mice, suggesting that the severe genomic instability and checkpoint defect of an initiated cell with reduced HUS1 can result in decreased tumor latency. Overall, Hus1$^{Neo/\Delta 1}$ mice developed strikingly fewer papillomas than Hus1$^{+}$ mice, while Hus1$^{Neo/Neo}$ mice developed an intermediate number. This result demonstrates that overall, mice with reduced levels of HUS1 show reduced transformation capacity *in vivo*, however, a small number of tumors are still able to form. This correlates with the cell culture data, which shows that in most cell lines expressing reduced HUS1 levels, cells show reduced ability to be transformed, but that transformation is possible in at least one cell line of each genotype. Taken together, these data suggest that reduced levels of HUS1 are not compatible with transformation and tumor development.

Reduced levels of HUS1 also correlated with reduced tumor size. When comparing the largest papilloma on the back of each mouse, Hus1$^{Neo/\Delta 1}$ mice

developed smaller papillomas than $Hus1^{+}$ mice, and $Hus1^{Neo/Neo}$ mice developed an intermediate sized average largest papilloma. This suggests that cells with reduced levels of HUS1 cannot expand to form papillomas as large as $Hus1^{+}$ papillomas. This is consistent with the soft agar assay data, which shows that the colonies that are able to form in $Hus1^{Neo/\Delta 1}$ cells are much smaller than $Hus1^{+}$ colonies, demonstrating difficulty to undergo rapid, oncogene-induced proliferation when there are insufficient levels of HUS1.

In some mouse models, a decrease in papilloma formation can be attributed to increased sensitivity to DMBA or TPA treatment. For example, BRCA2+/- mice, which express reduced levels of BRCA2, a DNA damage repair protein, develop papillomas at a slower rate than $BRCA2^{+/+}$ mice following DMBA treatment, but this is due to $BRCA2^{+/-}$ cell sensitivity to DMBA resulting in apoptosis (Yan et al., 2004). In the case of $Hus1^{Neo/Neo}$ and $Hus1^{Neo/\Delta 1}$, reduced papilloma number and size is not due to increased sensitivity, but rather due to a decreased ability of cells with reduced HUS1 to become transformed. This is further supported by the *in vitro* assays that do not make use of chemical carcinogens, but still show a reduced potential of cells with reduced *Hus1* expression to become transformed. Furthermore, the decreased ability to become transformed is directly related to the level of HUS1 reduction, as $Hus1^{Neo/\Delta 1}$ mice, which have a severe decrease in *Hus1* expression, also show a severe reduction in tumor number; whereas, $Hus1^{Neo/Neo}$ mice, with a moderate reduction in *Hus1* expression, develop a moderate number of papillomas, relative to $Hus1^{+}$ mice.

The data provided here are in contrast with other studies which have made use of a conditional *Rad9* knockout and *Rad1* heterozygotes. Because RAD9 and RAD1, along with HUS1, form the heterotrimeric 9-1-1 complex, one would predict that deficiencies in RAD9 or RAD1 would phenocopy the reduced tumorigenicity reported here. However, in these studies, *Rad9* inactivation in keratinocytes or *Rad1*

heterozygosity results in increased tumorigenesis using the same two-step skin carcinogenesis procedure to induce papilloma formation (Han et al., 2010; Hu et al., 2008). The mouse genetic background may play a role in tumor development. $Hus1^{Neo/\Delta_1}$ mice are maintained on a 129SvEv background, whereas *Rad9* conditional knockout mice and *Rad1* knockout mice were produced from a mixed 129SvEv and C57BL/6 background. Modifiers present in different strain backgrounds may also have an effect on tumor development. This discrepancy between tumor development in mice with partial *Hus1* expression, mice with conditionally inactivated *Rad9*, and *Rad1* heterozygous mice may be due to the level of checkpoint impairment. In the data presented here, *Hus1* is reduced to 20%-40% of wild-type expression, whereas the *Rad1* and *Rad9* studies utilize heterozygous mice and complete conditional knockout mice, respectively. However, in contrast with the $Rad1^{+/-}$ mice, $Hus1^{+/-}$ mice do not show increased genomic instability and $Rad9^{+/-}$ mice do not develop an increased number of papillomas in the same DMBA/TPA assays. In contrast with *Rad9* conditional inactivation in the skin, previous data from our lab shows that complete inactivation of *Hus1* in a tissue specific manner results in extensive cell death with no increase in spontaneous tumorigenesis (Chapter 2)(Yazinski et al., 2009). However, in *Rad9* conditional knockout cells, cell death and reconstitution of skin cells may function as a mechanism of tumor promotion, resulting in increased papilloma formation, or alternatively, keratinocytes may not have as high a requirement for RAD9 as mammary cells have for HUS1. Another difference between these studies is the cell type affected by checkpoint impairment. In the previous study, *Rad9* is inactivated exclusively in keratinocytes, whereas our $Hus1^{Neo/\Delta 1}$ mice globally express reduced HUS1 in all cell types. There may also be non-cell-autonomous effect in which surrounding cells with reduced *Hus1* expression may not be able to support sustained transformation and tumor growth. Finally, this inconsistency between the

phenotypes seen in *Hus1* hypomorph mice and phenotype of conditional *Rad9* knockout and *Rad1* heterozygous mice may be due to additional functions of RAD9, RAD1, or HUS1 outside of the 9-1-1 complex that have yet to be uncovered, which may be of critical importance for tumor initiation and development. For example, RAD9 has recently been shown to interact with BCL-2 and BCL-$x_L$ to induce apoptosis and furthermore, to play a role as a transcription factor which can activate transcription of p21 and induce apoptosis when overexpressed (Komatsu et al., 2000) (Yin et al., 2004).

Lower levels of HUS1 resulting in reduced tumor number is not universal to all tumor types and may be determined by the genetic composition of the tumor or cell type of origin. For example, $Hus1^{Neo/\Delta1}$ mice crossed to a *p53*-null background develop thymic lymphoma at the same rate as $Hus1^{+}$ *p53*-null mice (Levitt et al., 2007), suggesting reduced levels of HUS1 does not effect tumor development due to a p53-deficiency. This may be due to a requirement for p53 to respond to the damage induced by inhibition of *Hus1* in cells undergoing transformation to induce apoptosis or senescence, and thus prevent tumorigenesis. Alternatively, thymocytes have been shown to have a lower requirement for HUS1 (Francia et al., 2006), and proliferation of tumors originating from this tissue, such as thymic lymphoma seen in p53-null mice, may not be highly dependent on the ATR pathway. On the other hand, *Hus1*-inactivation in the mouse mammary gland in a *p53*-deficient background results in cell death, and does not result in mammary tumorigenesis. This suggests that in some tissue types, *Hus1*-inactivation actually sensitizes *p53*-null cells, which are normally resistant to apoptosis, to cell death. Because inactivation of *Hus1* and *p53* appears to be synthetic lethal in some cell types, *Hus1* may be a therapeutic target for *p53*-deficent tumors.

The results presented here fit well with the growing notion of "non-oncogene addiction" that posits that transformed cells may be "addicted" to DNA damage checkpoint proteins, and have a heavy reliance on their expression to survive transformation and sustain tumor development (Luo et al., 2009). Transformation is a process which results in elevated cellular stress due to increased proliferation and reactive oxygen species. This increased stress early in transformation continues throughout cancer development and growth (Benhar et al., 2002). Because of this, transformed cells may have a greater dependence on proteins involved in response to this stress, such as chaperone and DNA damage response proteins. The ATR pathway plays a critical role in response to DNA damage and stalled replication forks associated with normal S-phase progression. For this reason, the requirement for the ATR pathway may be higher in cells that have increased proliferation or hyper-replication, such as that seen in cells undergoing transformation. Because HUS1 is a critical component of the ATR pathway, reduced levels of *Hus1* expression may result in sensitivity to the cellular stress associated with transformation. Cells with reduced HUS1 that are forced to proliferate through oncogenic signaling may not be able to sustain this state of growth, and may instead induce senescence, apoptosis, or undergo mitotic catastrophe from the level of DNA damage sustained. This idea is supported by the reduced foci formation and colony formation in transformation assays of some $Hus1^{Neo/Neo}$ and $Hus1^{Neo/\Delta 1}$ cell culture lines, as well as reduced papilloma number and size seen in $Hus1^{Neo/Neo}$ and $Hus1^{Neo/\Delta 1}$ mice compared to $Hus1^{+}$ mice. Taken together, the cell culture and *in vivo* data presented here suggest that HUS1 may be involved in non-oncogene addiction in tumor cells since cells undergoing transformation or maintaining a transformed state are more dependent on the ATR pathway, which is normally involved in genome maintenance, resulting in decreased cancer development.

Several recent studies corroborate this idea of tumor cell addiction to DNA damage checkpoints. Cancer stem cells harvested from a murine model of mammary tumorigenesis upregulate several DNA damage response and repair proteins, including HUS1 (Zhang et al., 2008), suggesting an increased dependence on these proteins for tumor initiation. Human tumors have not been found to have loss of function of components of the ATR pathway (Bartek and Lukas, 2003), and several human tumor show increased expression of components of the Atr pathway, including upregulation of *Rad9* in breast and prostate cancers (Cheng et al., 2005; Zhu et al., 2008), increased expression of *Hus1* in ovarian tumors (de la Torre et al., 2008), and overexpression of *Chk1* in colorectal and breast cancers (Madoz-Gurpide et al., 2007; Verlinden et al., 2007). Taken together, the data presented here suggests that inhibition of *Hus1* or the ATR pathway may function as a potential target for cancer therapies. The idea of inactivation of DNA damage checkpoints as a potential therapeutic treatment is currently being tested through inhibitors targeted against the downstream effector in the ATR pathway, CHK1(Ashwell and Zabludoff, 2008; Chen et al., 2006). Inhibition of checkpoint proteins can lead to a checkpoint defect and genomic instability in rapidly proliferating cells, resulting in increased sensitivity of cancer cells to currently used chemotherapies which act by damaging DNA.

While inactivation of checkpoint proteins of the ATR pathway may decrease tumorigenesis in some contexts, mutations of many other DNA damage checkpoints of the parallel ATM pathway, such as *Atm*, *Chk2*, and *p53* instead results in an elevated tumor incidence in both mice and humans due to an increase in genomic instability (Bartek et al., 2007). Although defects in both ATR and ATM pathways result in genomic instability, ATM may play a less critical role in response to the type of stress induced by transformation and the rapid proliferation of tumor growth. This is supported by the fact that ATM and components of the ATM pathway are not essential

for embryonic growth and development (Shiloh, 2003). Instead, impairment of the ATM pathway results in a level and type of DNA damage that promotes tumorigenesis and does not result in extensive cell death in combination with the stresses of neoplastic proliferation.

While these experiments suggest that reduced levels of HUS1 result in decreased transformation and inhibition of tumor growth, there are limitations to our studies. Many of our cell culture transformation assays make use of immortalized cells, which are more readily transformed, to determine the transformation potential of cells with reduced HUS1. However, these cells have undergone spontaneous immortalization by random mutagenesis from repeated passing of cells. Testing the effect of oncogene-induced proliferation on primary cells or cells immortalized in the same way, i.e. through Large-T antigen expression, would better reflect the effect of reduced HUS1 on transformation without the added complexity of additional unknown mutations. Although our data suggest that decreased tumor formation following the two-step skin carcinogenesis protocol is not due to enhanced sensitivity to DMBA or TPA, we cannot completely exclude this possibility. In order to overcome this complication, we would like to induce tumors genetically, rather than with use of chemicals which act by damaging DNA. Additionally, we have only tested the effect of reduced HUS1 levels on skin tumorigenesis and would like to extend these studies to other tissue types in which oncogene activation results in tumorigenesis to determine if this model holds true.

# CHAPTER 4

# EFFECT OF ANTIOXIDANTS ON TUMORIGENESIS AND GENOMIC INSTABILITY

## *4.1 INTRODUCTION*

Mammalian cells are constantly assaulted by intrinsic and extrinsic stresses that can damage DNA, proteins, and lipids. Naturally occurring oxidative stress arising from metabolic byproducts or environmental factors can be one source of cellular damage. This is due to the increased reactive oxygen species (ROS) that result from high levels of oxygen, which can than react with DNA to produce adducts (Kawanishi et al., 2001), with lipids resulting in peroxidation (Bartsch and Nair, 2002), or with proteins to result in carbonylation (Nystrom, 2005). These molecular changes can result in cellular changes, such as increased proliferation, induction of senescence, or increased cell death, which then have a detrimental physiological impact on an organism, such as development of cancer, neurological diseases, or aging (Bartsch and Nair, 2002; Kawanishi et al., 2001; Nystrom, 2005). Because of the obvious toxic effect of increased ROS in a cell, the resulting molecular consequence of ROS, the mechanisms that act to correct these molecular changes, and preventative measures to preclude these molecular changes from occurring have been an important area of research. In particular, the effect of antioxidant treatment on transformation and tumorigenesis has yet to be fully understood.

ROS poses many difficulties to DNA replication and genome maintenance. The most common type of DNA damage to arise from an increase in ROS levels is the formation of 8-oxo-deoxyguanine (8-oxo-dG), but other oxidative DNA damage can occur. Unrepaired 8-oxo-dG can result in G→T transversions, resulting in permanent mutations in the DNA sequence, which can have detrimental effects, such as

activation of oncogenes (Kohen and Nyska, 2002). Additionally, these altered bases can be bypassed by error-prone translesion polymerases, which insert incorrect bases across from the damaged base, resulting in mutations. Helix distorting lesions can also pose a block to DNA replication, resulting in stalled forks, which can result in collapsed replication forks and DNA breaks (Wang, 2008).

DNA damage checkpoint proteins are known to respond to a variety of DNA lesions, including those resulting from increased oxidative stress, to maintain genomic integrity. There are two main, evolutionarily conserved DNA damage checkpoint pathways which respond to DNA damage, the ATM and the ATR pathways (Cimprich and Cortez, 2008). The ATM pathway responds primarily to double stranded DNA breaks (DSBs), and includes downstream effectors such as CHK2 and p53 (Kastan and Lim, 2000). The ATR pathway, on the other hand, responds to generation of single stranded DNA (ssDNA) which arises from stalled forks or bulky DNA lesions (Cimprich and Cortez, 2008). The ATM pathway has been shown to play a role in response to oxidative stress, and A-T patients and ATM deficient mice show a decreased antioxidant capacity (Barzilai and Yamamoto, 2004). Roles for the ATR pathway in response to oxidative stress are less clear. Because oxidative stress can cause bulky DNA adducts and stalled replication forks, it is possible that an increase in ROS will result in activation of the ATR pathway. The ATR pathway includes other components such as the 9-1-1 complex, which includes RAD9, RAD1, and HUS1, and downstream effector kinase, CHK1. Inactivation of any component of the ATR pathway results in embryonic lethality. HUS1 is an essential component of the 9-1-1 complex, a PCNA-like, heterotrimeric clamp, which is loaded onto RPA-coated ssDNA and acts as a scaffold to facilitate efficient activation of ATR and phosphorylation of CHK1. Additionally, the 9-1-1 complex has been shown to interact directly with components of the base excision repair (BER) pathway (Chang and Lu,

2005; Friedrich-Heineken et al., 2005; Shi et al., 2006; Smirnova et al., 2005; Toueille et al., 2004; Wang et al., 2004b; Wang et al., 2006), which responds to DNA damage caused by oxidative stress (Mitra et al., 2001).

Roles for the 9-1-1 complex in response to oxidative stress and in tumorigenesis have yet to be well characterized due in part to the fact that inactivation of any component of the ATR pathway results in embryonic lethality. In the present work, we made use of a previously described *Hus1* allelic series, which expresses incrementally reduced levels of HUS1 by combining $Hus1^{\Delta 1}$ allele which is null for *Hus1* expression, $Hus1^{Neo}$ allele which has a partial defect in *Hus1* expression, and $Hus1^{+}$ allele which is normal for *Hus1* expression. $Hus1^{Neo/\Delta 1}$ mice, which have about ~20% *Hus1* expression, allow us to study reduced levels of HUS1 while bypassing the embryonic lethality associated with complete germline inactivation of *Hus1* (Levitt et al., 2007). Here, we describe an essential role for the DNA damage checkpoint protein HUS1 in response to oxidative stress. Furthermore, we show the discrepancy between the severe phenotype of reduced *Hus1* expression in tissue culture and the more mild phenotype of reduced *Hus1* expression in mice is due to the increased oxidative stress associated with atmospheric oxygen levels. However, antioxidants cannot rescue all phenotypes of cells with reduced HUS1 levels, including hypersensitivity of *Hus1* hypomorph cells to high doses of aphidicolin, increased micronucleus levels in *Hus1* hypomorph mice, and lethality of *Hus1* knockout embryos, suggesting HUS1 plays a critical role in response to replicative stress, in addition to oxidative stress response. Furthermore, we have shown that antioxidant treatment has little effect on tumor growth or tumor regression following DMBA and TPA treatment, but significantly decreases malignant progression of skin tumors.

### *4.2 MATERIALS AND METHODS*

*Mice:*

Previously described $Hus1^{+/\Delta 1}$ and $Hus1^{+/Neo}$ mice (Levitt, 2007 #31) were maintained on a 129S6 inbred genetic background. $Hus1^{+/\Delta 1}$ and $Hus1^{+/Neo}$ mice were bred to generate experimental $Hus1^{Neo/\Delta 1}$ mice, as well as littermate control $Hus1^{+/+}$, $Hus1^{+/Neo}$, and $Hus1^{+/\Delta 1}$ mice. To generate $Hus1^{Neo/Neo}$ and control littermates, $Hus1^{+/Neo}$ mice were intercrossed. All animals were genotyped by PCR analysis of DNA extracted from tail tip biopsies. Wild-type mice were ordered from Jackson Laboratory. Mice were housed in accordance with institutional animal care and use guidelines.

*Generation of mouse embryonic fibroblasts (MEFs):*

$Hus1^{+/Neo}$ females were crossed to $Hus1^{+/\Delta 1}$ males in timed matings and embryos from pregnant females were harvested at 13.5dpc. After differentiated tissues (head, liver, and spleen) were removed, the remaining cells were plated in DMEM + 10% FBS, 1% non-essential amino acids, 1% l-glutamine, 1% penicillin-streptomycin. Cells were maintained on a 3T3 protocol (Todaro and Green, 1963), and passed every three days.

*Antioxidant and Aphidicolin treatment of cells:*

MEFs of the indicated genotypes at passage 1 were treated with N-acetyl-alanine (NAA) or N-acetyl-cysteine (NAC) (Sigma) to a final concentration of 5mM in DMEM + 10% FBS. Antioxidant or control media was changed daily. Cells were passed every three days and population doublings were determined using the formula Population doubling=$\log(n_f/n_o)/\log(2)$, where $n_o$ is the initial number of cells plated, and $n_f$ is the final number of cells (Blasco et al., 1997). Metaphase spreads were prepared at passages 1, 3, and 5 by treating cells with 0.15μg/ml colcemid for 1 hour,

harvesting the cells with trypsinization, swelling cells with hypotonization buffer (0.034M KCl and 0.017 sodium citrate), fixing cells with 75% methanol/25% acetic acid, dropping cells onto microscope slides, and staining slides with 2% Giemsa stain in Gurr buffer. Metaphase spreads were imaged at 100X magnification, and evaluated for aneuploidy, breaks, gaps, or acentric chromosomes using standard guidelines (Savage, 1976; Standing Committee on Human Cytogenetic Nomenclature. and Mitelman, 1995). For aphidicolin survival assays, MEFs of the indicated genotypes were treated with the indicated dose of aphidicolin at passage one. The media was removed 24 hours later and replaced with media containing either NAA or NAC. Cells were fed fresh media again 48 hours after treatment, and cells were harvested by trypsinization 72 hours following initial aphidicolin treatment. Surviving cells, as determined by trypan blue exclusion, were counted.

*Effect of antioxidant treatment on micronucleus formation in Hus1$^{Neo/\Delta 1}$ mice.*

Hus1$^{Neo/\Delta 1}$ and control Hus1$^{+}$ mice were bled and micronucleus levels were analyzed as performed by others (Reinholdt et al., 2004). Briefly, peripheral blood was collected from the mandibular vein directly into heparin and fixed in cold methanol. Cells were co-stained with anti-CD71-FITC (Biodesign International) and propidium iodide, and analyzed on a FACSCalibur flow cytometer (Becton-Dickinson). Following initial micronucleus measurements, mice were given 0.04M NAC water as their sole drinking source, and water was replaced weekly. Mice were reassayed at 1, 2, and 4 weeks of NAC water treatment.

*Effect of antioxidant treatment on Hus1$^{\Delta 1/\Delta 1}$ embryos:*

Female Hus1$^{+/\Delta 1}$ mice were bred with Hus1$^{+/\Delta 1}$ males in timed matings. Plugged females were untreated (water alone) or treated with 4mM NAC in water. Water was

changed weekly. Remaining water was measured in each bottle to confirm mice were consuming equal amounts of water. Embryos were harvested at 9.5dpc, imaged, and somites were quantified. The embryos were then fixed in 4% paraformaldehyde, dehydrated, paraffin embedded, and sectioned. Sections were rehydrated and stained using Feulgen-Schiff protocol, and the percentage of interphase, metaphase, and pyknotic cells was determined by cell morphology. Head folds of embryos from unstained sections were removed using Laser capture microdissection for genotyping by PCR as previously described (Espina et al., 2006).

*Effect of antioxidant treatment on papilloma development:*

Singly housed male FVB mice (n = 30) of the same age, ordered from the Jackson Laboratory, were shaved and treated with a single dose of DMBA (200nmol in acetone). One week later, mice were treated with repeated doses of TPA (5μg in acetone) twice weekly for twenty weeks. 65 days after initial DMBA treatment, half the mice (n = 15) were given 40mM NAC dissolved in water while the other half (n = 15) were given water alone, and drinking water was changed once weekly for the twenty weeks of treatment. 40mM NAC treatment was calculated based on 1 g NAC/kg body weight/day, which was shown to reduce DNA-adduct formation in rats exposed to carcinogens (Balansky et al., 1996). Papillomas were counted and measured twice weekly. One week and twenty weeks after the start of NAC treatment, two and three mice, respectively, from each group were injected with 50ug/g body weight BrdU for papilloma proliferation studies. At the conclusion of the study, the skin of the mice was harvested, fixed in 4% paraformaldehyde, dehydrated, embedded in paraffin, sectioned, stained by hematoxylin and eosin, and evaluated by a pathologist.

*BrdU Immunohistochemistry:*

Skin sections from two or three different mice for each treatment group at each time point were prepared and analyzed using the BrdU kit (Zymed-Invitrogen) to assess proliferation according to the manufacturer's directions. Approximately 500 cells in at least two fields of vision at 40X magnification were counted per papilloma. Statistical analysis was by two-tailed Student's t-test.

## *4.3 RESULTS*

### 4.3.1 Antioxidant treatment rescues the premature senescence and chromosomal aberrations of Hus1$^{Neo/\Delta1}$ cells, but does not rescue aphidicolin hypersensitivity.

Previous studies have shown that primary MEFs senesce in cell culture due to the increased oxidative stress of hyperoxic atmospheric conditions (~20% oxygen) associated with cell culture as compared to nomoxic levels (~3% oxygen) *in vivo* (Parrinello et al., 2003). Because HUS1 is known to respond DNA adducts and may play a role in BER, we wanted to test whether the premature senescence observed in Hus1$^{Neo/\Delta1}$ MEFs is due to sensitivity to oxidative stress. Hus1$^{+/+}$ or Hus1$^{Neo/\Delta1}$ MEFs were treated daily with either N-Acetyl-Alanine (NAA) or N-Acetyl-Cysteine (NAC) in cell culture media. NAC is a potent antioxidant due to the reactive thiol group which can act to neutralize ROS directly, as well as, serve as a precursor for the synthesis of glutathione, which acts to detoxify and protect cells from free radicals (Zafarullah et al., 2003). NAA, on the other hand, does not have any reactive side group, and should have no effect on levels of reactive oxygen species within a cell, and serves as a control in our experiments.

Primary Hus1$^{Neo/\Delta1}$ MEFs grown in atmospheric oxygen and treated with the control compound NAA senesced after 9 days in cell culture, as determined by the plateau in population doubling, as compared to Hus1$^{+/+}$ MEFs derived from the same

litter also treated with NAA which did not senesce until after 18 days in culture (Figure 4.1 A). Following treatment with NAC, $Hus1^{Neo/\Delta 1}$ MEFs did not senesce until after 21 days in culture, suggesting the initial premature senesce of these cells after 9 days in culture was due at least in part to increased oxidative stress associated with atmospheric oxygen which is relieved by antioxidant treatment. $Hus1^{+/+}$ MEFs treated with NAC also proliferated for a more prolonged period in cell culture compared to $Hus1^{+/+}$ MEFs in response to oxidative stress from culture conditions at atmospheric oxygen, which has been previously reported (Parrinello et al., 2003), but are not as sensitive to oxidative stress as $Hus1^{Neo/\Delta 1}$ cells. To confirm this premature senescence in cells with reduced levels of HUS1 is due impart to oxidative stress, primary $Hus1^{+}$ or $Hus1^{Neo/\Delta 1}$ MEFs derived from the same litter, were grown in low oxygen or normoxia from the time of initial preparation (Figure 4.1 C). As before, $Hus1^{+}$ cells grew well in atmospheric oxygen and began senescing after 25 days in culture, while $Hus1^{Neo/\Delta 1}$ cells underwent premature senescence after only 15 days in culture. $Hus1^{+}$ cells were grown in low oxygen conditions grew at a similar rate as $Hus1^{+}$ cells grown in atmospheric oxygen; however, the low oxygen $Hus1^{+}$ MEFs failed to senesce during the time course of the experiment, which has previously been observed (Parrinello et al., 2003). $Hus1^{Neo/\Delta 1}$ MEFs grown in low oxygen conditions grew markedly better than those grown in normal oxygen, though not as well as $Hus1^{+}$ cells. This difference in senesce initiation between $Hus1^{+/+}$ and $Hus1^{Neo/\Delta 1}$ MEFs suggests that HUS1 normally plays an important role in response to oxidative stress.
treated with NAA, suggesting that wild-type cells also undergo senesce

In order to evaluate the level of genomic instability in $Hus1^{+/+}$ and $Hus1^{Neo/\Delta 1}$ cells treated with NAA or NAC, I prepared metaphase spreads at passage 1, 3, and 5 (Figure 4.1 B). Metaphase spreads at passage 1 exhibited very little DNA damage, regardless of the genotype; however, $Hus1^{+/+}$ cells treated with NAC had no

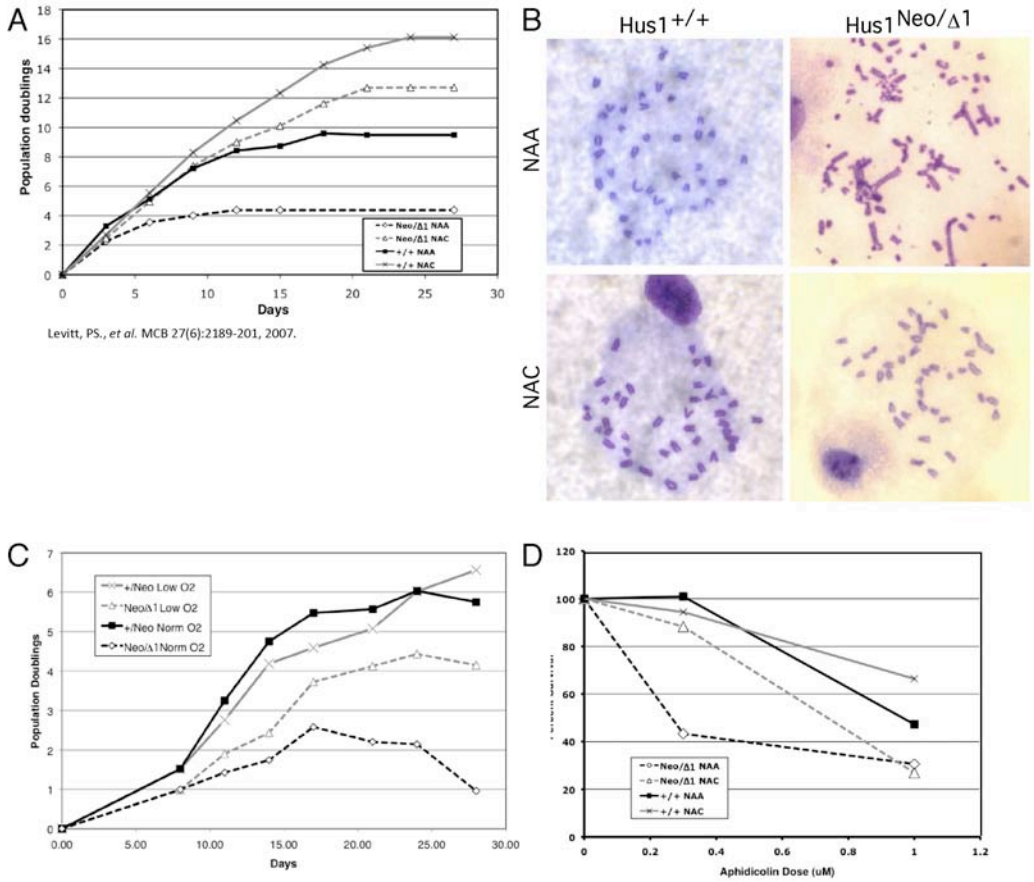


***Figure 4.1*** **Premature senescence and chromosomal aberrations of Hus1$^{Neo/\Delta1}$ cells can be rescued by antioxidant treatment, but sensitivity of Hus1$^{Neo/\Delta1}$ cells to a high dose aphidicolin cannot be rescued with antioxidant treatment.** (A) Hus1$^{+/+}$ or Hus1$^{Neo/\Delta1}$ MEFs were prepared and treated daily with NAA or NAC media. Cells were passed every three days, and population doublings were calculated. (B) Representative metaphase spreads from Hus1$^{+/+}$ or Hus1$^{Neo/\Delta1}$ treated with NAA or NAC at passage 3. (C) Hus1$^{+/Neo}$ or Hus1$^{Neo/\Delta1}$ MEFs were prepared and grown at low oxygen or normal oxygen conditions. Cells were passed every three days, and population doublings were calculated. (D) Hus1$^{+}$ and Hus1$^{Neo/\Delta1}$ cells treated with NAA or NAC were given a single dose of aphidicolin at the indicated concentration, and cell survival was measured 24 hours later using a trypan blue exclusion assay. Graphs are representative of the three separate primary MEF cell lines tested in each assay. *[(A)Published in* (Levitt et al., 2007)*;Experiments and Figures by S.A. Yazinski]*

Table 4.1: **Summary of chromosomal aberrations of metaphase spreads of Hus1$^{+/+}$ and Hus1$^{Neo/\Delta1}$ MEFs treated with NAA or NAC prepared at the given passage number** [a]

| | Genotype/ Treatment | Total Cells | Avg. Chrom./Cell | Breaks/Gaps | | Exchanges | | Acentric Chrom. | Extensive Damage | Cells with damage | #Abnormalities /Cell | |
|---|---|---|---|---|---|---|---|---|---|---|---|---|
| | | | | Total | Avg. | Total | Avg. | | | | 1-2 | >2 |
| Passage 1 | Neo/Δ1 NAA | 20 | 39.60 | 0 | 0.00 | 0 | 0.00 | 3 | 0 | 3 | 3 | 0 |
| | Neo/Δ1 NAC | 20 | 40 | 0 | 0.00 | 0 | 0.00 | 3 | 0 | 3 | 3 | 0 |
| | +/+ NAA | 20 | 39.60 | 0 | 0.00 | 0 | 0.00 | 1 | 0 | 2 | 2 | 0 |
| | +/+ NAC | 19 | 40.00 | 0 | 0.00 | 0 | 0.00 | 0 | 0 | 0 | 0 | 0 |
| Passage 3 | Neo/Δ1 NAA | 17 | 39.18 | 45 | 2.65 | 25 | 1.47 | 11 | 3 | 14 | 8 | 6 |
| | Neo/Δ1 NAC | 20 | 39.2 | 19 | 0.95 | 13 | 0.65 | 2 | 1 | 7 | 4 | 3 |
| | +/+ NAA | 19 | 39.68 | 12 | 0.63 | 4 | 0.21 | 2 | 0 | 7 | 5 | 2 |
| | +/+ NAC | 19 | 39.26 | 1 | 0.05 | 0 | 0.00 | 0 | 0 | 1 | 1 | 0 |
| Passage 5 | Neo/Δ1 NAA | | | | | | | | | | | |
| | Neo/Δ1 NAC | 20 | 36.2 | 6 | 0.30 | 0 | 0.00 | 0 | 0 | 5 | 5 | 0 |
| | +/+ NAA | 18 | 40.00 | 2 | 0.11 | 0 | 0.00 | 1 | 0 | 3 | 3 | 0 |
| | +/+ NAC | 19 | 40.00 | 1 | 0.05 | 0 | 0.00 | 0 | 0 | 1 | 1 | 0 |

[a] Hus1+ and Hus1$^{Neo/\Delta1}$ MEFs were fed media containing NAA or NAC after the first passage. MEFs were passed every three days, and metaphase spreads were prepared after 1, 3, and 5 passages. The first 20 metaphase spreads were evaluated for each genotype for each treatment.



chro

mosomal abnormalities (Table 4.1). At passage 3, where two independently derived cell lines were evaluated, $Hus1^{+/+}$ cells treated with NAA had low levels of damage, and these cells had even fewer abnormalities when treated with NAC. On the other hand, a majority of $Hus1^{Neo/\Delta 1}$ cells treated with NAA had a high level of chromosomal damage, including instances of extensive damage. Treatment with NAC reduced the number of abnormalities to a great extent and this level of damage was comparable to the $Hus1^{+/+}$ cells treated with NAA at the same passage number. Thissuggests that the increased level of chromosomal aberrations seen in metaphase spreads of $Hus1^{Neo/\Delta 1}$ MEFs is due to increased oxidative stress from tissue culture conditions which results in unrepaired DNA damage. At passage 5, no clear metaphase spreads of $Hus1^{Neo/\Delta 1}$ MEFs treated with NAA could be prepared, suggesting cells were not entering metaphase or were not surviving proliferation, while metaphase spreads of $Hus1^{Neo/\Delta 1}$ cells treated with NAC still had a low level of chromosomal aberrations (Figure 4.1 C and Table 4.1). This is consistent with the population doubling data, which shows that $Hus1^{Neo/\Delta 1}$ cells enter premature senescence at passage 5, while $Hus1^{Neo/\Delta 1}$ cells treated with NAC continue to proliferate until passage 7. Together, these results suggest that HUS1 plays a critical role in response to oxidative stress in order to maintain genomic integrity.

We next set out to test whether antioxidant treatment would reduce the sensitivity of $Hus1^{Neo/\Delta 1}$ cells to aphidicolin. $Hus1^{Neo/\Delta 1}$ cells had previously shown sensitivity to DNA damaging agents and replication inhibitors, such as aphidicolin, which acts by inhibiting Pol$\alpha$, and results in stalled replication forks (Levitt et al., 2005). Because HUS1 acts at the site of stalled forks, severe depletion of HUS1 could result in fork collapse and cell death. It is possible that the increased cell death following aphidicolin treatment is due to the compounding effects of the replication inhibitor and oxidative stress due to hyperoxic oxygen levels. The atmospheric oxygen

level may create a sensitized background in Hus1$^{Neo/\Delta1}$ cells, which then results in increased cell death following aphidicolin treatment compared to Hus1$^{+/+}$ cells. To test this, I treated Hus1$^{+}$ and Hus1$^{Neo/\Delta1}$ cells with NAA or NAC, followed by a single dose of aphidicolin. Cell survival was assessed 72 hours later using trypan blue exclusion assay. Following treatment with a low dose of aphidicolin (0.3μM), Hus1$^{+}$ cells did not show any decreased cell survival when compared with vehicle alone, while Hus1$^{Neo/\Delta1}$ cells showed hypersensitivity to aphidicolin at this dose (Figure 4.1 D). Treatment with NAC rescued the hypersensitivity of Hus1$^{Neo/\Delta1}$ cells to a low dose of aphidicolin, suggesting that atmospheric oxygen sensitizes Hus1$^{Neo/\Delta1}$ cells to treatment with the replication inhibitor. Following treatment with a high dose of aphidicolin (1.0μM), survival of Hus1$^{+}$ cells dropped to ~50%, but was slightly higher after treatment with NAC, with survival at ~65%. At this high dose of aphidicolin, Hus1$^{Neo/\Delta1}$ cells showed decreased survival (~30%) relative to Hus1$^{+}$ cells. This enhanced sensitivity to a high dose of aphidicolin was not rescued by treatment with NAC, and survival of Hus1$^{Neo/\Delta1}$ cells still remained low (~30%). This suggests that the limited amount of HUS1 in Hus1$^{Neo/\Delta1}$ cells is not enough to respond to the level of genomic instability incurred by a high dose of aphidicolin, and that all defects seen in Hus1$^{Neo/\Delta1}$ cannot be attributed to hypersensitivity to oxidative stress alone.

**4.3.2 Mice with reduced levels of HUS1 show an increase in micronucleus formation that cannot be rescued by treatment with an antioxidant.** Because cells with reduced levels of HUS1 were found to be hypersensitive oxidative stress, which resulted in chromosomal aberrations in culture, we next wanted to determine if antioxidant treatment could rescue the genomic instability seen in mice with reduced levels of HUS1. Hus1$^{Neo/\Delta1}$ mice have an increased level of micronuclei compared to Hus1$^{+}$ mice (Levitt et al., 2007). Normally, red blood cells expel their nucleus as they

reach full maturity, resulting in an anucleated cell. However, mice with heightened chromosomal instability form micronuclei, acentric fragments of chromosomal DNA due to the chromosomal instability. This fragment is then retained in the mature red blood cell. The percentage of red blood cells that retain a micronucleus reflects the level of genomic instability. To quantify this population, cells isolated from peripheral blood were double labeled with CD71, which labels reticulocytes and erythrocytes progenitor cells, and propidium iodide (PI), which labels DNA (Reinholdt et al., 2004). These cells were run through FACS, and $CD71^{-}$ $PI^{+}$ cells, which are mature erythrocytes that still retain DNA, were gated.

To test whether antioxidant treatment could reduce the level of genomic instability in $Hus1^{Neo/\Delta1}$ mice, we treated $Hus1^{+}$ (n = 6) and $Hus1^{Neo/\Delta1}$ (n = 4) mice with 0.04M NAC in their drinking water, and monitored changes in the micronucleus level overtime for each mouse. As expected, following initial bleeds, $Hus1^{+}$ mice had a low level of micronucleus formation (0.153%) while $Hus1^{Neo/\Delta1}$ mice had a much higher initial level of micronuclei (0.408%) (Table 4.2). To determine how this level changed over time, a ratio of initial micronucleus level to final micronucleus level was determine for each mouse at 1 week, 2 weeks, and 4 weeks after the start of NAC treatment, with NAC water being changed every week. The ratio of change was averaged for each genotype and plotted (Table 4.2 and Figure 4.2). Although $Hus^{+}$ mice began with low micronucleus levels (0.153%), the level actually became lower over time (0.113% at 4 weeks after the start of NAC treatment) after 4 weeks of NAC treatment. The micronucleus level of $Hus1^{Neo/\Delta1}$ mice did not change following NAC treatment suggesting that NAC treatment did not relieve the increase in genomic instability seen in peripheral red blood cells. The average micronucleus levels of $Hus1^{+}$ mice did decrease over the four week NAC treatment, suggesting that

antioxidant treatment did have a positive effect on decreasing the low level genomic instability in these mice.

**4.3.4 Embryonic lethality caused by *Hus1*-deficiency is not rescued by antioxidant treatment *in utero*.** Because cells with reduced HUS1 levels were found to be hypersensitive to oxidative stress, which could then be rescued by treatment with antioxidant treatment (Figure 4.1), we next set out to test if antioxidant treatment could partially rescue the embryonic lethality seen in $Hus1^{\Delta 1/\Delta 1}$ embryos, which are null for *Hus1* expression. $Hus1^{\Delta 1/\Delta 1}$ embryos die mid-gestationally with elevated levels of apoptosis due to a high level of genomic instability. Previous studies have shown that the genomic instability resulting from a deficiency in ATM, another DNA damage checkpoint protein, can be rescued by antioxidant treatment. ATM-null mice treated with NAC *in utero* showed a decrease in oxidative stress, in DNA deletions, in neurobehavioral defects, and in tumor incidence, all which are normally elevated in ATM-deficient mice (Browne et al., 2004; Reliene et al., 2004; Reliene and Schiestl, 2006; Schubert et al., 2004). This prompted us to test whether treatment of *Hus1*-null embryos with NAC *in utero* can partially rescue the heightened level of apoptosis.

$Hus1^{+}$ (which includes both $Hus1^{+/+}$ and $Hus1^{+/\Delta 1}$) and $Hus1^{\Delta 1/\Delta 1}$ embryos were untreated or treated with NAC throughout gestation. The embryos were harvested at 8.5dpc, embedded, sectioned, and stained by Feulgen-Schiff technique (Figure 4.3 A and B). Embryos were genotyped by Laser microdissection using unstained, sectioned tissue from the headfold. Stained cells from the headfold of the embryos were scored as interphase, mitotic, or apoptotic by morphology. As expected, untreated $Hus1^{\Delta 1/\Delta 1}$ embryos had a marked increase in apoptotic cells (11%) compared to levels of $Hus1^{+}$ embryos (1%). There was no change in the distribution of cells in $Hus1^{+}$ cells following NAC treatment, with a similar level of mitosis (7%) and apoptosis (1%)

Table 4.2: Summary of micronucleus formation over time in $Hus1^{+}$ and $Hus1^{Neo/\Delta1}$ mice treated with NAC[a]

| Genotype | Percent RBCs with MN before NAC | Percent RBCs with MN one week after NAC | Percent RBC with MN two weeks after NAC | Percent RBCs with MN four weeks after NAC |
|---|---|---|---|---|
| +/+ | 0.16 | 0.15 | 0.14 | 0.12 |
| +/Δ1 | 0.12 | 0.13 | 0.12 | 0.11 |
| +/Δ1 | 0.12 | 0.16 | 0.16 | 0.12 |
| +/Neo | 0.21 | 0.14 | 0.11 | 0.12 |
| +/Neo | 0.17 | 0.15 | 0.13 | 0.12 |
| +/Neo | 0.14 | 0.16 | 0.19 | 0.09 |
| Neo/Δ1 | 0.35 | 0.37 | 0.31 | 0.33 |
| Neo/Δ1 | 0.28 | 0.33 | 0.35 | 0.32 |
| Neo/Δ1 | 0.56 | 0.53 | 0.54 | 0.41 |
| Neo/Δ1 | 0.44 | 0.5 | 0.43 | 0.48 |

| Genotype (N) | Avg. 0 week | Avg. 1 week | Avg. 2 week | Avg. 4 week |
|---|---|---|---|---|
| + (6) | 0.15 | 0.15 | 0.14 | 0.11 |
| Neo/Δ1 (4) | 0.41 | 0.43 | 0.41 | 0.39 |

[a] $Hus1^{+}$ and $Hus1^{Neo/\Delta1}$ mice were initially bled, and baseline micronucleus levels (MN) in mature red blood cells (RBC) were determined for each mouse. Mice were then treated with 0.04M NAC in their drinking water. Mice were reassayed from peripheral blood samples taken at 1 week, 2 weeks, and 4 weeks after the start of NAC water treatment.

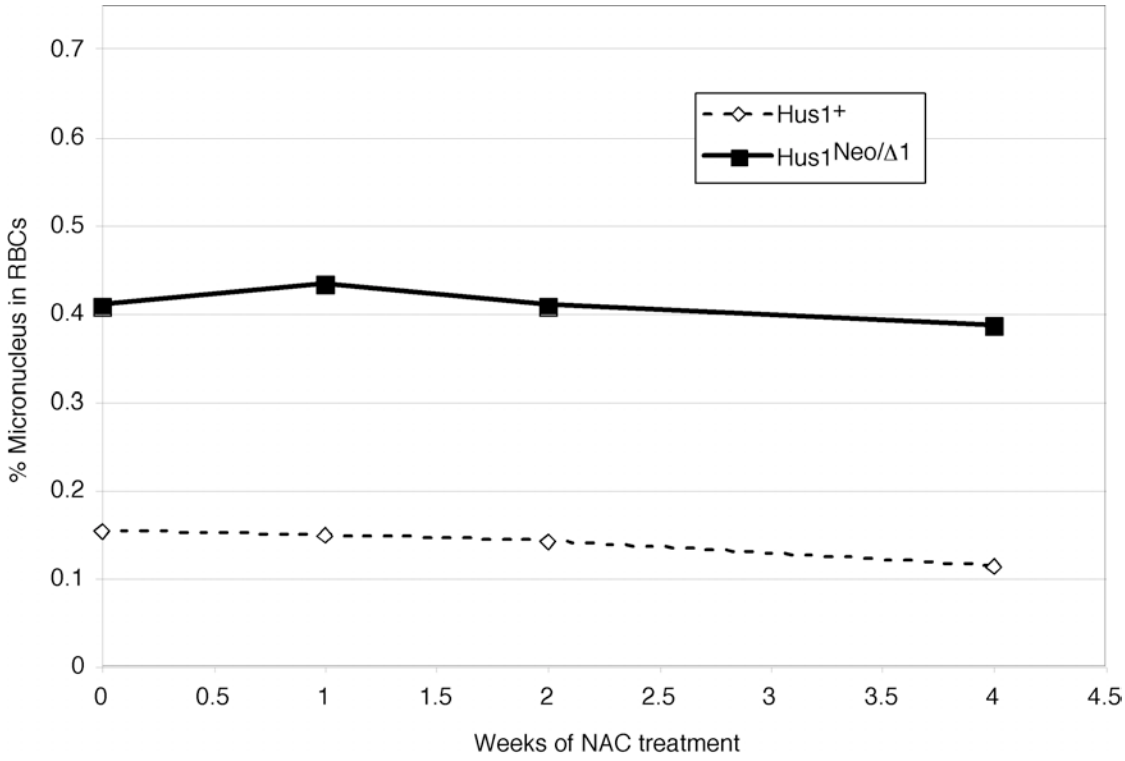


***Figure 4.2*** **The heightened level of micronucleus in Hus1$^{Neo/\Delta1}$ mice is not rescued by antioxidant treatment.** Peripheral blood from Hus1$^{+/+}$ or Hus1$^{Neo/\Delta1}$ mice was collected and sorted for erythrocytes containing micronucleus DNA, and this initial measurement served as a baseline. Mice were then placed on 0.04M NAC water as their sole water source. Micronucleus levels were measured at 1, 2, and 4 weeks after antioxidant treatment began, and the final/initial micronucleus level was calculated. Micronucleus levels remained high in Hus1$^{Neo/\Delta1}$ mice, even following 4 weeks of NAC treatment. *[Experiment and figure by S.A. Yazinski]*

following the antioxidant treatment. Hus1$^{\Delta1/\Delta1}$ embryos also showed no improvement in morphology (Figure 4.3 B) or levels of apoptosis (Figure 4.3 C) following NAC treatment. NAC treated Hus1$^{\Delta1/\Delta1}$ embryos were as underdeveloped as untreated Hus1$^{\Delta1/\Delta1}$ embryos and had elevated levels of apoptosis (9%), indicating that NAC treatment did not have a rescuing effect on *Hus1*-deficient embryos. These data suggest a fundamental role for HUS1 in embryonic development apart from response to oxidative stress.

**4.3.5 Effect of NAC treatment on papilloma development following a two-step carcinogenesis treatment.** Both tumor initiation and development have shown to result in an increase in oxidative stress in transformed cells, which can result in increased DNA damage (Benhar et al., 2002; Klaunig et al., 2010). This increased oxidative stress may provide a mechanism for an increased mutation rate that can aid tumor development. Based on this reasoning, antioxidant treatment before or during tumorigenesis has been shown to have an effect on cancer treatment and progression (Zafarullah et al., 2003). However, NAC treatment has also been shown to be anti-apoptotic and promote growth and survival, and may act to enhance tumorigenesis. In order to determine the effect of antioxidant treatment following transformation, we made use of the well-characterized carcinogen-induced skin papilloma model of tumorigenesis (Yuspa, 1994). In this experiment, wild-type mice of the same age were shaved and treated with 12-7-dimethylbenz(a)-anthracene (DMBA) and 12-O-tetradecanoylphorbol-13-acetate (TPA) to induce skin papillomas. Because these mice were all of the same age, hair cycle should be synchronized among these mice and should not generate differences in papilloma growth. DMBA causes specific A-T transversions at the second nucleotide of codon 61 of the Harvey-ras (H-ras) gene,

***Figure 4.3*** **NAC treatment cannot rescue the increased apoptosis seen in Hus1$^{\Delta 1/\Delta 1}$ embryos.** Hus1$^{+/\Delta 1}$ female mice were placed on bottled water or 0.04M NAC water, and then were bred to Hus1$^{+/\Delta 1}$ mice to generate Hus1$^{+/+}$, Hus1$^{+/\Delta 1}$, and Hus1$^{\Delta 1/\Delta 1}$ embryos. Representative (A) Hus1$^{+/+}$ and (B) Hus1$^{\Delta 1/\Delta 1}$ embryos at day 9.5 dpc stained by Feulgen-Schiff technique taken at low magnification (upper panels) or high magnification (lower panels). Embryos on the left of each panel were harvested from females that were given water, while embryos on the right of each panel were harvested from females that were given NAC water. Arrow heads in panel B indicate pyknotic nuclei. (C) Interphase, mitotic, and apoptotic cells from the head folds of embryos from Hus1$^{+}$ (n = 8) and Hus1$^{\Delta 1/\Delta 1}$ (n = 5) embryos treated with water, or from Hus1$^{+}$ (n = 9) and Hus1$^{\Delta 1/\Delta 1}$ (n = 7) embryos treated with NAC, were quantified based on morphology. *[Experiments (NAC treatment, timed matings, dissections, and genotyping) and figures by S. Yazinski; experiments (embedding, sectioning, staining, counting, and genotyping) by A. Ramanathan]*

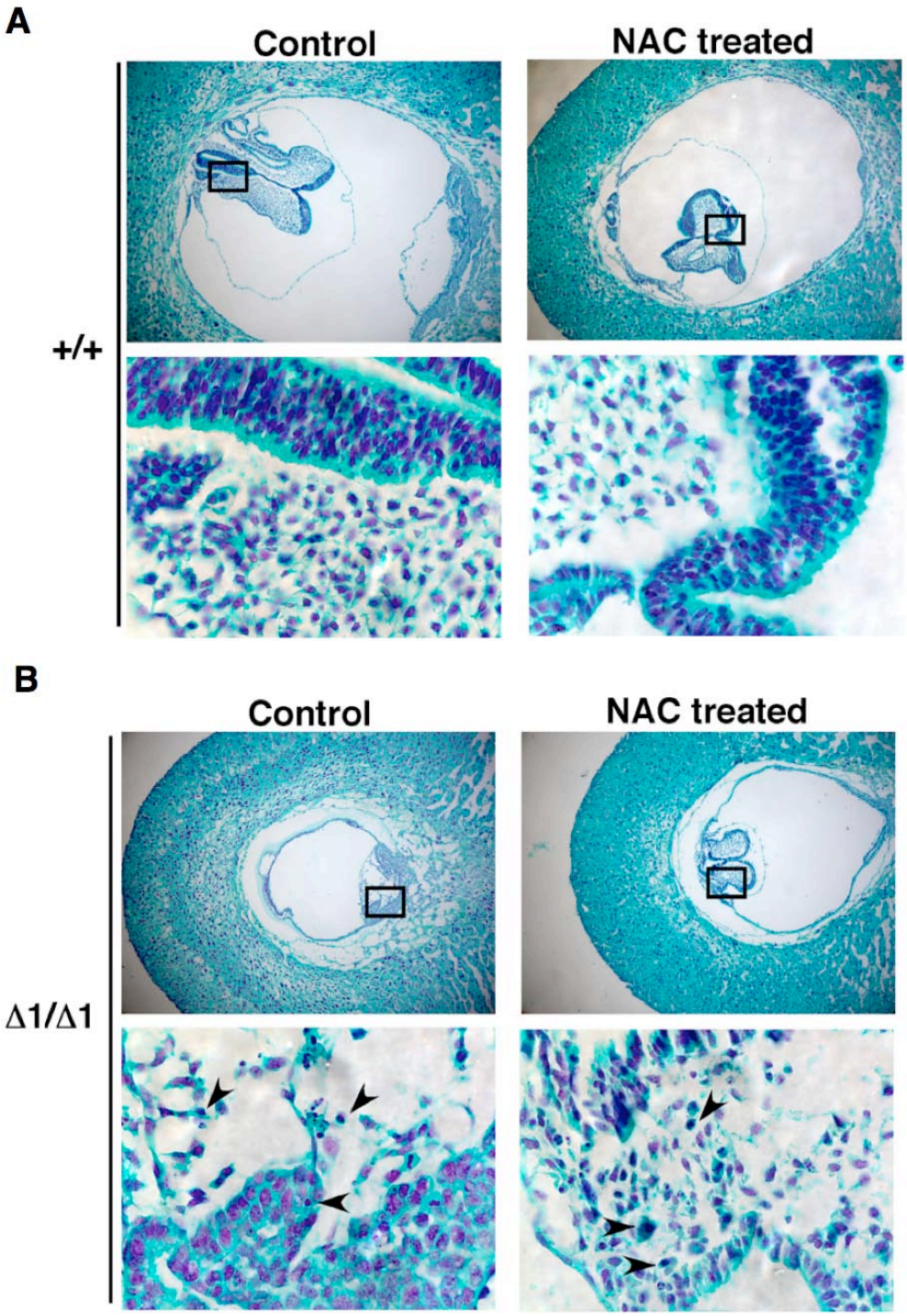
A
Control
NAC treated
+/+
B
Control
NAC treated
Δ1/Δ1

Figure 4.3 (Continued)

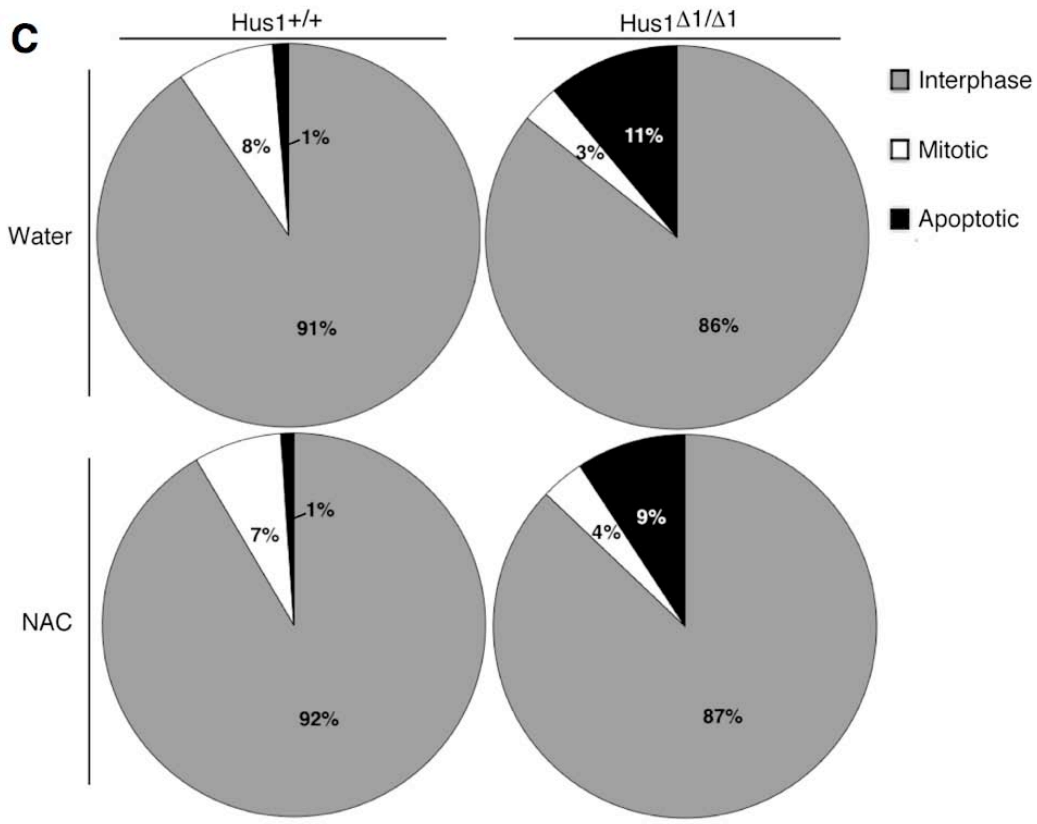

resulting in H-ras activation, and is a well-characterized tumor initiator (Quintanilla et al., 1986). TPA is potent tumor promoter that acts through activation of protein kinase C (PKC) (Angel et al., 1987). DMBA is applied once to the skin, while TPA is applied twice weekly for twenty weeks, resulting in skin papilloma formation. After tumor growth had begun, 65 days post DMBA treatment, mice were divided into two groups, a control group which received normal bottled water, and a treatment group, which received NAC water. This time point allowed us to determine that all mice had in fact begun developing tumors. However, NAC 65 days after initiation of tumor growth precludes us from understanding the role of antioxidant treatment on prevention of initiation. Because NAC can break down over time, the water for both groups was changed weekly. Papilloma number and size was documented. At the conclusion of the experiment, there was no significant difference in papilloma number or size due to NAC treatment (Figure 4.4 A).

In order to determine if there was a change in tumor growth, either acute or progressive, following NAC treatment, skin samples containing papillomas from control mice or mice treated with NAC were harvested following administration of BrdU at one week or 20 weeks after NAC treatments began. Sections from papillomas were sectioned and stained, and BrdU positive cells were quantified (Figure 4.4 B). There was no significant difference in proliferation rates of papillomas after one week or 20 weeks of NAC treatment, suggesting that antioxidant treatment alone does not alter papilloma proliferation.

In order to determine the effect of antioxidant treatment on tumor progression, H&E stained sections were prepared from the papillomas of all mice at the conclusion of the experiment. Papillomas from mice treated with NAC progressed to malignancy at a significantly lower frequency than papillomas from mice that were fed water alone ($p < 0.001$) (Table 4.3). This suggests that antioxidant treatment can decrease the

malignant progression of skin tumors. This is further supported by data in other model systems which suggest that antioxidants can reduce angiogenesis and inflammation associated with tumor growth, which then prevents tumor progression (Zafarullah et al., 2003).

## 4.4 ***DISCUSSION***

DNA damage checkpoint proteins play a key role in response to oxidative stress, which can be toxic to cells and result in diseases, such as cancer, in organisms. In order to determine what role the DNA damage checkpoint protein HUS1 plays in response to oxidative stress, we have made use of the *Hus1* allelic series to reduce the levels of HUS1. Primary $Hus1^{Neo/\Delta 1}$ cells senesce rapidly under standard culture conditions, which is hyperoxic compared to physiological oxygen levels (Levitt et al., 2007). This premature senescence can be relieved by treatment with a potent antioxidant, NAC, or by growth in low oxygen conditions, suggesting that HUS1 normally plays a critical role in response to oxidative stress (Figure 4.1 A). ROS can result in the formation of 8-oxo-dG, which if unrepaired, can result in G→T transversions, and permanent mutations which can have detrimental effects on a cell and an organism. Base excision repair (BER) machinery specifically can recognize and repair oxidative lesions to prevent mutations. The 9-1-1 complex has been shown to interact with components of BER, which may be one reason cells deficient for *Hus1* have an increased sensitivity to oxidative stress. Additionally, the 9-1-1 complex is known to stabilize replication forks, which may become stalled in hyperoxic conditions, due to bulky DNA lesions or breakdown of other important macromolecules. The lack of HUS1, and thus the lack of functional 9-1-1 complex, may result in increased fork collapse and double stranded breaks (Branzei and Foiani; Zhu and Weiss, 2007). This is further supported by the chromosomal instability seen

***Figure 4.4*** **No significant difference in papilloma number or size in wild-type mice treated with NAC and no significant change in proliferation rate within papillomas.** 30 wild-type FVB mice of the same age were shaved and treated with a single dose of DMBA followed by repeated doses of TPA for 20 weeks. After visible papillomas began to form 65 days after DMBA treatment, mice were divided into two groups with half the mice were placed on 0.04M NAC water as their sole water source, while half the mice were placed on normal bottled water. This antioxidant water was changed weekly. (A) Papilloma number and size were measured twice weekly. There was no significant difference between papilloma number ($p = 0.191$) or size ($p = 0.361$) between non-treated and NAC treated mice as assessed by mixed model analysis (linear regression with covariant structure). (B) Representative images of BrdU staining in papillomas of non-treated and NAC treated mice at 10X and 40X magnification. (C) Quantification of BrdU staining in papillomas of control (n = 4 papillomas from 2 mice) and NAC treated (n = 4 papillomas from 2 mice) mice following acute NAC treatment, and quantification of BrdU staining in large papillomas of control (n = 4 papillomas from 2 mice) and NAC treated (n = 6 papillomas from 3 mice) mice 20 weeks after the start of NAC treatment. At least two sections were counted for each papilloma. There was no significant differences in proliferation between control and NAC treated papillomas at 1 week ($p = 0.388$) or at 20 weeks ($p = 0.344$) by two-tailed Students t-Test. *[Experiments and figures by S.A. Yazinski]*

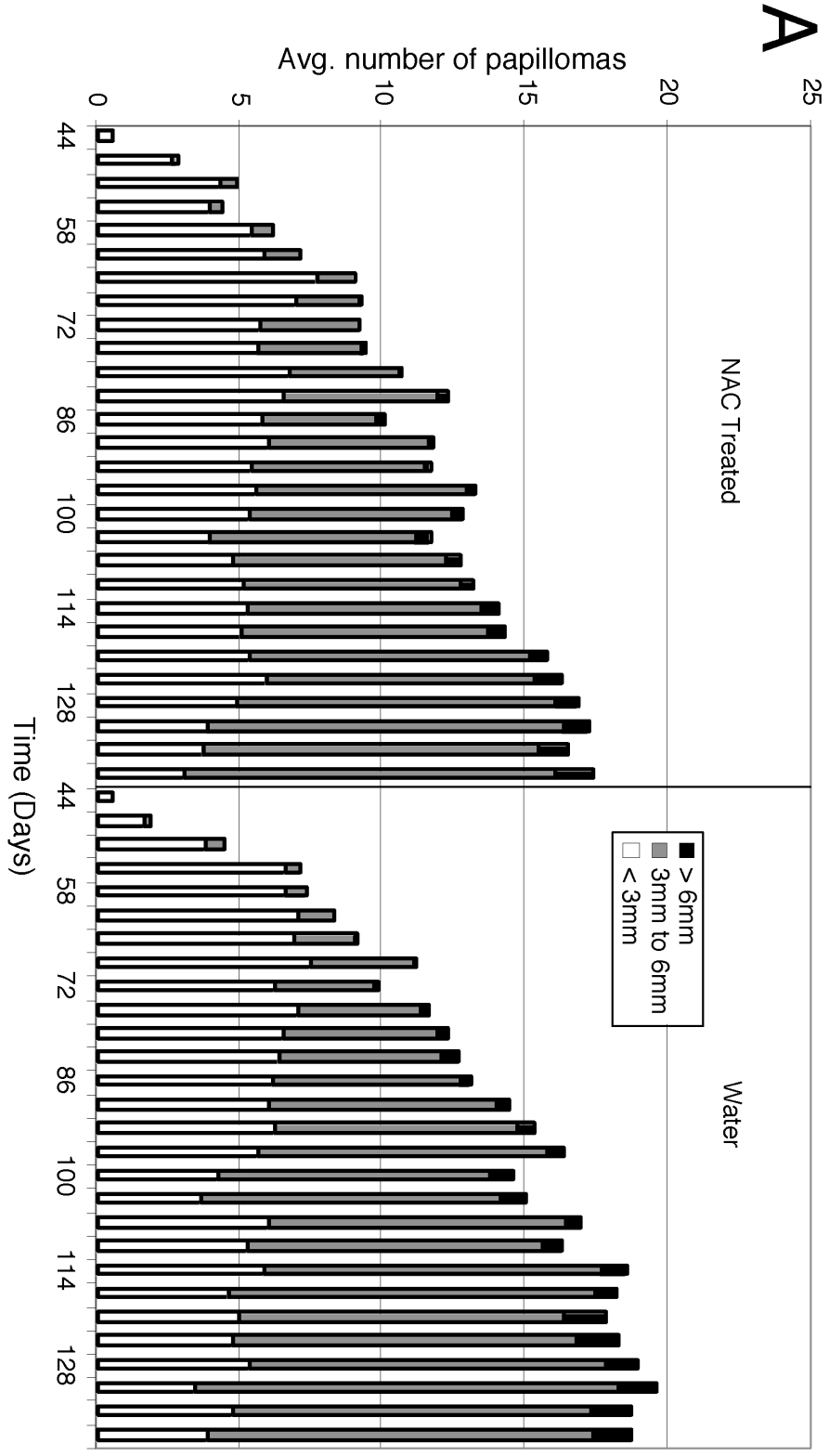
A
Avg. number of papillomas
0
5
10
15
20
25
NAC Treated
Water
> 6mm
3mm to 6mm
< 3mm
Time (Days)
44
58
72
86
100
114
128
44
58
72
86
100
114
128

Figure 4.4 (Continued)

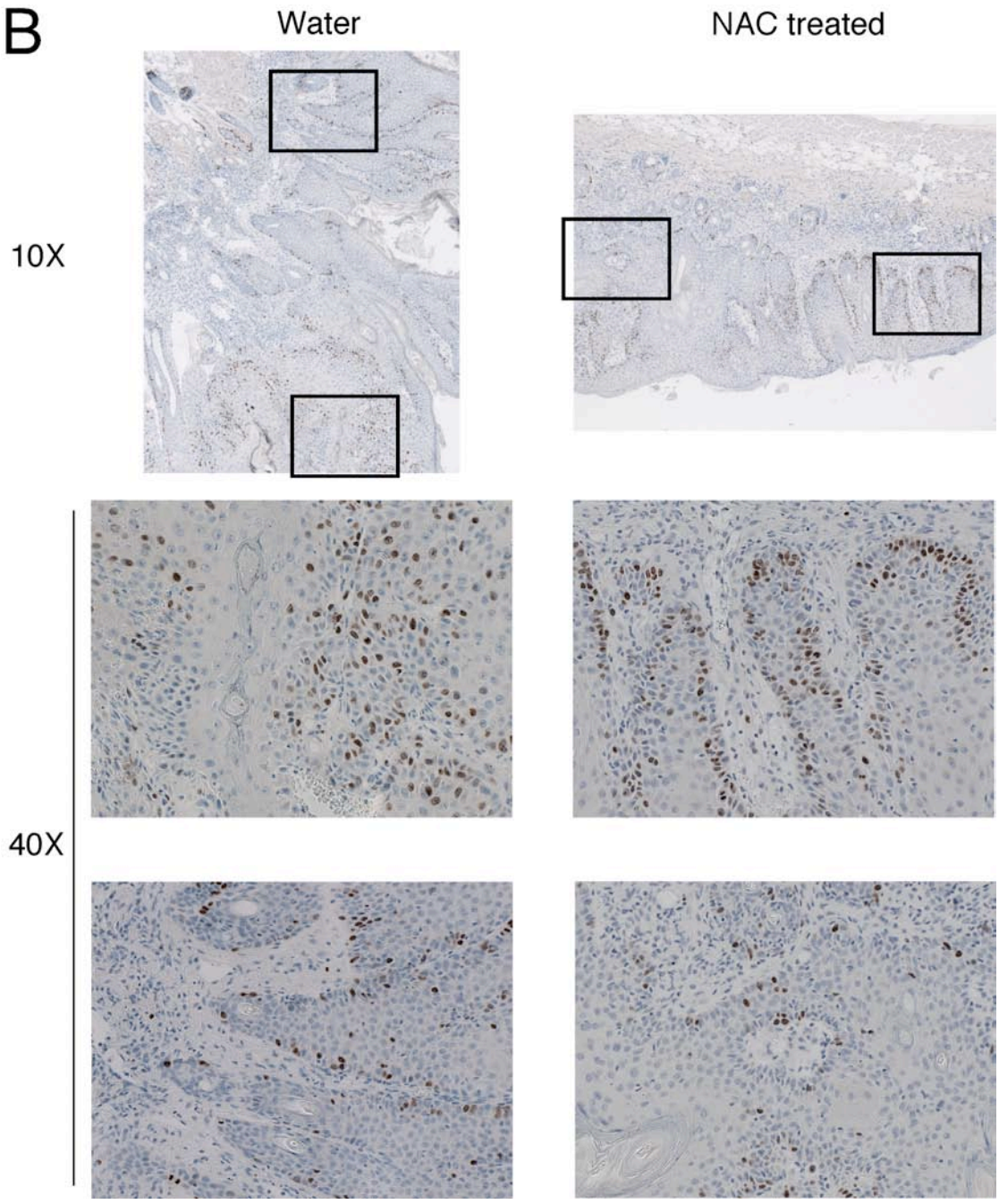

Figure 4.4 (Continued)

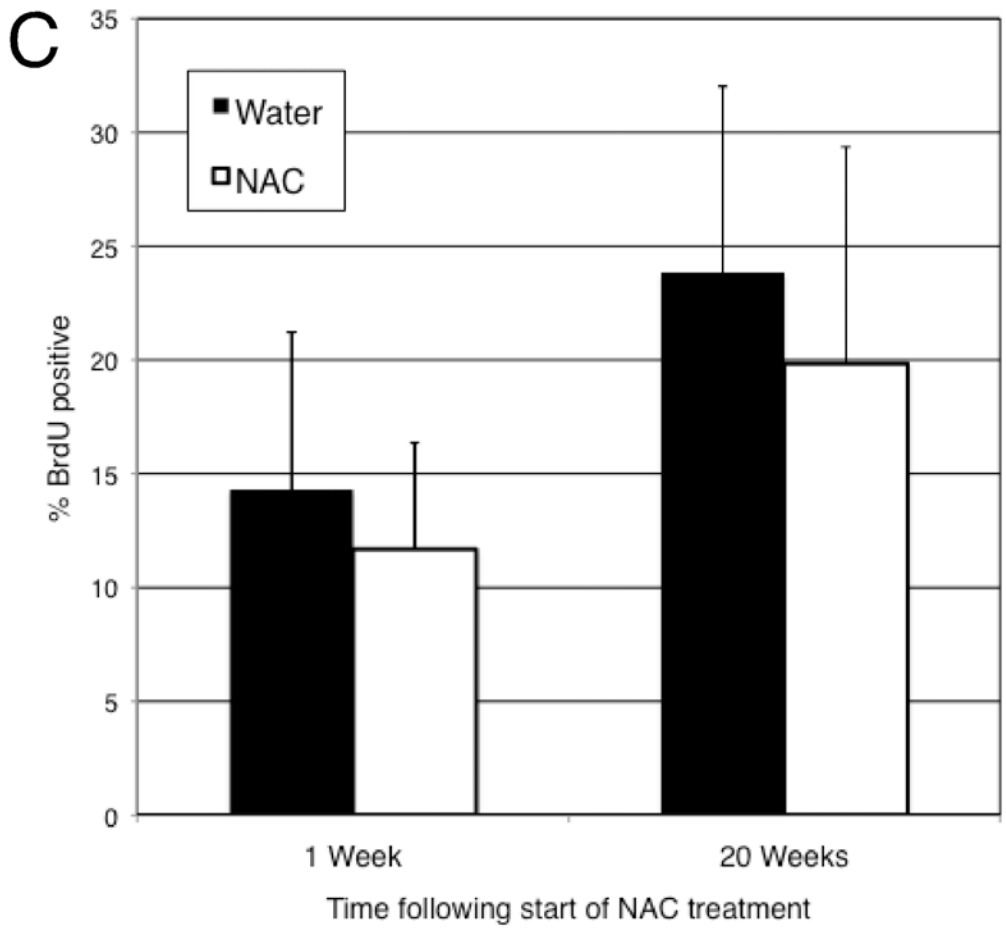

***Table 4.3*** **Summary of histological evaluation of papillomas arising from a two-step skin carcinogenesis treatment in wild-type FVB mice treated with water or NAC[a]**

| Treatment | Non-Malignant | Malignant | Total |
|---|---|---|---|
| **NAC** | 77 | 13 | 90 |
| **Water** | 42 | 38 | 80 |
| **Total** | 119 | 51 | 170 |

[a]Sections of skin papillomas of wild-type FVB mice with (n = 15) or without (n=15) treatment of NAC in their drinking water were H&E stained and evaluated for malignancy by a pathologist. A malignant tumor was determined as a papilloma with non-defined borders with cells that had begun to migrate below the basal epidermal layer. Mice that were given antioxidant supplement in their drinking water had significantly fewer papillomas progress to malignancy than control mice that received only water ($p < 0.001$ by Pearson Chi-Square). *[Experiment by S.A. Yazinski; Malignancy evaluated by R. Peters]*

in metaphase spreads prepared from Hus1$^{Neo/\Delta1}$ cells that were not treated with NAC (Figure 4.1 B). Additionally, antioxidant treatment was able to rescue the hypersensitivity of Hus1$^{Neo/\Delta1}$ cells to low doses of aphidicolin, a replication inhibitor, suggesting that DNA damage from oxidative stress occupies the available HUS1, sensitizing these cells to aphidicolin treatment. However, when the oxidative stress is relieved, Hus1$^{Neo/\Delta1}$ cell have enough HUS1 to cope with aphidicolin inhibition of replication. However, when the system is overloaded with replication inhibitor, Hus1$^{Neo/\Delta1}$ cells no longer have enough HUS1 to stabilize stalled forks, resulting in cell death.

This rescue of genomic instability by antioxidant treatment seen in Hus1$^{Neo/\Delta1}$ cells with severe replication defects in culture (Figure 4.1) suggested that antioxidant treatment of Hus1$^{Neo/\Delta1}$ mice may reduce the high level of genomic instability *in vivo*, as assessed by micronucleus assay. However, NAC treatment of Hus1$^{Neo/\Delta1}$ mice in drinking water was not able to reduce micronucleus levels (Figure 4.2). This may be because the NAC may be metabolized in such a way that the antioxidant does not reach the erythroid progenitor population. Also, NAC may have a more long term effect that was not detected in our assay which only measured micronucleus in erythrocytes out to 28 days (4 weeks) after NAC treatment, while the turn over rate for erythrocytes in mice is about 60 days (Walker et al., 1984). Alternatively, this may be because the genomic instability of Hus1$^{Neo/\Delta1}$ mice assessed by micronucleus assay is not due to oxidative stress, but rather, due to another defect resulting from inadequate levels of HUS1, such as increased replication stress in proliferative tissues. That HUS1 has additional functions beyond responding to oxidative stress was further confirmed by treatment of Hus1$^{\Delta1/\Delta1}$ embryos with antioxidants *in utero* which has no effect on levels of apoptosis and embryonic lethality (Figure 4.3). Again, this critical requirement for HUS1 during embryonic development, even when levels of ROS are

decreased, further supports the idea that HUS1 is plays an important role in response to replication stress and stalled forks during high rates of proliferation.

Because antioxidant treatment had such a remarkable effect on genomic instability in cell culture (Figure 4.1), we wanted to determine what effect NAC treatment would have on the growth of tumors, which have been shown to have increased genomic instability. Antioxidants did not significantly alter the number or size of tumors that developed; however, NAC treatment did significantly reduce the number of papillomas that progressed to malignancy (Figure 4.4). It is not surprising that antioxidant treatment, which was given after tumor initiation, did not halt tumor growth or result in tumor regression, as the mutation in H-ras from DMBA treatment is permanent, and TPA, which promotes tumor development, is still continually delivered. Antioxidant treatment did not affect the tumor cells themselves, as proliferation rates between treated and untreated tumors were not significantly different. However, antioxidant treatment was able prevent malignant progression, despite continuous applications of TPA. This may be due to a reduction in inflammation or angiogenesis due to NAC treatment (Zafarullah et al., 2003), which then prevents tumor cell invasion and metastasis (Makrilia et al., 2009; Moore et al., 2010). By this reasoning, the antioxidant treatment does not affect the tumor growth itself, but rather acts on surrounding cells to prevent malignant progression. On the other hand, NAC may also prevent further oxidative damage to the tumor cells themselves. In this way, NAC would prevent mutations in tumor cells required for malignant progression and impede aggressive tumor growth. These ideas are validated by studies which have found decreased malignancy in certain tumors following NAC treatment (Estensen et al., 1999; Goldman et al., 2000; Kawakami et al., 2001). Our results indicate a beneficial effect of NAC treatment following tumor initiation; however, our study did not determine the long term effect of NAC treatment

prior to tumor initiation. Because tumors have high levels of oxidative stress and genomic instability, NAC treatment prior to initiating events may actually lower the stress in cells undergoing transformation, and allow cells to become transformed more efficiently. Additionally, this lower stress level may also allow cancer cells to grow more aggressively. Further studies are needed to better understand the role antioxidant treatment plays in tumor initiation and development.

# CHAPTER 5

# SUMMARY, MODELS, AND FUTURE DIRECTIONS

The ATR DNA damage checkpoint pathway is essential and responds to various DNA lesions which result in single stranded DNA. HUS1 is an indispensable component of the ATR pathway, and germline deletion of *Hus1* results in embryonic lethality (Weiss et al., 2000). Conditional inactivation of *Hus1* in cultured cells had previously been shown to result in genomic instability, increased chromosomal breaks at common fragile sites, proliferation defects, and apoptosis that cannot be rescued by inactivation of *p53* (Zhu and Weiss, 2007). Reduced expression of wild-type HUS1 also resulted in increased genomic instability and chromosomal aberrations in culture, as well as sensitivity to DNA damaging agents (Levitt et al., 2007). Taken together, these data suggest HUS1 acts to maintain genomic integrity in order to allow proliferation and survival of cultured cells under normal conditions and in response to DNA damaging agents. This suggests that HUS1 may also play a role in tumor suppression, as an increase in genomic instability correlates with tumor susceptibility.

## 5.1 An essential role for HUS1 in mammary gland development and tissue homeostasis

In order to determine the role of HUS1 in tumorigenesis, we made use of a conditional *Hus1* knockout mouse to inactivate *Hus1* in the mouse mammary gland. This allowed us to bypass the embryonic lethality of germline inactivation while studying the consequences of deletion of *Hus1* at a specific time and tissue. We found that *Hus1*-null cells were not present and that levels of DNA damage and apoptosis were elevated in conditional *Hus1* knockout mammary glands. However, conditional *Hus1* knockout mammary glands appeared grossly normal. This suggested that *Hus1*-

null cells were being cleared from the mouse mammary gland by apoptosis due to increased genomic instability and DNA damage. *Hus1* loss resulted in cell death, rather than tumorigenesis. However, clearance of these *Hus1*-null cells may have promoted compensatory proliferation of surrounding *Hus1*-retaining cells, as there were no morphological defects following clearance of a large number of cells from the mammary gland. This may be due to compensatory signaling from other DNA damage proteins that recognize the severe DNA damage in *Hus1*-null cells and induce apoptosis to prevent tumorigenesis (Figure 5.1).

We next set out to determine if loss of *p53* could prevent apoptosis and clearance of *Hus1*-null cells from the mammary gland. Conditional *Hus1* knockout, *p53*-deficient mammary glands retained *Hus1*-null cells, suggesting that p53 normally induces apoptosis in response to *Hus1*-deficiency-induced DNA damage and promotes clearance of these cells. Surprisingly, the levels of DNA damage and apoptosis were significantly higher in conditional Hus1 knockout mammary glands in the absence of p53. This may be due to delayed induction of apoptosis to a narrow window of time in a *p53*-deficient setting or lack of clearance of these damaged cells. Furthermore, retention of *Hus1*-null cells was accompanied by severe morphological abnormalities in the mammary gland, resulting in nursing defects of conditional *Hus1* knockout, *p53*-deficient mice. The cause of this loss of tissue homeostasis has yet to be determined. A dominant inhibitory signal from apoptotic cells remaining in the mammary gland may prevent compensatory growth. Alternatively, clearance of apoptotic cells may act as a positive growth signal in normal conditions, and, because apoptotic cells are not cleared from conditional *Hus1* knockout mammary glands, there may not be a positive growth center for regeneration. This shows that a combined loss of *Hus1* and *p53* results in loss of tissue homeostasis, but does not result in tumorigenesis. Furthermore, these data suggest that loss of *Hus1* is not likely

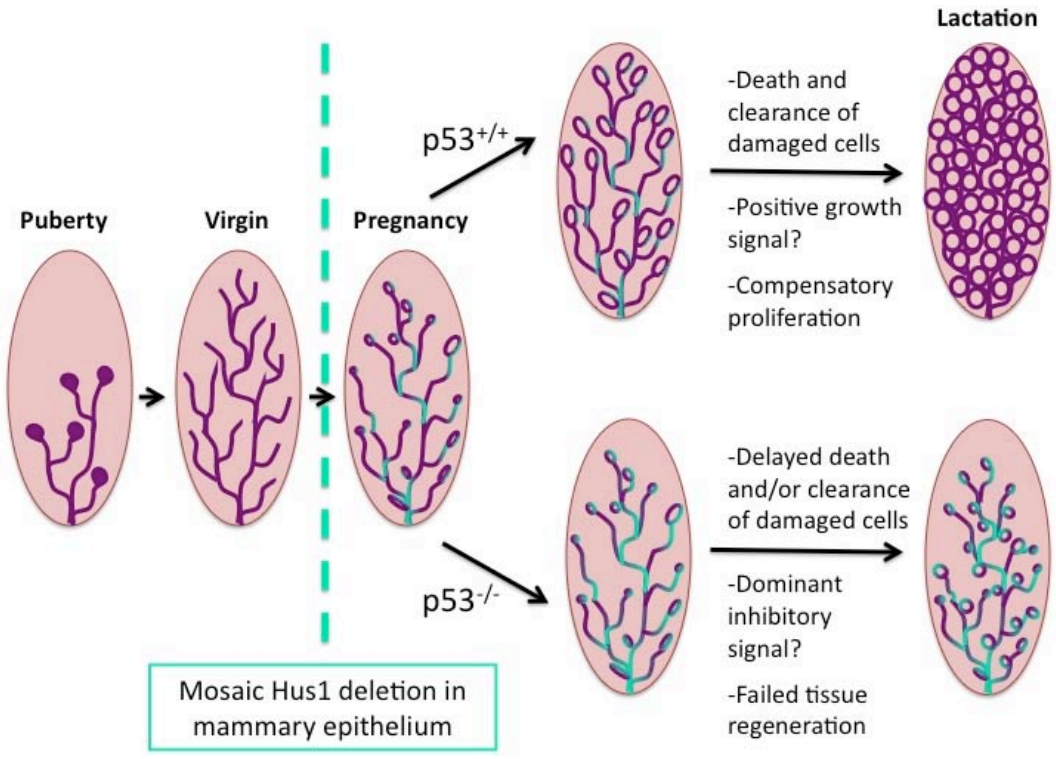


***Figure 5.1*** **Model for interaction between Hus1 and p53 in maintenance of tissue homeostasis in the mouse mammary gland.** Conditional Hus1 inactivation is achieved in the mammary gland of pregnant mice using Cre-recombinase expression driven by the Blg promoter sequence. Following Hus1 inactivation, cells experience increased genomic instability, resulting in DNA damage and cell death. Clearance of these cells may signal for compensatory proliferation, as this level of cell death does not result in morphological abnormalities, resulting in a functional mammary gland. Following Hus1 inactivation in the absence of p53, there is a greater increase in DNA damage and, surprisingly, a greater increase in apoptosis. This may be due to a failure to clear dead cells or delayed apoptosis occurring in a more narrow window of time. This retention or increase in apoptotic cells in the mammary gland resulted in failed tissue regeneration and striking morphological abnormalities that were not compatible with milk production or with nursing pups. Overall, these results establish an essential role for Hus1 in the survival and proliferation of mammary epithelium and identify a novel role for p53 in mammary gland tissue regeneration and homeostasis.

to contribute to tumorigenesis, and, in fact, may sensitize *p53*-null cells, which are generally resistant to apoptosis, to cell death. This may be because inactivation of *p53* results in genomic instability, which, when combined with *Hus1*-inactivation, elevates the level of DNA damage to level which induces p53-independent apoptosis.

### 5.2 Reduced HUS1 levels result in impaired tumorigenesis

While complete *Hus1* inactivation results in severe genomic instability which is not compatible with cellular survival, this does not exclude the possibility that partial reduction in HUS1 levels, which also results in genomic instability, may have a different effect on tumorigenesis. Cells with a partial reduction in *Hus1* expression have increased levels of genomic instability and are sensitive to DNA damaging agents (Levitt et al., 2007). However, mice expressing reduced levels of HUS1 ($Hus1^{Neo/\Delta1}$ mice) are grossly normal and are born at expected frequencies (Levitt et al., 2007), making them an ideal tool to study the effect of reduced levels of HUS1 on transformation and subsequent tumorigenesis. In preliminary experiments, $Hus1^{Neo/\Delta1}$ cells, despite a higher basal level of genomic instability, showed a decreased probability of becoming transformed as measured by focus formation assays and soft agar assays. To better understand the effect of reduced HUS1 on tumorigenesis, $Hus1^{Neo/\Delta1}$ mice were subjected to two-step skin carcinogenesis protocol which induces skin papillomas. In agreement with the cell culture data, $Hus1^{Neo/\Delta1}$ mice developed fewer and smaller papillomas than control littermates. The reduced papilloma development in $Hus1^{Neo/\Delta1}$ mice was not associated with sensitivity to either DMBA or TPA treatment, the chemicals which induce and promote tumor development, respectively. Taken together, the cell culture transformation assays and the skin tumorigenesis study suggest that reduced levels of HUS1 inhibit tumorigenesis (Figure 5.2).

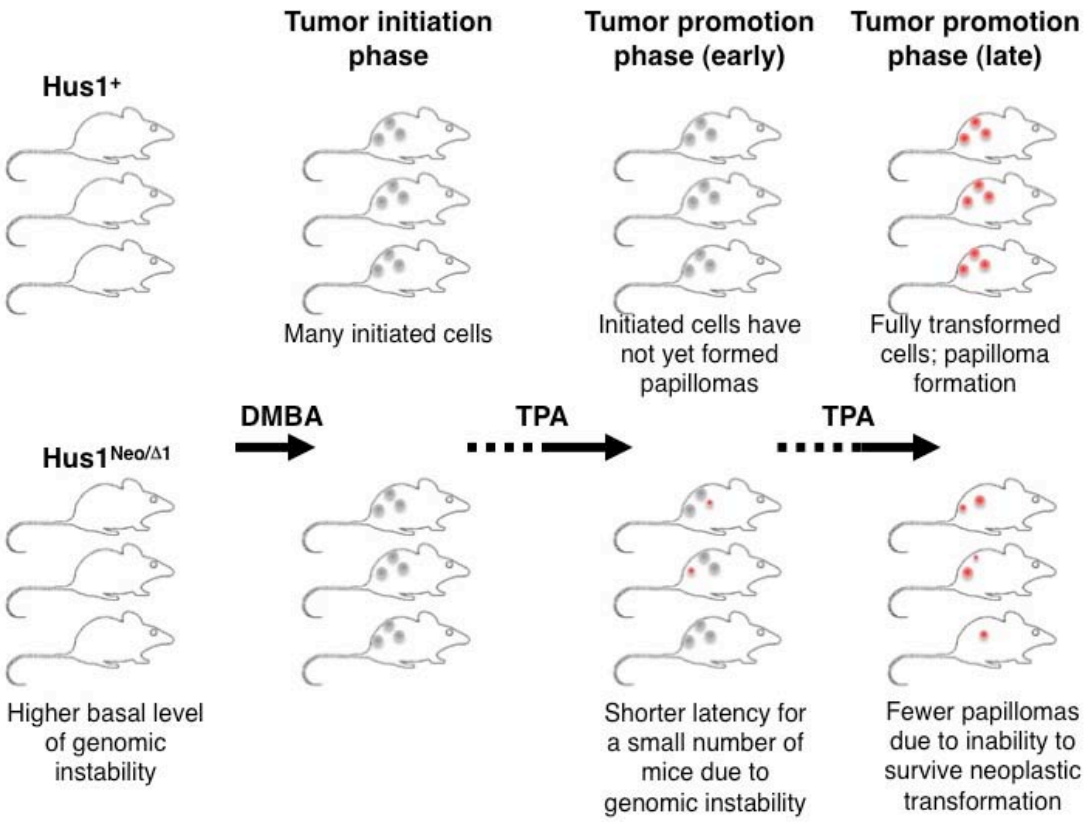


***Figure 5.2*** **Model for reduced Hus1 expression resulting in reduced skin papilloma formation.** $Hus1^{+}$ mice, with wild-type levels of Hus1, and $Hus1^{Neo/\Delta1}$ mice, with reduced levels of Hus1, were treated with a single dose of DMBA to induce tumor development, and were treated with TPA twice weekly for twenty weeks to promote tumor development. A small number of $Hus1^{Neo/\Delta1}$ mice developed papillomas with a shorter latency than $Hus1^{+}$ mice, perhaps due to a higher basal level of genomic instability resulting in $Hus^{Neo/\Delta1}$ skin cells being more ready transformed. However, at the conclusion of 20 weeks, $Hus^{Neo/\Delta1}$ mice had significantly fewer papillomas than $Hus1^{+}$ mice. We hypothesize this is due to a requirement for Hus1 in order for cells to survive transformation and to undergo oncogene-induced proliferation.

**5.3 Model for the effect of reduced HUS1 levels on tumorigenesis.**

The data presented here, along with previous data from our lab and others, allow us to formulate a model for the effect of reduced levels of HUS1 on tumorigenesis. Complete inactivation of *Hus1* results in severe genomic instability, which may not be compatible with rapid proliferation, such as that which occurs during tumor growth. This is supported by the fact that germline inactivation of *Hus1* results in embryonic lethality, suggesting HUS1 is essential during rapid embryonic proliferation. Furthermore, HUS1 is necessary for survival of rapidly proliferating mammary gland epithelial cells, as *Hus1*-deficient cells are cleared from the mammary gland during pregnancy. Additionally, conditional *Hus1* inactivation in cultured cells results in delayed S-phase progression, increased DNA breaks at common fragile sites, and increased apoptosis. Taken together, these data suggest that *Hus1* inactivation likely does not contribute to tumor initiation and growth, as rapid proliferation in the absence of *Hus1* results in cell death.

A partial defect in *Hus1* expression has a different cellular phenotype than complete *Hus1* inactivation. $Hus1^{Neo/\Delta 1}$ mice, which express only 20% wild-type *Hus1*, are grossly normal and born at expected frequencies, suggesting that this level of *Hus1* expression permits embryo growth and normal mouse development. Overall, $Hus1^{Neo/\Delta 1}$ mice have only mild phenotypes, such as increased sensitivity to some DNA damaging agents as well as a higher level of micronucleus formation. These characteristics indicate that these mice have a higher basal level of genomic instability, but that these genome maintenance defects have little effect on an unstressed mouse, as $Hus1^{Neo/\Delta 1}$ mice show no increase in spontaneous tumor development. $Hus1^{Neo/\Delta 1}$ cells exhibit more severe phenotypes than $Hus1^{Neo/\Delta 1}$ mice, including increased genomic instability, premature senescence, and hypersensitivity to DNA damaging agents and oxidative stress. When $Hus^{Neo/\Delta 1}$ cells were tested in transformation assays,

there were variable results between immortalized cell lines, though these cells are less able to be transformed overall. This variability between cell lines may be due to mutations incurred during the transformation process, and variability decreased as the stringency of the assay increased. This decreased ability of cells with reduced levels of HUS1 to undergo transformation was further confirmed *in vivo*, as $Hus1^{Neo/\Delta 1}$ mice developed fewer and smaller skin papillomas following a two-step skin carcinogenesis treatment. These results suggest that the high level of genomic instability in $Hus1^{Neo/\Delta 1}$ mice is compatible with normal cell proliferation, but cannot support the rapid proliferation of neoplastic transformation. $Hus1^{Neo/Neo}$ mice, with a less severe reduction in Hus1 expression, show an intermediate phenotype, developing more papillomas than $Hus1^{Neo/\Delta 1}$ mice, but fewer than $Hus1^{+}$. This suggests that the ability of cells be transformed directly relates to the level of *Hus1* expression. Taken together, these experiments demonstrate that transformed cells may require HUS1 in order to survive the stress of oncogene-induced proliferation (Figure 5.3).

Hus1 is an essential checkpoint protein that is critical for response to replication and oxidative stresses. The process of transformation results in increased oxidative stress as well as increased proliferation. Without sufficient levels of HUS1, cells cannot survive these stresses of transformation and neoplastic proliferation. However, this effect may be tissue specific. Some tissues have more tolerance for loss of HUS1, and HUS1 may not be required for transformation of these tissue types. This may be because of a more prominent function of other redundant checkpoint proteins, such as those of the ATM pathway or DNA-PK, in these tissues. Therefore, reduced levels of HUS1 may not result in decreased tumorigenesis in every tissue type. This effect may also depend on interactions with other DNA damage proteins. Tumors which are initiated by mutations in other DNA damage checkpoint proteins, rather than initiated by oncogenes, may not be sensitive to *Hus1*-loss. For example, reduced

***Figure 5.3*** **Model for the effect of reduced Hus1 on transformation.** Cells expressing wild-type levels of Hus1 have normal checkpoint mechanisms in place, and have no genome maintenance defects. Despite normal checkpoint function, a certain number of these cells become transformed after addition of two oncogenes as measured by cell culture transformation assays. Accordingly, a certain number of cells of $Hus1^{+}$ mice also become transformed after a two-step skin carcinogenesis treatment, resulting skin papilloma formation. On the other hand, $Hus1^{Neo/Neo}$ and $Hus1^{Neo/\Delta 1}$ cells have a higher basal level of genomic instability. Despite this, cells are less readily transformed as measured by cell culture transformation assays. $Hus1^{Neo/Neo}$ and $Hus1^{Neo/\Delta 1}$ mice also develop fewer skin papillomas following DMBA and TPA treatment. Additionally, the level of Hus1 expression correlates with the level of tumorigenesis and is inversely related to the level of genomic instability, such that the low level of Hus1 expression results in a small number of papillomas, but very high levels of genomic instability. Complete germline inactivation of Hus1 results in embryonic lethality due to severe genomic instability. Similarly, complete conditional Hus1 inactivation also results in increased DNA damage and apoptosis, but does not cause tumor development. Taken together, this points to an essential role for Hus1 in survival of transformation and in neoplastic proliferation.

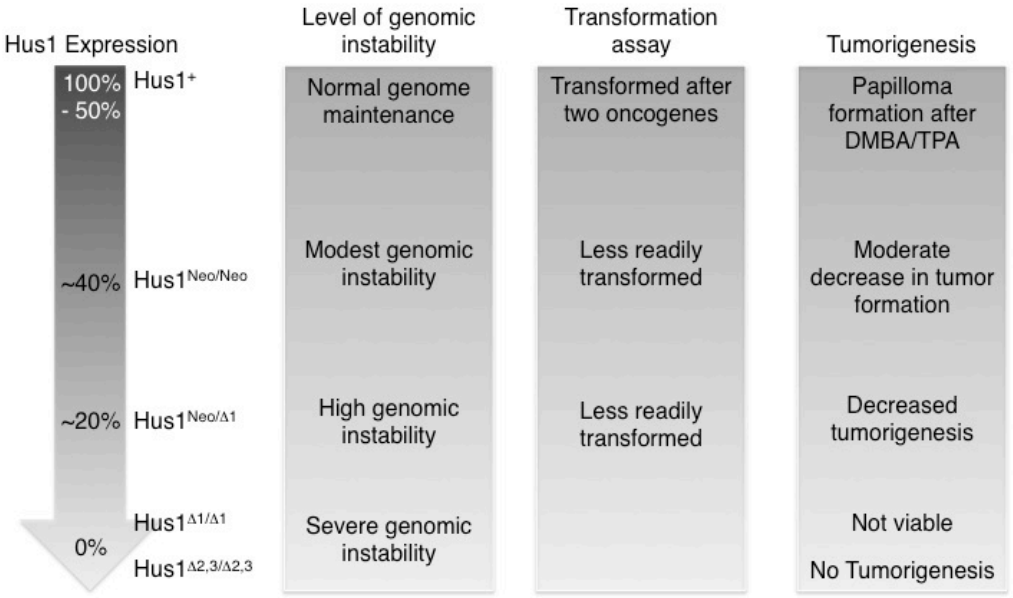
Hus1 Expression
Level of genomic instability
Transformation assay
Tumorigenesis
100% - 50%
Hus1+
Normal genome maintenance
Transformed after two oncogenes
Papilloma formation after DMBA/TPA
~40%
Hus1Neo/Neo
Modest genomic instability
Less readily transformed
Moderate decrease in tumor formation
~20%
Hus1Neo/Δ1
High genomic instability
Less readily transformed
Decreased tumorigenesis
0%
Hus1Δ1/Δ1
Hus1Δ2,3/Δ2,3
Severe genomic instability
Not viable
No Tumorigenesis

levels of HUS1 does not affect lymphoma incidence promoted by loss of p53 (Levitt et al., 2007) or ATM (Balmus, et al., manuscript in preparation). In order for reduced levels of HUS1 to result in decreased tumorigenesis, cells may require the remaining DNA damage checkpoint proteins to be in place in order to respond to the damage resulting from *Hus1* loss to induce senescence or apoptosis, and prevent tumorigenesis.

**5.4 Model for the role of the ATR pathway in tumorigenesis.**

The results described here, along with results from other labs describing other components of the ATR pathway, provide insight into the roles of the ATR in prevention of genomic instability, in maintenance of tissue homeostasis, and in tumor suppression. Some reports suggest that inactivation of or mutations in the ATR pathway may result in increased tumorigenesis due to genomic instability. Several components of the ATR pathway, such as ATR, CHK1, RAD9, and RAD1, have been suggested to be haploinsufficient for tumor suppression (Fang et al., 2004; Hu et al., 2008; Lam et al., 2004; Liu et al., 2000). While other reports suggest that impairment of the ATR pathway results in a heightened levels of genomic instability that is incompatible with hyper-proliferation resulting in decreased tumor development (Cho et al., 2005; Jardim et al., 2009; Kinzel et al., 2002; Luo et al., 2009; Luo et al., 2001; Yuki et al., 2008; Zhu et al., 2008). The dependence on the ATR pathway for proliferation is seen clearly during embryogenesis, as inactivation of any component of the ATR pathway is not compatible with life (Brown and Baltimore, 2000; Budzowska et al., 2004; Han et al.; Hopkins et al., 2004; Liu et al., 2000; Takai et al., 2000; Weiss et al., 2000). Additionally, there are several examples of increased expression of checkpoint proteins in human tumors, suggesting that tumors have an increased dependency on these factors (Cheng et al., 2005; de la Torre et al., 2008;

Madoz-Gurpide et al., 2007; Verlinden et al., 2007; Zhu et al., 2008). Reducing expression of several components of the ATR pathway has a tumor preventative phenotype and also sensitizes tumor cells to therapeutic treatments.

These conflicting reports may be due to tissue specific requirements for DNA damage responsive elements. For example, certain cell types of cancer origin may have less dependence on components of the ATR pathway for survival, such as certain types of prostate cancers, endometrial cancers, colon cancers, and stomach cancers. For these types of cancer, a lower level of components of the ATR pathway would result in genomic instability and higher mutation rate that would be advantageous to the rapidly dividing tumor cells. While other cell types of cancer origin may have a greater dependence on components of that ATR pathway, such as breast cancers, some types of prostate cancer, ovarian cancers, and some colon cancers. For these types of cancers, lower levels of *Atr* expression are not compatible with rapid proliferation, and results in cell death following oncogene activation or transformation due to the increased stress and genomic instability.

The extent of reduced expression of each checkpoint protein may also have an effect on tumorigenesis. Heterozygosity for components of the ATR pathway, expressing only half the wild-type level, may result in a modest increase in genomic instability, which may result in increased mutation rate and accelerated tumorigenesis. A more drastic decrease in checkpoint expression can result in severe genomic instability. This, in combination with the increased stress level of replication and oxidative stress associated with neoplastic proliferation, may result in DNA damage incompatible with cell survival. Thus, an extreme decrease in protein expression of certain checkpoint proteins may actually prevent tumorigenesis, while having very little effect on normal cells which are proliferating at a slower rate and retain other redundant, though less vital, checkpoint pathways.

While there are many indicators that inhibitors of checkpoint proteins in the ATR pathway may be effective in treatment of cancer, the effect of checkpoint inhibition on specific cell type and the level of inhibition must be more clearly understood, so as to prevent tumor promotion. Additionally, the consequences of inactivation of components of the ATR pathway on tissue homeostasis and other critical processes, such as meiosis, must be further understood. The information provided here further shows the importance of understanding the genetic makeup of tumors cells prior to treatment, in order to determine the effectiveness of combinational therapy. For example, the synthetic lethal effect of combined inactivation of p53 with components of the ATR pathway can be exploited to target cells deficient for p53. The effectiveness of inhibitors of the ATR pathway may depend on a combination of tissue type, genetic fingerprint of the tumor, and level of checkpoint reduction. In certain tissue types, ATR inhibition may increase the risk for tumor development (Figure 5.4). Clearly, the role of the ATR pathway in tumorigenesis is not a simple story, and many questions still remain.

## 5.5 FUTURE DIRECTIONS

While the data presented here indicate that reduced levels of HUS1 result in decreased tumorigenesis, there is evidence that inhibition of other components of the ATR pathway in various tissue types may have a tumor promoter effect. We cannot be sure that reduced HUS1 levels will result in reduced tumor formation in other tissue types. In fact, reduced levels of HUS1 does not decrease lymphoma incidence induced by p53 or ATM deficiency. Furthermore, the mechanism by which reduced levels of HUS1 result in decreased skin papillomas has yet to be determined.

One caveat of our results that $Hus1^{Neo/\Delta 1}$ mice develop fewer skin papillomas is that chemical carcinogens were used in the two-step skin carcinogenesis experiments.

***Figure 5.4*** **Overall model for the effect of reduced function of the Atr pathway on transformation and tumor development.** In response to oncogenic stimuli, most cells with normal checkpoint function will induce senescence or apoptosis to prevent transformation. However, some cells will become transformed, allowing cancer to develop. In cells that are deficient for components of the Atr pathway, there are at least two possible outcomes following a signal of oncogene-induced proliferation. If the oncogenic signal occurs in a tissue which has a low requirement for the Atr pathway, loss of the Atr pathway may result in increased genomic instability that can enhance transformation ability and result in increased tumorigenesis. This same effect can occur if there is only moderate reduction of function of the Atr pathway, such that there is enough Atr checkpoint function to allow cells to survive, but not enough to prevent a modest increased in genomic instability, which can accelerate tumorigenesis. A second possibility is that reduced Atr function results in reduced tumorigenesis. This can be due to a tissue specific requirement for Atr function. In this case, when cells receive an oncogenic signal, they cannot survive the rapid proliferation and stress associated with transformation without Atr function, and may induce senescence, apoptosis, or undergo mitotic catastrophe. Similarly, an extreme decrease in Atr function can result in severe genomic instability that can be detrimental to cell survival in a stressed state, such as during transformation. This too would result in induction of senescence, apoptosis, or mitotic catastrophe in cells with oncogenic signaling, resulting in decreased tumorigenesis.

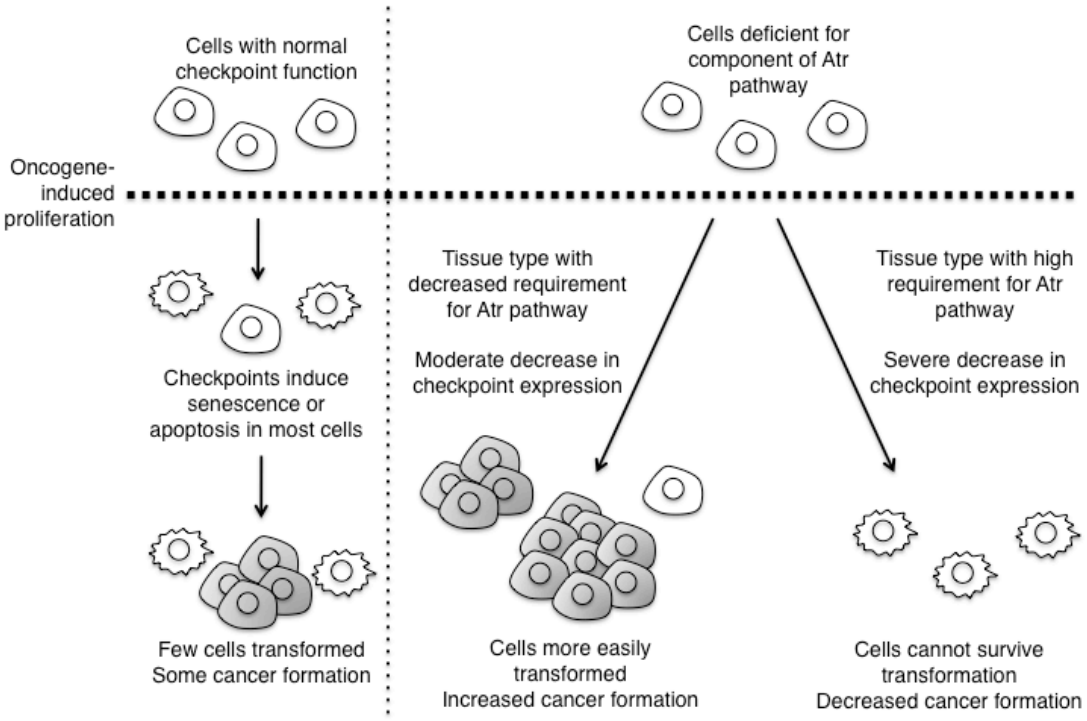
Cells with normal checkpoint function
Cells deficient for component of Atr pathway
Oncogene-induced proliferation
Checkpoints induce senescence or apoptosis in most cells
Few cells transformed
Some cancer formation
Tissue type with decreased requirement for Atr pathway
Moderate decrease in checkpoint expression
Cells more easily transformed
Increased cancer formation
Tissue type with high requirement for Atr pathway
Severe decrease in checkpoint expression
Cells cannot survive transformation
Decreased cancer formation

Because $Hus1^{Neo/\Delta1}$ cells and mice have shown increased sensitivity to certain DNA damaging agents, it is possible the skin of $Hus1^{Neo/\Delta1}$ mice is sensitive to the chemicals DMBA and TPA, which induce and promote tumor development. Although we tested the acute effect of both DMBA and TPA on cells in culture expressing reduced levels of HUS1 and on skin sections from mice expressing reduced HUS1 levels, and found no heightened sensitivity, we still cannot rule out a long term effect of these genotoxic chemicals on cell survival. In order to further understand the effect of reduced levels of HUS1 on tumorigenesis without the use of chemical carcinogens, we would like to induce tumors using other methods, including genetically inducing mammary tumorigenesis in mice with incrementally reduced levels of HUS1.

**5.6.1 Mouse models of mammary tumorigenesis.** As a second mechanism to induce tumor formation in mice with reduced HUS1 levels, we will make use of the well characterized MMTV-Neu and MMTV-PyMT mice to drive tumorigenesis specifically in the mammary gland of female mice (Guy et al., 1992a; Guy et al., 1992b). These mice overexpress Neu or PyMT, two potent oncogenes, driven by the long terminal repeats of the murine mammary tumor virus sequence. MMTV-$Neu^{Tg}$ mice or MMTV-$PyMT^{Tg}$ mice were crossed to $Hus1^{+/Neo}$ mice. The resulting $Hus^{+/Neo}$ MMTV-$Neu^{Tg}$ or $Hus^{+/Neo}$ MMTV-$PyMT^{Tg}$ offspring were bred to $Hus1^{+/\Delta1}$ mice to generate control $Hus1^{+}$ MMTV-$Neu^{Tg}$ or $Hus^{+}$ MMTV-$PyMT^{Tg}$ and experimental $Hus1^{Neo/\Delta1}$ MMTV-$Neu^{Tg}$ or $Hus1^{Neo/\Delta1}$ MMTV-$PyMT^{Tg}$ female littermates. These mice were then aged until tumor development or to 20 months, and onset of tumor development was noted, as well as, tumor size and number upon dissection. $Hus1^{+}$MMTV-$Neu^{Tg}$ mice developed more tumors than $Hus1^{Neo/\Delta1}$MMTV-$Neu^{Tg}$ mice (Figure 5.5 A, B and Table 5.1). However, the MMTV-Neu transgene on a 129 background was only 30% effective at inducing a single mammary tumor after an

***Figure 5.5*** **Hus1$^{+}$ MMTV-Neu$^{+}$ and Hus1$^{Neo/\Delta1}$ MMTV-Neu$^{+}$ mice develop mammary tumors, while Hus1$^{Neo/\Delta1}$ mice are leaner and develop uterine pathology, regardless of MMTV-Neu transgene status.** (A) Representative H&E stained image of a MMTV-Neu induced mammary tumor from a Hus1$^{+}$ MMTV-Neu$^{+}$ mouse. Scale bar represents 200μm. (B) Kaplan-Meier plot showing fraction of tumor free survival over time for all Hus1$^{+}$ MMTV-Neu$^{+}$ and Hus1$^{Neo/\Delta1}$ MMTV-Neu$^{+}$ mice. Mice were euthanized when a mammary tumor developed, when uterine pathology developed, or at 600 days. There are no statistically significant difference in tumor free survival between Hus1$^{+}$ MMTV-Neu$^{+}$ and Hus1$^{Neo/\Delta1}$ MMTV-Neu$^{+}$ ($p=0.466$ by Log Rank survival test). (C) Image showing body size difference between Hus1$^{+}$ and Hus1$^{Neo/\Delta1}$ mice on a mixed background. (D) Weight differences across age between Hus1$^{+}$ and Hus1$^{Neo/\Delta1}$ on a mixed 129SvEv and FVB background. (E) Abnormal uterine pathology found more frequently in Hus1$^{Neo/\Delta1}$ mice than Hus1$^{+}$ mice, regardless of MMTV-Neu transgene status. Arrowhead indicates start of right uterine horn, which has grossly normal uterine morphology. Scale bar represents 1cm. *[Experiments and figures by S.A. Yazinski]*

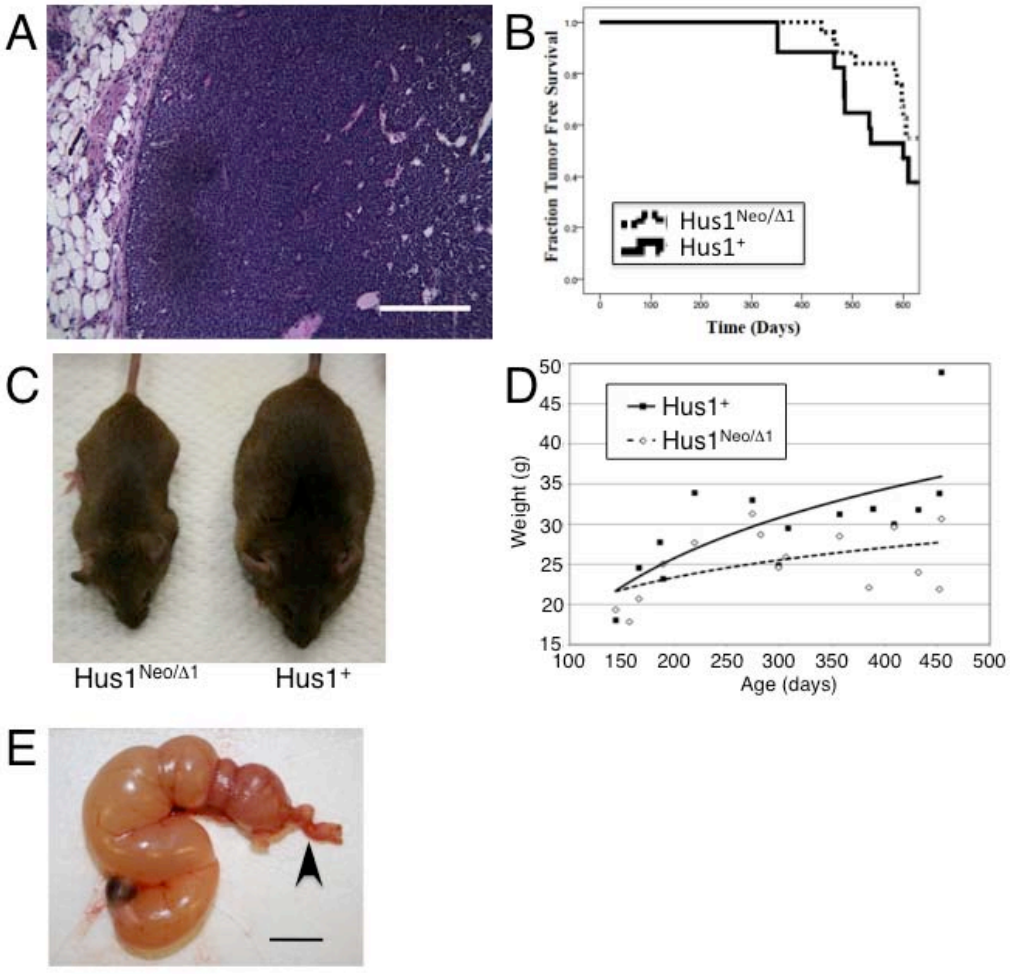
A
B
Fraction Tumor Free Survival
Hus1Neo/Δ1
Hus1+
Time (Days)
C
Hus1Neo/Δ1
Hus1+
D
Hus1+
Hus1Neo/Δ1
Weight (g)
Age (days)
E

**Table 5.1 Summary of tumor development in MMTV-Neu$^{+}$ Hus1$^{+}$ and MMTV-Neu$^{+}$ Hus1$^{Neo/\Delta1}$ mice[a]**

| Genotype | # of Animals Assessed | # with Mammary Tumors | Average Latency for Mammary Tumors | # with Uterine Pathology | Average Latency for Uterine Pathology |
|---|---|---|---|---|---|
| MMTV-Neu$^{+}$ Hus1$^{+}$ | 23 | 7 (30.43%) | 523 days | 1 (4.34%) | 481 days |
| MMTV-Neu$^{+}$ Hus1$^{Neo/\Delta1}$ | 15 | 3 (20.0%) | 456 days | 6 (40.0%) | 508 days |
| MMTV-Neu$^{-}$ Hus1$^{+}$ | 3 | 0 | 0 | 0 | 0 |
| MMTV-Neu$^{-}$ Hus1$^{Neo/\Delta1}$ | 3 | 0 | 0 | 1 (33.3%) | 604 days |

[a]MMTV-Neu$^{+}$ Hus1$^{+}$ and MMTV-Neu$^{+}$ Hus1$^{Neo/\Delta1}$ mice were generated and aged 20 months or until tumor formation. The tumor latency and frequency was determined for each genotype.

extended 20 month latency, making it difficult to determine the contribution of reduced Hus1 on reduced mammary tumor development. There was no significant difference in tumor latency (p=0.466). Additionally, $Hus1^{+}$ mice were much heavier and had more adipose tissue than $Hus1^{Neo/\Delta1}$ mice on this strain background (Figure 5.5 C and D). Because increased adipose tissue has been shown to increase inflammation, and inflammation has been linked to cancer development, the resulting decreased tumor burden in $Hus1^{Neo/\Delta1}$ mice may be due to decreased fat and inflammation rather than decreased levels of Hus1 directly (van Kruijsdijk et al., 2009). The results were further complicated due to an increased number of $Hus1^{Neo/\Delta1}$ mice, with or without MMTV-$Neu^{Tg}$ that died from uterine hemorrhaging, which may have prevented mammary tumor development (Figure 5.5 F). To clarify this, a more robust genetic model of mammary tumorigenesis was used, MMTV-PyMT transgenic mice. MMTV-PyMT mice, which express polyomavirus middle T oncogene specifically in the mammary epithelium, should develop mammary tumors within 6 weeks of age, and affect multiple mammary glands (Guy et al., 1992a). Thus, by comparing tumor number and size in MMTV-$PyMT^{Tg}$ $Hus1^{+}$ and $Hus1^{Neo/\Delta1}$ mice, we can more accurately assess the effect reduced levels of Hus1 on oncogene induced tumorigenesis, without the added complications of advanced mouse age and low frequency of tumor development. Based on results in cell culture transformation assays as well as skin tumorigenesis studies, we hypothesize that there will be a reduced tumor burden in $Hus1^{Neo/\Delta1}$ mice bearing MMTV-$PyMT^{Tg}$ relative to $Hus1^{+}$ mice.

**5.6.2 Intranasal or intratracheal instillation of AdenoCre Virus used to conditionally activate Kras while simultaneously inactivating *Hus1* in the mouse lung.** While reduced levels of HUS1 resulted in decreased skin tumorigenesis, the

effect of complete inactivation of *Hus1* on oncogene-induced tumorigenesis has yet to be determined. Previous data using conditional inactivation of *Hus1* in the mouse mammary gland suggest that *Hus1*-null cells are unable to survive rapid proliferation. However, forced proliferation by activated oncogenes in a tissue with a lower requirement for HUS1 may have a different effect than natural proliferation in the mouse mammary gland. In order to determine the role for HUS1 in oncogene-induced tumorigenesis in the lung, mice harboring a conditionally active Kras allele (LSL-$Kras^{G12D}$) (Jackson et al., 2001) were crossed with conditional Hus1 knockout mice ($Hus1^{Flox/Flox}$) (Levitt et al., 2005). $Hus1^{+/Flox}$ LSL-$Kras^{G12D}$ mice, with only one conditional *Hus1* allele serve as controls, as these mice retain one wild-type *Hus1* allele following recombination, and should not be subject to selection from loss of *Hus1*. Mice were anesthetized and $6.67X10^8$ PFU adenovirus expressing Cre-recombinase was administered in 40ul of MEM/$CaCl_2$ either drop wise into a single nostril or directly into a catheter inserted in the trachea for intranasal or intratracheal instillation, respectively (DuPage et al., 2009). Following intranasal instillation, mice were given a single burst of pressurized air into the nostril to ensure virus was forced into the lungs, and not trapped in the nasal passage. Intranasal instillation achieves efficient recombination when the virus reaches the lung; however, because the virus is not directly delivered to the lungs, some virus can be swallowed or coughed up prior to reaching the lungs, resulting in variability of infectivity. Intratracheal instillation is a more efficient method to deliver virus directly to the lungs, though this method is more invasive. As previously reported, expression of $Kras^{G12D}$ results in induction of tumorigenesis specifically in the lung. We hypothesize that inactivation of *Hus1* in cells which express constitutively active Kras will result in cell death or induction of senescence; thus, $Hus1^{Flox/Flox}$ LSL-$Kras^{G12D}$ mice will have a reduced tumor burden

*Figure 5.6* **Intranasal instillation can be used to effectively deliver virus to mouse lungs which can be used to conditionally activate $Kras^{G12D}$ to induce tumor growth.** (A) Mouse lungs infected with vehicle alone (PBS) or an adenovirus expressing LacZ. (B) Mouse lungs from either $Kras^{+}$ (right) or LSL-$Kras^{G12D}$ (left) mice infected with adenovirus expressing Cre-recombinase. LSL-$Kras^{G12D}$ mice develop tumors following recombination and activation of $Kras^{G12D}$, while $Kras^{+}$ mice do not. (C) Hematoxylin and Eosin stained sections of $Kras^{G12D}$ induced tumors 8 weeks following infection with AdenoCre virus. *[(A)Experiment and figure by S.A. Yazinski; (B and C) Experiment and figure by S.A. Yazinski and K. Hume]*

A

PBS

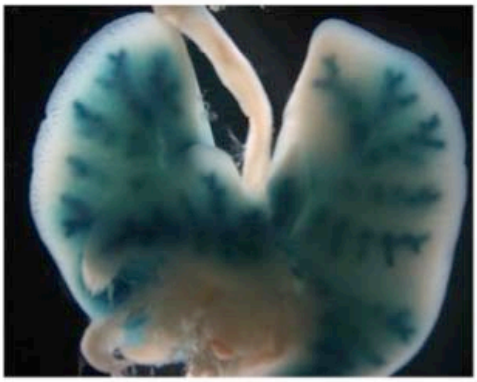

Adeno-LacZ Virus

B 20 weeks post-infection:

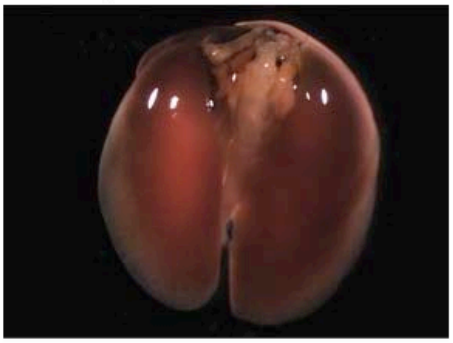

$Kras^{+/+}$

$Kras^{+/LSL}$

C 8 weeks post infection:

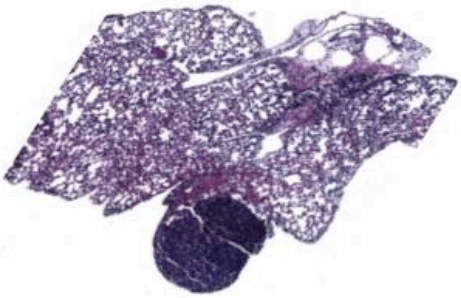

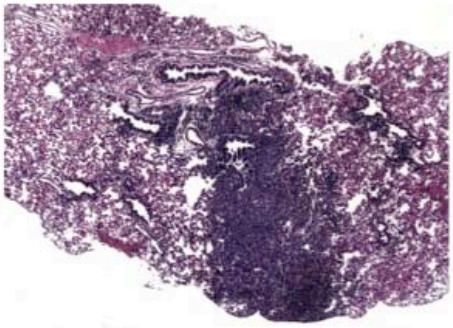

H&E stained sections at 10X

compared to Hus1$^{+/Flox}$ LSL-Kras$^{G12D}$ mice following AdenoCre administration (Figure 5.6).

**5.6.3 Mechanism of reduced *Hus1* expression resulting in decreased tumorigenesis.** As previously discussed, reduced *Hus1* expression resulted in decreased transformation in cell culture and decreased papilloma formation in mice following a two-step skin carcinogenesis protocol. We hypothesize that this may be due to cell death or senescence in cells with a high basal level of genomic instability due to reduced *Hus1* expression following the increased oxidative and replicative stresses associated with neoplastic transformation. To test this, we will harvest cells expressing incrementally reduced levels of *Hus1* following addition of activated oncogenes at various time points to determine if the parallel ATM pathway is activated, if apoptosis is induced, or if senescence is induced. Additionally, papillomas and surrounding skin in mice with reduced levels of *Hus1* will be stained for markers of DNA damage, apoptosis, and senescence to determine if there is increased genomic instability in the few resulting papillomas, and if the surrounding skin cells, which did not develop papillomas, induce senescence or apoptosis in response to oncogenic stimuli. The experiments proposed here will clarify the effect of reduced *Hus1* expression on oncogene-induced proliferation.

Taken together, the data outlined here suggests that impairment of *Hus1*, or the ATR pathway, may be a possible drug targets, either alone or in combination with chemotherapeutics, to treat cancers.

# REFERENCES


Ahmed, M., and Rahman, N. (2006). ATM and breast cancer susceptibility. Oncogene *25*, 5906-5911.

Ahmed, S., and Hodgkin, J. (2000). MRT-2 checkpoint protein is required for germline immortality and telomere replication in C. elegans. Nature *403*, 159-164.

Akagi, K., Sandig, V., Vooijs, M., Van der Valk, M., Giovannini, M., Strauss, M., and Berns, A. (1997). Cre-mediated somatic site-specific recombination in mice. Nucleic Acids Res *25*, 1766-1773.

Alderton, G.K., Joenje, H., Varon, R., Borglum, A.D., Jeggo, P.A., and O'Driscoll, M. (2004). Seckel syndrome exhibits cellular features demonstrating defects in the ATR-signalling pathway. Hum Mol Genet *13*, 3127-3138.

Ali, S.H., and DeCaprio, J.A. (2001). Cellular transformation by SV40 large T antigen: interaction with host proteins. Semin Cancer Biol *11*, 15-23.

Angel, P., Imagawa, M., Chiu, R., Stein, B., Imbra, R.J., Rahmsdorf, H.J., Jonat, C., Herrlich, P., and Karin, M. (1987). Phorbol ester-inducible genes contain a common cis element recognized by a TPA-modulated trans-acting factor. Cell *49*, 729-739.

Arlt, M.F., Durkin, S.G., Ragland, R.L., and Glover, T.W. (2006). Common fragile sites as targets for chromosome rearrangements. DNA Repair (Amst) *5*, 1126-1135.

Ashwell, S., and Zabludoff, S. (2008). DNA damage detection and repair pathways--recent advances with inhibitors of checkpoint kinases in cancer therapy. Clin Cancer Res *14*, 4032-4037.

Bai, H., Madabushi, A., Guan, X., and Lu, A.L. (2010). Interaction between human mismatch repair recognition proteins and checkpoint sensor Rad9-Rad1-Hus1. DNA Repair (Amst) *9*, 478-487.

Balansky, R., Izzotti, A., Scatolini, L., D'Agostini, F., and De Flora, S. (1996). Induction by carcinogens and chemoprevention by N-acetylcysteine of adducts to mitochondrial DNA in rat organs. Cancer Res *56*, 1642-1647.

Bao, S., Lu, T., Wang, X., Zheng, H., Wang, L.E., Wei, Q., Hittelman, W.N., and Li, L. (2004). Disruption of the Rad9/Rad1/Hus1 (9-1-1) complex leads to checkpoint signaling and replication defects. Oncogene *23*, 5586-5593.

Bartek, J., Bartkova, J., and Lukas, J. (2007). DNA damage signalling guards against activated oncogenes and tumour progression. Oncogene *26*, 7773-7779.

Bartek, J., and Lukas, J. (2003). Chk1 and Chk2 kinases in checkpoint control and cancer. Cancer Cell *3*, 421-429.

Bartek, J., and Lukas, J. (2007). DNA damage checkpoints: from initiation to recovery or adaptation. Curr Opin Cell Biol *19*, 238-245.

Bartkova, J., Horejsi, Z., Koed, K., Kramer, A., Tort, F., Zieger, K., Guldberg, P., Sehested, M., Nesland, J.M., Lukas, C., *et al*. (2005). DNA damage response as a candidate anti-cancer barrier in early human tumorigenesis. Nature *434*, 864-870.

Bartsch, H., and Nair, J. (2002). Potential role of lipid peroxidation derived DNA damage in human colon carcinogenesis: studies on exocyclic base adducts as stable oxidative stress markers. Cancer Detect Prev *26*, 308-312.

Barzilai, A., and Yamamoto, K. (2004). DNA damage responses to oxidative stress. DNA Repair (Amst) *3*, 1109-1115.

Begus-Nahrmann, Y., Lechel, A., Obenauf, A.C., Nalapareddy, K., Peit, E., Hoffmann, E., Schlaudraff, F., Liss, B., Schirmacher, P., Kestler, H., *et al*. (2009). p53 deletion impairs clearance of chromosomal-instable stem cells in aging telomere-dysfunctional mice. Nat Genet *41*, 1138-1143.

Benhar, M., Engelberg, D., and Levitzki, A. (2002). ROS, stress-activated kinases and stress signaling in cancer. EMBO Rep *3*, 420-425.

Bermudez, V.P., Lindsey-Boltz, L.A., Cesare, A.J., Maniwa, Y., Griffith, J.D., Hurwitz, J., and Sancar, A. (2003). Loading of the human 9-1-1 checkpoint complex

onto DNA by the checkpoint clamp loader hRad17-replication factor C complex in vitro. Proc Natl Acad Sci U S A *100*, 1633-1638.

Bertoni, F., Codegoni, A.M., Furlan, D., Tibiletti, M.G., Capella, C., and Broggini, M. (1999). CHK1 frameshift mutations in genetically unstable colorectal and endometrial cancers. Genes Chromosomes Cancer *26*, 176-180.

Blasco, M.A., Lee, H.W., Hande, M.P., Samper, E., Lansdorp, P.M., DePinho, R.A., and Greider, C.W. (1997). Telomere shortening and tumor formation by mouse cells lacking telomerase RNA. Cell *91*, 25-34.

Boles, N.C., Peddibhotla, S., Chen, A.J., Goodell, M.A., and Rosen, J.M. Chk1 haploinsufficiency results in anemia and defective erythropoiesis. PLoS One *5*, e8581.

Branzei, D., and Foiani, M. Maintaining genome stability at the replication fork. Nat Rev Mol Cell Biol *11*, 208-219.

Brown, E.J., and Baltimore, D. (2000). ATR disruption leads to chromosomal fragmentation and early embryonic lethality. Genes Dev *14*, 397-402.

Browne, S.E., Roberts, L.J., 2nd, Dennery, P.A., Doctrow, S.R., Beal, M.F., Barlow, C., and Levine, R.L. (2004). Treatment with a catalytic antioxidant corrects the neurobehavioral defect in ataxia-telangiectasia mice. Free Radic Biol Med *36*, 938-942.

Budzowska, M., Jaspers, I., Essers, J., de Waard, H., van Drunen, E., Hanada, K., Beverloo, B., Hendriks, R.W., de Klein, A., Kanaar, R.*, et al*. (2004). Mutation of the mouse Rad17 gene leads to embryonic lethality and reveals a role in DNA damage-dependent recombination. Embo J *23*, 3548-3558.

Burrows, A.E., and Elledge, S.J. (2008). How ATR turns on: TopBP1 goes on ATRIP with ATR. Genes Dev *22*, 1416-1421.

Carrassa, L., Montelatici, E., Lazzari, L., Zangrossi, S., Simone, M., Broggini, M., and Damia, G. (2010). Role of Chk1 in the differentiation program of hematopoietic stem cells. Cell Mol Life Sci *67*, 1713-1722.

Casper, A.M., Nghiem, P., Arlt, M.F., and Glover, T.W. (2002). ATR regulates fragile site stability. Cell *111*, 779-789.

Cha, R.S., and Kleckner, N. (2002). ATR homolog Mec1 promotes fork progression, thus averting breaks in replication slow zones. Science *297*, 602-606.

Chang, D.Y., and Lu, A.L. (2005). Interaction of checkpoint proteins Hus1/Rad1/Rad9 with DNA base excision repair enzyme MutY homolog in fission yeast, Schizosaccharomyces pombe. J Biol Chem *280*, 408-417.

Chen, C.C., Kennedy, R.D., Sidi, S., Look, A.T., and D'Andrea, A. (2009). CHK1 inhibition as a strategy for targeting Fanconi Anemia (FA) DNA repair pathway deficient tumors. Mol Cancer *8*, 24.

Chen, Z., Xiao, Z., Gu, W.Z., Xue, J., Bui, M.H., Kovar, P., Li, G., Wang, G., Tao, Z.F., Tong, Y., *et al*. (2006). Selective Chk1 inhibitors differentially sensitize p53-deficient cancer cells to cancer therapeutics. Int J Cancer *119*, 2784-2794.

Cheng, C.K., Chow, L.W., Loo, W.T., Chan, T.K., and Chan, V. (2005). The cell cycle checkpoint gene Rad9 is a novel oncogene activated by 11q13 amplification and DNA methylation in breast cancer. Cancer Res *65*, 8646-8654.

Cho, S.H., Toouli, C.D., Fujii, G.H., Crain, C., and Parry, D. (2005). Chk1 is essential for tumor cell viability following activation of the replication checkpoint. Cell Cycle *4*, 131-139.

Cimprich, K.A., and Cortez, D. (2008). ATR: an essential regulator of genome integrity. Nat Rev Mol Cell Biol *9*, 616-627.

Coppe, J.P., Patil, C.K., Rodier, F., Sun, Y., Munoz, D.P., Goldstein, J., Nelson, P.S., Desprez, P.Y., and Campisi, J. (2008). Senescence-associated secretory phenotypes reveal cell-nonautonomous functions of oncogenic RAS and the p53 tumor suppressor. PLoS Biol *6*, 2853-2868.

Costanzo, V., and Gautier, J. (2003). Single-strand DNA gaps trigger an ATR- and Cdc7-dependent checkpoint. Cell Cycle *2*, 17.

Cuadrado, M., Martinez-Pastor, B., Murga, M., Toledo, L.I., Gutierrez-Martinez, P., Lopez, E., and Fernandez-Capetillo, O. (2006). ATM regulates ATR chromatin loading in response to DNA double-strand breaks. J Exp Med *203*, 297-303.

de Klein, A., Muijtjens, M., van Os, R., Verhoeven, Y., Smit, B., Carr, A.M., Lehmann, A.R., and Hoeijmakers, J.H. (2000). Targeted disruption of the cell-cycle checkpoint gene ATR leads to early embryonic lethality in mice. Curr Biol *10*, 479-482.

de la Torre, J., Gil-Moreno, A., Garcia, A., Rojo, F., Xercavins, J., Salido, E., and Freire, R. (2008). Expression of DNA damage checkpoint protein Hus1 in epithelial ovarian tumors correlates with prognostic markers. Int J Gynecol Pathol *27*, 24-32.

Delacroix, S., Wagner, J.M., Kobayashi, M., Yamamoto, K., and Karnitz, L.M. (2007). The Rad9-Hus1-Rad1 (9-1-1) clamp activates checkpoint signaling via TopBP1. Genes Dev *21*, 1472-1477.

Dore, A.S., Kilkenny, M.L., Rzechorzek, N.J., and Pearl, L.H. (2009). Crystal structure of the rad9-rad1-hus1 DNA damage checkpoint complex--implications for clamp loading and regulation. Mol Cell *34*, 735-745.

DuPage, M., Dooley, A.L., and Jacks, T. (2009). Conditional mouse lung cancer models using adenoviral or lentiviral delivery of Cre recombinase. Nat Protoc *4*, 1064-1072.

Durkin, S.G., Arlt, M.F., Howlett, N.G., and Glover, T.W. (2006). Depletion of CHK1, but not CHK2, induces chromosomal instability and breaks at common fragile sites. Oncogene *25*, 4381-4388.

Ellison, V., and Stillman, B. (2003). Biochemical characterization of DNA damage checkpoint complexes: clamp loader and clamp complexes with specificity for 5' recessed DNA. PLoS Biol *1*, E33.

Espina, V., Wulfkuhle, J.D., Calvert, V.S., VanMeter, A., Zhou, W., Coukos, G., Geho, D.H., Petricoin, E.F., 3rd, and Liotta, L.A. (2006). Laser-capture microdissection. Nat Protoc *1*, 586-603.

Estensen, R.D., Levy, M., Klopp, S.J., Galbraith, A.R., Mandel, J.S., Blomquist, J.A., and Wattenberg, L.W. (1999). N-acetylcysteine suppression of the proliferative index

in the colon of patients with previous adenomatous colonic polyps. Cancer Lett *147*, 109-114.

Fan, Y., and Bergmann, A. (2008). Distinct mechanisms of apoptosis-induced compensatory proliferation in proliferating and differentiating tissues in the Drosophila eye. Dev Cell *14*, 399-410.

Fang, Y., Tsao, C.C., Goodman, B.K., Furumai, R., Tirado, C.A., Abraham, R.T., and Wang, X.F. (2004). ATR functions as a gene dosage-dependent tumor suppressor on a mismatch repair-deficient background. Embo J *23*, 3164-3174.

Francia, S., Weiss, R.S., Hande, M.P., Freire, R., and d'Adda di Fagagna, F. (2006). Telomere and telomerase modulation by the mammalian Rad9/Rad1/Hus1 DNA-damage-checkpoint complex. Curr Biol *16*, 1551-1558.

Freedman, V.H., and Shin, S.I. (1974). Cellular tumorigenicity in nude mice: correlation with cell growth in semi-solid medium. Cell *3*, 355-359.

Friedrich-Heineken, E., Toueille, M., Tannler, B., Burki, C., Ferrari, E., Hottiger, M.O., and Hubscher, U. (2005). The two DNA clamps Rad9/Rad1/Hus1 complex and proliferating cell nuclear antigen differentially regulate flap endonuclease 1 activity. J Mol Biol *353*, 980-989.

Fu, Y., Zhu, Y., Zhang, K., Yeung, M., Durocher, D., and Xiao, W. (2008). Rad6-Rad18 mediates a eukaryotic SOS response by ubiquitinating the 9-1-1 checkpoint clamp. Cell *133*, 601-611.

Gatei, M., Sloper, K., Sorensen, C., Syljuasen, R., Falck, J., Hobson, K., Savage, K., Lukas, J., Zhou, B.B., Bartek, J., *et al*. (2003). Ataxia-telangiectasia-mutated (ATM) and NBS1-dependent phosphorylation of Chk1 on Ser-317 in response to ionizing radiation. J Biol Chem *278*, 14806-14811.

Goldman, Y., Peled, A., and Shinitzky, M. (2000). Effective elimination of lung metastases induced by tumor cells treated with hydrostatic pressure and N-acetyl-L-cysteine. Cancer Res *60*, 350-358.

Gorgoulis, V.G., Vassiliou, L.V., Karakaidos, P., Zacharatos, P., Kotsinas, A., Liloglou, T., Venere, M., Ditullio, R.A., Jr., Kastrinakis, N.G., Levy, B., *et al*. (2005).

Activation of the DNA damage checkpoint and genomic instability in human precancerous lesions. Nature *434*, 907-913.

Greenow, K.R., Clarke, A.R., and Jones, R.H. (2009). Chk1 deficiency in the mouse small intestine results in p53-independent crypt death and subsequent intestinal compensation. Oncogene *28*, 1443-1453.

Griffith, E., Walker, S., Martin, C.A., Vagnarelli, P., Stiff, T., Vernay, B., Al Sanna, N., Saggar, A., Hamel, B., Earnshaw, W.C., *et al*. (2008). Mutations in pericentrin cause Seckel syndrome with defective ATR-dependent DNA damage signaling. Nat Genet *40*, 232-236.

Griffith, J.D., Lindsey-Boltz, L.A., and Sancar, A. (2002). Structures of the human Rad17-replication factor C and checkpoint Rad 9-1-1 complexes visualized by glycerol spray/low voltage microscopy. J Biol Chem *277*, 15233-15236.

Guy, C.T., Cardiff, R.D., and Muller, W.J. (1992a). Induction of mammary tumors by expression of polyomavirus middle T oncogene: a transgenic mouse model for metastatic disease. Mol Cell Biol *12*, 954-961.

Guy, C.T., Webster, M.A., Schaller, M., Parsons, T.J., Cardiff, R.D., and Muller, W.J. (1992b). Expression of the neu protooncogene in the mammary epithelium of transgenic mice induces metastatic disease. Proc Natl Acad Sci U S A *89*, 10578-10582.

Han, L., Hu, Z., Liu, Y., Wang, X., Hopkins, K.M., Lieberman, H.B., and Hang, H. (2010). Mouse Rad1 deletion enhances susceptibility for skin tumor development. Mol Cancer *9*, 67.

Heatwole, V.M. (1999). TUNEL assay for apoptotic cells. Methods Mol Biol *115*, 141-148.

Helt, C.E., Cliby, W.A., Keng, P.C., Bambara, R.A., and O'Reilly, M.A. (2005a). Ataxia telangiectasia mutated (ATM) and ATM and Rad3-related protein exhibit selective target specificities in response to different forms of DNA damage. J Biol Chem *280*, 1186-1192.

Helt, C.E., Wang, W., Keng, P.C., and Bambara, R.A. (2005b). Evidence that DNA damage detection machinery participates in DNA repair. Cell Cycle *4*, 529-532.

Hoeijmakers, J.H. (2001). Genome maintenance mechanisms for preventing cancer. Nature *411*, 366-374.

Hofmann, E.R., Milstein, S., Boulton, S.J., Ye, M., Hofmann, J.J., Stergiou, L., Gartner, A., Vidal, M., and Hengartner, M.O. (2002). Caenorhabditis elegans HUS-1 is a DNA damage checkpoint protein required for genome stability and EGL-1-mediated apoptosis. Curr Biol *12*, 1908-1918.

Hopkins, K.M., Auerbach, W., Wang, X.Y., Hande, M.P., Hang, H., Wolgemuth, D.J., Joyner, A.L., and Lieberman, H.B. (2004). Deletion of mouse rad9 causes abnormal cellular responses to DNA damage, genomic instability, and embryonic lethality. Mol Cell Biol *24*, 7235-7248.

Hu, Z., Liu, Y., Zhang, C., Zhao, Y., He, W., Han, L., Yang, L., Hopkins, K.M., Yang, X., Lieberman, H.B., *et al*. (2008). Targeted deletion of Rad9 in mouse skin keratinocytes enhances genotoxin-induced tumor development. Cancer Res *68*, 5552-5561.

Jacks, T., Remington, L., Williams, B.O., Schmitt, E.M., Halachmi, S., Bronson, R.T., and Weinberg, R.A. (1994). Tumor spectrum analysis in p53-mutant mice. Curr Biol *4*, 1-7.

Jackson, E.L., Willis, N., Mercer, K., Bronson, R.T., Crowley, D., Montoya, R., Jacks, T., and Tuveson, D.A. (2001). Analysis of lung tumor initiation and progression using conditional expression of oncogenic K-ras. Genes Dev *15*, 3243-3248.

Jardim, M.J., Wang, Q., Furumai, R., Wakeman, T., Goodman, B.K., and Wang, X.F. (2009). Reduced ATR or Chk1 expression leads to chromosome instability and chemosensitization of mismatch repair-deficient colorectal cancer cells. Mol Biol Cell *20*, 3801-3809.

Jazayeri, A., Falck, J., Lukas, C., Bartek, J., Smith, G.C., Lukas, J., and Jackson, S.P. (2006). ATM- and cell cycle-dependent regulation of ATR in response to DNA double-strand breaks. Nat Cell Biol *8*, 37-45.

Jerry, D.J., Kuperwasser, C., Downing, S.R., Pinkas, J., He, C., Dickinson, E., Marconi, S., and Naber, S.P. (1998). Delayed involution of the mammary epithelium in BALB/c-p53null mice. Oncogene *17*, 2305-2312.

Kai, M., and Wang, T.S. (2003). Checkpoint activation regulates mutagenic translesion synthesis. Genes Dev *17*, 64-76.

Kannouche, P.L., Wing, J., and Lehmann, A.R. (2004). Interaction of human DNA polymerase eta with monoubiquitinated PCNA: a possible mechanism for the polymerase switch in response to DNA damage. Mol Cell *14*, 491-500.

Kastan, M.B., and Lim, D.S. (2000). The many substrates and functions of ATM. Nat Rev Mol Cell Biol *1*, 179-186.

Kawakami, S., Kageyama, Y., Fujii, Y., Kihara, K., and Oshima, H. (2001). Inhibitory effect of N-acetylcysteine on invasion and MMP-9 production of T24 human bladder cancer cells. Anticancer Res *21*, 213-219.

Kawanishi, S., Hiraku, Y., and Oikawa, S. (2001). Mechanism of guanine-specific DNA damage by oxidative stress and its role in carcinogenesis and aging. Mutat Res *488*, 65-76.

Kendall, S.D., Linardic, C.M., Adam, S.J., and Counter, C.M. (2005). A network of genetic events sufficient to convert normal human cells to a tumorigenic state. Cancer Res *65*, 9824-9828.

Kinzel, B., Hall, J., Natt, F., Weiler, J., and Cohen, D. (2002). Downregulation of Hus1 by antisense oligonucleotides enhances the sensitivity of human lung carcinoma cells to cisplatin. Cancer *94*, 1808-1814.

Klaunig, J.E., Kamendulis, L.M., and Hocevar, B.A. (2010). Oxidative stress and oxidative damage in carcinogenesis. Toxicol Pathol *38*, 96-109.

Knudson, A.G. (2001). Two genetic hits (more or less) to cancer. Nat Rev Cancer *1*, 157-162.

Kohen, R., and Nyska, A. (2002). Oxidation of biological systems: oxidative stress phenomena, antioxidants, redox reactions, and methods for their quantification. Toxicol Pathol *30*, 620-650.

Komatsu, K., Miyashita, T., Hang, H., Hopkins, K.M., Zheng, W., Cuddeback, S., Yamada, M., Lieberman, H.B., and Wang, H.G. (2000). Human homologue of S.

pombe Rad9 interacts with BCL-2/BCL-xL and promotes apoptosis. Nat Cell Biol *2*, 1-6.

Kumagai, A., Lee, J., Yoo, H.Y., and Dunphy, W.G. (2006). TopBP1 activates the ATR-ATRIP complex. Cell *124*, 943-955.

Lam, M.H., Liu, Q., Elledge, S.J., and Rosen, J.M. (2004). Chk1 is haploinsufficient for multiple functions critical to tumor suppression. Cancer Cell *6*, 45-59.

Levitt, P.S., Liu, H., Manning, C., and Weiss, R.S. (2005). Conditional inactivation of the mouse Hus1 cell cycle checkpoint gene. Genomics *86*, 212-224.

Levitt, P.S., Zhu, M., Cassano, A., Yazinski, S.A., Liu, H., Darfler, J., Peters, R.M., and Weiss, R.S. (2007). Genome maintenance defects in cultured cells and mice following partial inactivation of the essential cell cycle checkpoint gene Hus1. Mol Cell Biol *27*, 2189-2201.

Lewis, K.A., Bakkum-Gamez, J., Loewen, R., French, A.J., Thibodeau, S.N., and Cliby, W.A. (2007). Mutations in the ataxia telangiectasia and rad3-related-checkpoint kinase 1 DNA damage response axis in colon cancers. Genes Chromosomes Cancer *46*, 1061-1068.

Lewis, K.A., Mullany, S., Thomas, B., Chien, J., Loewen, R., Shridhar, V., and Cliby, W.A. (2005). Heterozygous ATR mutations in mismatch repair-deficient cancer cells have functional significance. Cancer Res *65*, 7091-7095.

Liu, Q., Guntuku, S., Cui, X.S., Matsuoka, S., Cortez, D., Tamai, K., Luo, G., Carattini-Rivera, S., DeMayo, F., Bradley, A., *et al*. (2000). Chk1 is an essential kinase that is regulated by Atr and required for the G(2)/M DNA damage checkpoint. Genes Dev *14*, 1448-1459.

Logan, J., and Shenk, T. (1984). Adenovirus tripartite leader sequence enhances translation of mRNAs late after infection. Proc Natl Acad Sci U S A *81*, 3655-3659.

Luo, J., Solimini, N.L., and Elledge, S.J. (2009). Principles of cancer therapy: oncogene and non-oncogene addiction. Cell *136*, 823-837.

Luo, Y., Rockow-Magnone, S.K., Joseph, M.K., Bradner, J., Butler, C.C., Tahir, S.K., Han, E.K., Ng, S.C., Severin, J.M., Gubbins, E.J., *et al*. (2001). Abrogation of G2 checkpoint specifically sensitize p53 defective cells to cancer chemotherapeutic agents. Anticancer Res *21*, 23-28.

MacDougall, C.A., Byun, T.S., Van, C., Yee, M.C., and Cimprich, K.A. (2007). The structural determinants of checkpoint activation. Genes Dev *21*, 898-903.

Madoz-Gurpide, J., Canamero, M., Sanchez, L., Solano, J., Alfonso, P., and Casal, J.I. (2007). A proteomics analysis of cell signaling alterations in colorectal cancer. Mol Cell Proteomics *6*, 2150-2164.

Maier, B., Gluba, W., Bernier, B., Turner, T., Mohammad, K., Guise, T., Sutherland, A., Thorner, M., and Scrable, H. (2004). Modulation of mammalian life span by the short isoform of p53. Genes Dev *18*, 306-319.

Majka, J., Binz, S.K., Wold, M.S., and Burgers, P.M. (2006). Replication protein A directs loading of the DNA damage checkpoint clamp to 5'-DNA junctions. J Biol Chem *281*, 27855-27861.

Majka, J., and Burgers, P.M. (2004). The PCNA-RFC families of DNA clamps and clamp loaders. Prog Nucleic Acid Res Mol Biol *78*, 227-260.

Makrilia, N., Lappa, T., Xyla, V., Nikolaidis, I., and Syrigos, K. (2009). The role of angiogenesis in solid tumours: an overview. Eur J Intern Med *20*, 663-671.

Maniwa, Y., Yoshimura, M., Bermudez, V.P., Yuki, T., Okada, K., Kanomata, N., Ohbayashi, C., Hayashi, Y., Hurwitz, J., and Okita, Y. (2005). Accumulation of hRad9 protein in the nuclei of nonsmall cell lung carcinoma cells. Cancer *103*, 126-132.

Matheu, A., Maraver, A., Klatt, P., Flores, I., Garcia-Cao, I., Borras, C., Flores, J.M., Vina, J., Blasco, M.A., and Serrano, M. (2007). Delayed ageing through damage protection by the Arf/p53 pathway. Nature *448*, 375-379.

Matsuoka, S., Ballif, B.A., Smogorzewska, A., McDonald, E.R., 3rd, Hurov, K.E., Luo, J., Bakalarski, C.E., Zhao, Z., Solimini, N., Lerenthal, Y., *et al*. (2007). ATM and ATR substrate analysis reveals extensive protein networks responsive to DNA damage. Science *316*, 1160-1166.

Matsuoka, S., Rotman, G., Ogawa, A., Shiloh, Y., Tamai, K., and Elledge, S.J. (2000). Ataxia telangiectasia-mutated phosphorylates Chk2 in vivo and in vitro. Proc Natl Acad Sci U S A *97*, 10389-10394.

McNees, C.J., Tejera, A.M., Martinez, P., Murga, M., Mulero, F., Fernandez-Capetillo, O., and Blasco, M.A. (2010). ATR suppresses telomere fragility and recombination but is dispensable for elongation of short telomeres by telomerase. J Cell Biol *188*, 639-652.

Menoyo, A., Alazzouzi, H., Espin, E., Armengol, M., Yamamoto, H., and Schwartz, S., Jr. (2001). Somatic mutations in the DNA damage-response genes ATR and CHK1 in sporadic stomach tumors with microsatellite instability. Cancer Res *61*, 7727-7730.

Merry, C., Fu, K., Wang, J., Yeh, I.J., and Zhang, Y. (2009). Targeting the checkpoint kinase Chk1 in cancer therapy. Cell Cycle *9*, 279-283.

Mitra, S., Boldogh, I., Izumi, T., and Hazra, T.K. (2001). Complexities of the DNA base excision repair pathway for repair of oxidative DNA damage. Environ Mol Mutagen *38*, 180-190.

Moore, M.M., Chua, W., Charles, K.A., and Clarke, S.J. (2010). Inflammation and cancer: causes and consequences. Clin Pharmacol Ther *87*, 504-508.

Muller-Rover, S., Handjiski, B., van der Veen, C., Eichmuller, S., Foitzik, K., McKay, I.A., Stenn, K.S., and Paus, R. (2001). A comprehensive guide for the accurate classification of murine hair follicles in distinct hair cycle stages. J Invest Dermatol *117*, 3-15.

Murga, M., Bunting, S., Montana, M.F., Soria, R., Mulero, F., Canamero, M., Lee, Y., McKinnon, P.J., Nussenzweig, A., and Fernandez-Capetillo, O. (2009). A mouse model of ATR-Seckel shows embryonic replicative stress and accelerated aging. Nat Genet *41*, 891-898.

Myers, K., Gagou, M.E., Zuazua-Villar, P., Rodriguez, R., and Meuth, M. (2009). ATR and Chk1 suppress a caspase-3-dependent apoptotic response following DNA replication stress. PLoS Genet *5*, e1000324.

Nakamura, T.M., Moser, B.A., and Russell, P. (2002). Telomere binding of checkpoint sensor and DNA repair proteins contributes to maintenance of functional fission yeast telomeres. Genetics *161*, 1437-1452.

Navadgi-Patil, V.M., and Burgers, P.M. (2009). A tale of two tails: activation of DNA damage checkpoint kinase Mec1/ATR by the 9-1-1 clamp and by Dpb11/TopBP1. DNA Repair (Amst) *8*, 996-1003.

Nystrom, T. (2005). Role of oxidative carbonylation in protein quality control and senescence. Embo J *24*, 1311-1317.

O'Driscoll, M., Dobyns, W.B., van Hagen, J.M., and Jeggo, P.A. (2007). Cellular and clinical impact of haploinsufficiency for genes involved in ATR signaling. Am J Hum Genet *81*, 77-86.

O'Driscoll, M., Ruiz-Perez, V.L., Woods, C.G., Jeggo, P.A., and Goodship, J.A. (2003). A splicing mutation affecting expression of ataxia-telangiectasia and Rad3-related protein (ATR) results in Seckel syndrome. Nat Genet *33*, 497-501.

Pandita, R.K., Sharma, G.G., Laszlo, A., Hopkins, K.M., Davey, S., Chakhparonian, M., Gupta, A., Wellinger, R.J., Zhang, J., Powell, S.N., *et al*. (2006). Mammalian Rad9 plays a role in telomere stability, S- and G2-phase-specific cell survival, and homologous recombinational repair. Mol Cell Biol *26*, 1850-1864.

Parrilla-Castellar, E.R., Arlander, S.J., and Karnitz, L. (2004). Dial 9-1-1 for DNA damage: the Rad9-Hus1-Rad1 (9-1-1) clamp complex. DNA Repair (Amst) *3*, 1009-1014.

Parrinello, S., Samper, E., Krtolica, A., Goldstein, J., Melov, S., and Campisi, J. (2003). Oxygen sensitivity severely limits the replicative lifespan of murine fibroblasts. Nat Cell Biol *5*, 741-747.

Pennarun, G., Hoffschir, F., Revaud, D., Granotier, C., Gauthier, L.R., Mailliet, P., Biard, D.S., and Boussin, F.D. (2010). ATR contributes to telomere maintenance in human cells. Nucleic Acids Res.

Quintanilla, M., Brown, K., Ramsden, M., and Balmain, A. (1986). Carcinogen-specific mutation and amplification of Ha-ras during mouse skin carcinogenesis. Nature *322*, 78-80.

Ragland, R.L., Arlt, M.F., Hughes, E.D., Saunders, T.L., and Glover, T.W. (2009). Mice hypomorphic for Atr have increased DNA damage and abnormal checkpoint response. Mamm Genome *20*, 375-385.

Reinholdt, L., Ashley, T., Schimenti, J., and Shima, N. (2004). Forward genetic screens for meiotic and mitotic recombination-defective mutants in mice. Methods Mol Biol *262*, 87-107.

Reliene, R., Fischer, E., and Schiestl, R.H. (2004). Effect of N-acetyl cysteine on oxidative DNA damage and the frequency of DNA deletions in atm-deficient mice. Cancer Res *64*, 5148-5153.

Reliene, R., and Schiestl, R.H. (2006). Antioxidant N-acetyl cysteine reduces incidence and multiplicity of lymphoma in Atm deficient mice. DNA Repair (Amst) *5*, 852-859.

Rodier, F., Campisi, J., and Bhaumik, D. (2007). Two faces of p53: aging and tumor suppression. Nucleic Acids Res *35*, 7475-7484.

Roos-Mattjus, P., Hopkins, K.M., Oestreich, A.J., Vroman, B.T., Johnson, K.L., Naylor, S., Lieberman, H.B., and Karnitz, L.M. (2003). Phosphorylation of human Rad9 is required for genotoxin-activated checkpoint signaling. J Biol Chem *278*, 24428-24437.

Ruzankina, Y., Pinzon-Guzman, C., Asare, A., Ong, T., Pontano, L., Cotsarelis, G., Zediak, V.P., Velez, M., Bhandoola, A., and Brown, E.J. (2007). Deletion of the developmentally essential gene ATR in adult mice leads to age-related phenotypes and stem cell loss. Cell Stem Cell *1*, 113-126.

Ruzankina, Y., Schoppy, D.W., Asare, A., Clark, C.E., Vonderheide, R.H., and Brown, E.J. (2009). Tissue regenerative delays and synthetic lethality in adult mice after combined deletion of Atr and Trp53. Nat Genet *41*, 1144-1149.

Sabbioneda, S., Minesinger, B.K., Giannattasio, M., Plevani, P., Muzi-Falconi, M., and Jinks-Robertson, S. (2005). The 9-1-1 checkpoint clamp physically interacts with polzeta and is partially required for spontaneous polzeta-dependent mutagenesis in Saccharomyces cerevisiae. J Biol Chem *280*, 38657-38665.

Sanchez, Y., Wong, C., Thoma, R.S., Richman, R., Wu, Z., Piwnica-Worms, H., and Elledge, S.J. (1997). Conservation of the Chk1 checkpoint pathway in mammals: linkage of DNA damage to Cdk regulation through Cdc25. Science *277*, 1497-1501.

Savage, J.R. (1976). Classification and relationships of induced chromosomal structual changes. J Med Genet *13*, 103-122.

Scholzen, T., and Gerdes, J. (2000). The Ki-67 protein: from the known and the unknown. J Cell Physiol *182*, 311-322.

Schubert, R., Erker, L., Barlow, C., Yakushiji, H., Larson, D., Russo, A., Mitchell, J.B., and Wynshaw-Boris, A. (2004). Cancer chemoprevention by the antioxidant tempol in Atm-deficient mice. Hum Mol Genet *13*, 1793-1802.

Seckel, H.P.G. (1960). Bird-headed dwarfs; studies in developmental anthropology including human proportions (Springfield, Ill., C. C. Thomas).

Selbert, S., Bentley, D.J., Melton, D.W., Rannie, D., Lourenco, P., Watson, C.J., and Clarke, A.R. (1998). Efficient BLG-Cre mediated gene deletion in the mammary gland. Transgenic Res *7*, 387-396.

Serrano, M., Lin, A.W., McCurrach, M.E., Beach, D., and Lowe, S.W. (1997). Oncogenic ras provokes premature cell senescence associated with accumulation of p53 and p16INK4a. Cell *88*, 593-602.

Shechter, D., Costanzo, V., and Gautier, J. (2004). Regulation of DNA replication by ATR: signaling in response to DNA intermediates. DNA Repair (Amst) *3*, 901-908.

Shi, G., Chang, D.Y., Cheng, C.C., Guan, X., Venclovas, C., and Lu, A.L. (2006). Physical and functional interactions between MutY glycosylase homologue (MYH) and checkpoint proteins Rad9-Rad1-Hus1. Biochem J *400*, 53-62.

Shi, Y., Evans, J.E., and Rock, K.L. (2003). Molecular identification of a danger signal that alerts the immune system to dying cells. Nature *425*, 516-521.

Shiloh, Y. (2003). ATM and related protein kinases: safeguarding genome integrity. Nat Rev Cancer *3*, 155-168.

Shiomi, Y., Shinozaki, A., Nakada, D., Sugimoto, K., Usukura, J., Obuse, C., and Tsurimoto, T. (2002). Clamp and clamp loader structures of the human checkpoint protein complexes, Rad9-1-1 and Rad17-RFC. Genes Cells *7*, 861-868.

Shiotani, B., and Zou, L. (2009). Single-stranded DNA orchestrates an ATM-to-ATR switch at DNA breaks. Mol Cell *33*, 547-558.

Sidi, S., Sanda, T., Kennedy, R.D., Hagen, A.T., Jette, C.A., Hoffmans, R., Pascual, J., Imamura, S., Kishi, S., Amatruda, J.F., *et al*. (2008). Chk1 suppresses a caspase-2 apoptotic response to DNA damage that bypasses p53, Bcl-2, and caspase-3. Cell *133*, 864-877.

Silberstein, G.B. (2001). Postnatal mammary gland morphogenesis. Microsc Res Tech *52*, 155-162.

Smirnova, E., Toueille, M., Markkanen, E., and Hubscher, U. (2005). The human checkpoint sensor and alternative DNA clamp Rad9-Rad1-Hus1 modulates the activity of DNA ligase I, a component of the long-patch base excision repair machinery. Biochem J *389*, 13-17.

Sohn, S.Y., and Cho, Y. (2009). Crystal structure of the human rad9-hus1-rad1 clamp. J Mol Biol *390*, 490-502.

Soussi, T. (2007). p53 alterations in human cancer: more questions than answers. Oncogene *26*, 2145-2156.

Standing Committee on Human Cytogenetic Nomenclature., and Mitelman, F. (1995). ISCN 1995 : an international system for human cytogenetic nomenclature (1995) : recommendations of the International Standing Committee on Human Cytogenetic Nomenclature, Memphis, Tennessee, USA, October 9-13, 1994 (Basel ;, New York : Karger).

Steele, V.E., Sharma, S., Mehta, R., Elmore, E., Redpath, L., Rudd, C., Bagheri, D., Sigman, C.C., and Kelloff, G.J. (1996). Use of in vitro assays to predict the efficacy of chemopreventive agents in whole animals. J Cell Biochem Suppl *26*, 29-53.

Stelter, P., and Ulrich, H.D. (2003). Control of spontaneous and damage-induced mutagenesis by SUMO and ubiquitin conjugation. Nature *425*, 188-191.

Tabin, C.J., and Weinberg, R.A. (1985). Analysis of viral and somatic activations of the cHa-ras gene. J Virol *53*, 260-265.

Takai, H., Tominaga, K., Motoyama, N., Minamishima, Y.A., Nagahama, H., Tsukiyama, T., Ikeda, K., Nakayama, K., Nakanishi, M., and Nakayama, K. (2000). Aberrant cell cycle checkpoint function and early embryonic death in Chk1(-/-) mice. Genes Dev *14*, 1439-1447.

Tibbetts, R.S., Brumbaugh, K.M., Williams, J.M., Sarkaria, J.N., Cliby, W.A., Shieh, S.Y., Taya, Y., Prives, C., and Abraham, R.T. (1999). A role for ATR in the DNA damage-induced phosphorylation of p53. Genes Dev *13*, 152-157.

Todaro, G.J., and Green, H. (1963). Quantitative studies of the growth of mouse embryo cells in culture and their development into established lines. J Cell Biol *17*, 299-313.

Toueille, M., El-Andaloussi, N., Frouin, I., Freire, R., Funk, D., Shevelev, I., Friedrich-Heineken, E., Villani, G., Hottiger, M.O., and Hubscher, U. (2004). The human Rad9/Rad1/Hus1 damage sensor clamp interacts with DNA polymerase beta and increases its DNA substrate utilisation efficiency: implications for DNA repair. Nucleic Acids Res *32*, 3316-3324.

Tyner, S.D., Venkatachalam, S., Choi, J., Jones, S., Ghebranious, N., Igelmann, H., Lu, X., Soron, G., Cooper, B., Brayton, C., *et al*. (2002). p53 mutant mice that display early ageing-associated phenotypes. Nature *415*, 45-53.

Valentin-Vega, Y.A., Okano, H., and Lozano, G. (2008). The intestinal epithelium compensates for p53-mediated cell death and guarantees organismal survival. Cell Death Differ *15*, 1772-1781.

van Kruijsdijk, R.C., van der Wall, E., and Visseren, F.L. (2009). Obesity and cancer: the role of dysfunctional adipose tissue. Cancer Epidemiol Biomarkers Prev *18*, 2569-2578.

Vandivier, R.W., Henson, P.M., and Douglas, I.S. (2006). Burying the dead: the impact of failed apoptotic cell removal (efferocytosis) on chronic inflammatory lung disease. Chest *129*, 1673-1682.

Vassileva, V., Millar, A., Briollais, L., Chapman, W., and Bapat, B. (2002). Genes involved in DNA repair are mutational targets in endometrial cancers with microsatellite instability. Cancer Res *62*, 4095-4099.

Venclovas, C., and Thelen, M.P. (2000). Structure-based predictions of Rad1, Rad9, Hus1 and Rad17 participation in sliding clamp and clamp-loading complexes. Nucleic Acids Res *28*, 2481-2493.

Verlinden, L., Vanden Bempt, I., Eelen, G., Drijkoningen, M., Verlinden, I., Marchal, K., De Wolf-Peeters, C., Christiaens, M.R., Michiels, L., Bouillon, R., *et al*. (2007). The E2F-regulated gene Chk1 is highly expressed in triple-negative estrogen receptor /progesterone receptor /HER-2 breast carcinomas. Cancer Res *67*, 6574-6581.

Vidanes, G.M., Bonilla, C.Y., and Toczyski, D.P. (2005). Complicated tails: histone modifications and the DNA damage response. Cell *121*, 973-976.

Volkmer, E., and Karnitz, L.M. (1999). Human homologs of Schizosaccharomyces pombe rad1, hus1, and rad9 form a DNA damage-responsive protein complex. J Biol Chem *274*, 567-570.

Walker, W.S., Singer, J.A., Morrison, M., and Jackson, C.W. (1984). Preferential phagocytosis of in vivo aged murine red blood cells by a macrophage-like cell line. Br J Haematol *58*, 259-266.

Walsh, T., and King, M.C. (2007). Ten genes for inherited breast cancer. Cancer Cell *11*, 103-105.

Wang, L., Hsu, C.L., Ni, J., Wang, P.H., Yeh, S., Keng, P., and Chang, C. (2004a). Human checkpoint protein hRad9 functions as a negative coregulator to repress androgen receptor transactivation in prostate cancer cells. Mol Cell Biol *24*, 2202-2213.

Wang, W., Brandt, P., Rossi, M.L., Lindsey-Boltz, L., Podust, V., Fanning, E., Sancar, A., and Bambara, R.A. (2004b). The human Rad9-Rad1-Hus1 checkpoint complex stimulates flap endonuclease 1. Proc Natl Acad Sci U S A *101*, 16762-16767.

Wang, W., Lindsey-Boltz, L.A., Sancar, A., and Bambara, R.A. (2006). Mechanism of stimulation of human DNA ligase I by the Rad9-rad1-Hus1 checkpoint complex. J Biol Chem *281*, 20865-20872.

Wang, X., Guan, J., Hu, B., Weiss, R.S., Iliakis, G., and Wang, Y. (2004c). Involvement of Hus1 in the chain elongation step of DNA replication after exposure to camptothecin or ionizing radiation. Nucleic Acids Res *32*, 767-775.

Wang, Y. (2008). Bulky DNA lesions induced by reactive oxygen species. Chem Res Toxicol *21*, 276-281.

Watanabe, K., Tateishi, S., Kawasuji, M., Tsurimoto, T., Inoue, H., and Yamaizumi, M. (2004). Rad18 guides poleta to replication stalling sites through physical interaction and PCNA monoubiquitination. Embo J *23*, 3886-3896.

Weinert, T.A., and Hartwell, L.H. (1988). The RAD9 gene controls the cell cycle response to DNA damage in Saccharomyces cerevisiae. Science *241*, 317-322.

Weiss, R.S., Enoch, T., and Leder, P. (2000). Inactivation of mouse Hus1 results in genomic instability and impaired responses to genotoxic stress. Genes Dev *14*, 1886-1898.

Weiss, R.S., Kostrub, C.F., Enoch, T., and Leder, P. (1999). Mouse Hus1, a homolog of the Schizosaccharomyces pombe hus1+ cell cycle checkpoint gene. Genomics *59*, 32-39.

Weiss, R.S., Leder, P., and Vaziri, C. (2003). Critical role for mouse Hus1 in an S-phase DNA damage cell cycle checkpoint. Mol Cell Biol *23*, 791-803.

Weiss, R.S., Matsuoka, S., Elledge, S.J., and Leder, P. (2002). Hus1 acts upstream of chk1 in a mammalian DNA damage response pathway. Curr Biol *12*, 73-77.

Wells, B.S., Yoshida, E., and Johnston, L.A. (2006). Compensatory proliferation in Drosophila imaginal discs requires Dronc-dependent p53 activity. Curr Biol *16*, 1606-1615.

Wilsker, D., and Bunz, F. (2007). Loss of ataxia telangiectasia mutated- and Rad3-related function potentiates the effects of chemotherapeutic drugs on cancer cell survival. Mol Cancer Ther *6*, 1406-1413.

Xu, M., Bai, L., Gong, Y., Xie, W., Hang, H., and Jiang, T. (2009). Structure and functional implications of the human rad9-hus1-rad1 cell cycle checkpoint complex. J Biol Chem *284*, 20457-20461.

Yan, D.H., Wen, Y., Su, L.K., Xia, W., Wang, S.C., Zhang, S., Gan, L., Lee, D.F., Spohn, B., Frey, J.A., *et al*. (2004). A delayed chemically induced tumorigenesis in Brca2 mutant mice. Oncogene *23*, 1896-1901.

Yazinski, S.A., Westcott, P.M., Ong, K., Pinkas, J., Peters, R.M., and Weiss, R.S. (2009). Dual inactivation of Hus1 and p53 in the mouse mammary gland results in accumulation of damaged cells and impaired tissue regeneration. Proc Natl Acad Sci U S A *106*, 21282-21287.

Yin, Y., Zhu, A., Jin, Y.J., Liu, Y.X., Zhang, X., Hopkins, K.M., and Lieberman, H.B. (2004). Human RAD9 checkpoint control/proapoptotic protein can activate transcription of p21. Proc Natl Acad Sci U S A *101*, 8864-8869.

Yuki, T., Maniwa, Y., Doi, T., Okada, K., Nishio, W., Hayashi, Y., and Okita, Y. (2008). DNA damage sensor protein hRad9, a novel molecular target for lung cancer treatment. Oncol Rep *20*, 1047-1052.

Yuspa, S.H. (1994). The pathogenesis of squamous cell cancer: lessons learned from studies of skin carcinogenesis--thirty-third G. H. A. Clowes Memorial Award Lecture. Cancer Res *54*, 1178-1189.

Yuspa, S.H. (1998). The pathogenesis of squamous cell cancer: lessons learned from studies of skin carcinogenesis. J Dermatol Sci *17*, 1-7.

Zafarullah, M., Li, W.Q., Sylvester, J., and Ahmad, M. (2003). Molecular mechanisms of N-acetylcysteine actions. Cell Mol Life Sci *60*, 6-20.

Zalvide, J., and DeCaprio, J.A. (1995). Role of pRb-related proteins in simian virus 40 large-T-antigen-mediated transformation. Mol Cell Biol *15*, 5800-5810.

Zaugg, K., Su, Y.W., Reilly, P.T., Moolani, Y., Cheung, C.C., Hakem, R., Hirao, A., Elledge, S.J., and Mak, T.W. (2007). Cross-talk between Chk1 and Chk2 in double-mutant thymocytes. Proc Natl Acad Sci U S A *104*, 3805-3810.

Zhang, M., Behbod, F., Atkinson, R.L., Landis, M.D., Kittrell, F., Edwards, D., Medina, D., Tsimelzon, A., Hilsenbeck, S., Green, J.E., *et al*. (2008). Identification of tumor-initiating cells in a p53-null mouse model of breast cancer. Cancer Res *68*, 4674-4682.

Zhao, H., Thompson, R.B., Lockatell, V., Johnson, D.E., and Mobley, H.L. (1998). Use of green fluorescent protein to assess urease gene expression by uropathogenic Proteus mirabilis during experimental ascending urinary tract infection. Infect Immun *66*, 330-335.

Zhu, A., Zhang, C.X., and Lieberman, H.B. (2008). Rad9 has a functional role in human prostate carcinogenesis. Cancer Res *68*, 1267-1274.

Zhu, M., and Weiss, R.S. (2007). Increased common fragile site expression, cell proliferation defects, and apoptosis following conditional inactivation of mouse Hus1 in primary cultured cells. Mol Biol Cell *18*, 1044-1055.

Zighelboim, I., Schmidt, A.P., Gao, F., Thaker, P.H., Powell, M.A., Rader, J.S., Gibb, R.K., Mutch, D.G., and Goodfellow, P.J. (2009). ATR mutation in endometrioid endometrial cancer is associated with poor clinical outcomes. J Clin Oncol *27*, 3091-3096.

Zou, L., Cortez, D., and Elledge, S.J. (2002). Regulation of ATR substrate selection by Rad17-dependent loading of Rad9 complexes onto chromatin. Genes Dev *16*, 198-208.

Zou, L., and Elledge, S.J. (2003). Sensing DNA damage through ATRIP recognition of RPA-ssDNA complexes. Science *300*, 1542-1548.

Zou, L., Liu, D., and Elledge, S.J. (2003). Replication protein A-mediated recruitment and activation of Rad17 complexes. Proc Natl Acad Sci U S A *100*, 13827-13832.